Title
Some features of the anatomical and physiological organization of the central nucleus of the inferior colliculus

Author
Roth, George Linn

Publication Date
1977

Peer reviewed|Thesis/dissertation

SOME FEATURES OF THE ANATOMICAL AND PHYSIOLOGICAL ORGANIZATION OF THE CENTRAL NUCLEUS OF THE INFERIOR COLLICULUS: IMPLICATIONS FOR ITS ROLE IN THE PROCESSING OF AUDITORY INFORMATION

by

George Linn Roth
B.A., University of California, Berkeley, 1966

DISSERTATION

Submitted in partial satisfaction of the requirements for the degree of

DOCTOR OF PHILOSOPHY

in

PHYSIOLOGY

in the

GRADUATE DIVISION

(San Francisco)

of the

UNIVERSITY OF CALIFORNIA

Table of Contents

Acknowledgements

I would like to extend my sincerest thanks and appreciation to a number of people who were involved in this project and in my graduate education. In particular, I would like to thank Dr. Michael Merzenich, who shared his knowledge, enthusiasm, and advice, and Dr. Lindsay Aitkin, who provided invaluable experience and insights. Both participated in many of the experiments reported here, and Dr. Aitkin constructed four of the illustrations. Richard Andersen - who also participated in many of these studies - Mark White, David Zealear, Dr. Patricia Leake, and Paul Knight contributed to my graduate education in a variety of personal, and professional, ways. To all, and each, of these people I extend my gratitude as a friend, and as a colleague.

This research was partially supported by NIH Grant NS-10414, by the Colemen Fund, and by Hearing Research, Inc.

Abstract

This thesis reports the results of a series of neuroanatomical and neurophysiological experiments conducted in the central nucleus of the inferior colliculus (ICC) of the cat. Anatomical studies have defined the origins and topography of the brain stem afferents to ICC and have demonstrated that at least many of these projections remain segregated within the nucleus. Physiological studies in ICC have shown that neurons with similar response properties - response properties that often mimic those observed in the brain stem nuclei that project to ICC - are segregated within that structure. In addition, studies of a large population of ICC neurons whose discharge rates are a sensitive function of interaural time differences indicate that the contralateral (and perhaps part of the ispilateral) free sound field is represented within the ICC. The anatomical and physiological data derived in these studies can be directly related and provide strong evidence that anatomically, physiologically, and functionally distinct subdivisions of ICC exist. The implications of these findings with regard to the central neural processing of auditory information is discussed.

I. Introduction

The central nucleus of the inferior colliculus is a complex structure in the midbrain tectum. Its physiological organization is only superficially understood. Microelectrode studies have demonstrated that there is a systematic representation of the auditory sensory epithelium, the basilar membrane, within the central nucleus, and anatomical studies have defined a laminar pattern of organization that is the structural framework of that physiological order. Beyond this fundamental information, little else is known regarding the physiology and anatomy of the central nucleus, or the function(s) that this structure might subserve.

All auditory information (all input to the central nucleus) is ultimately derived from the cochlear branch of the VIIIth nerve. Fibers of this nerve are distributed within the cochlear nuclear complex to provide input to the cell groups of its three main divisions (the anteroventral, posteroventral, and dorsal cochlear nuclei). Axons from definable cell "fields" of these subdivisions innervate specific brain stem auditory nuclei. Some of these nuclei (e.g. the medial superior olive) receive binaural input; others (e.g. the medial nucleus of the trapazoid body) are strictly monaural. By virtue of the distribution of primary information to the very different populations of neurons in the cochlear nuclear complex and the specific redistribution of that information to particular brain stem nuclei, different aspects of auditory sensation are

apparently derived from a common input delivered via the auditory nerve. Thus, each of a large number of brain stem nuclei or cell fields abstracts different information from this common input, as reflected by the very different response properties of neurons in these different nuclei and cell fields.

Most experimental evidence indicates that ascending information from these brain stem auditory nuclei (including the entire cochlear nuclear complex) terminates in the central nucleus of the inferior colliculus, and is then fed forward to the auditory forebrain. Thus, a large number of inputs from these lower structures converges on the central nucleus, is somehow processed within its cochleotopic order, and is then relayed to the medial geniculate body. However, no experimental evidence exists to suggest how input from the various projecting brain stem nuclei is distributed or how the very different information from these sources is processed therein. Within the cochleotopic organization of the central nucleus, other rules of order must exist.

In order to determine some basic features of the functional organization of the central nucleus of the inferior colliculus, a series of neurophysiological and neuroanatomical experiments were conducted in the nucleus of the cat. By using a combined neurophysiological-neuroanatomical approach, principles of the functional organization could be directly related to their structural substrate, thereby providing additional insight into the basic processing of auditory information within this nucleus. This thesis reports the results of those experiments.

II. Review of Anatomical Literature

A. Structure of the Central Nucleus of the Inferior Colliculus

It is generally agreed that there are three major subdivisions in the mammalian inferior colliculus (IC), as first distinguished by Ramon y Cajal (1911). These subdivisions include a pericentral or roof nucleus ("ecorce internucleaire" or "ecorce superieure"), and external nucleus ("ecorce externe"), and a central nucleus ("noyau du tubercule quadrijuneau posterieur"). Rockel and Jones (1973 a,b,c) recently described these three major divisions in detail in the cat IC (Figure 1); their subdivision of the nucleus is compatible with and extends Ramon y Cajal's brief text. The central nucleus (ICC) is approximately ovoidal in shape, and occupies most of the volume of the colliculus. The pericentral division (ICP) consists of a sheet of cells approximately .5-.75 mm thick that overlies the dorsal and caudal aspects of ICC and extends down a short distance over the rostral surface of ICC (Figure 1-B). On its lateral edge, ICP merges with the external nucleus (ICX), a slightly thicker sheet of cells that covers the lateral portion of ICC and more anteriorally encompasses much of the rostral surface of ICC (Figure 1-B,C).

There is little agreement among anatomists regarding the borders and "cell groups" of these subdivisions. However, the central nucleus has a distinctly laminar appearance in Golgi preparations (first noted by Morest, 1964 a,b), which serves

to delimit it from the surrounding grey matter. This laminar organization has been described in all recent Golgi studies and constitutes the fundamental feature of the anatomical organization of ICC that is presently recognized. In the cat ICC, Rockel and Jones (1973 a,b) classified about 60% of the neurons as "principle cells". Dendritic arborizations of these principle cells tend to be oriented in parallel throughout most of ICC, and incoming lateral lemniscal fibers (conveying all major ascending inputs) run tangential to the major axis of dendritic orientation. This parallel alignment of dendrites and axons accounts for the laminar appearance of ICC in Golgi preparations and is evident in the three standard planes of section (Figures 2,3,4). In addition, the orientation of the principle cell somas can parallel the laminae to a greater (Ryugo and Killackey, 1977) or lesser (Rockel and Jones, 1973 a) degree, apparently depending upon the species and plane of section.

Golgi studies in man (Geniec and Morest, 1971), squirrel and rhesus monkeys (FitzPatrick, 1975; Fullerton, 1976), rat (Ryugo and Killackey, 1977), and tree shrew (Oliver, 1977) have confirmed this laminar pattern of organization, and physiological studies (Merzenich and Reid, 1974; FitzPatrick, 1975) have directly related this anatomical organization to the cochleotopic order found in ICC. Data reported in this thesis were derived from the laminated central nucleus of the inferior colliculus.

The anatomy of the IC has also been studied in Nissl preparations in the cat (van Noort, 1969; Goldberg and Moore, 1967), rhesus

monkey (Goldberg and Moore, 1967), and kangaroo rat (Webster et al., 1968). The lamination of ICC and the borders of all three subdivisions are blurred or indistinct in these preparations, and the anatomy cannot be easily correlated with the physiology of the IC. For this reason, subdivisions described in these studies were not employed in the interpretation of experimental results.

B. Brain Stem Afferents to the Central Nucleus: Degeneration Studies

The ICC receives input from many brain stem auditory nuclei, including the cochlear nuclear complex (CN), the medial (MSO) and lateral (LSO) superior olives, and the dorsal (DNLL) and ventral (VNLL) nuclei of the lateral lemniscus (NLL). These projections were initially defined by anterograde fiber degeneration studies (using Marchi and Nauta methods) and by a few retrograde cell degeneration studies. Because of inconsistencies in these studies, projections in any one animal (including cat) have never been well defined. Although species differences might be a factor, inconsistencies probably stem from limitations in experimental methods (e.g. interruption of fibers of passage) and analysis of results (e.g. interpretation of preterminal degeneration).

1. Projections from the Cochlear Nucleus

Some early degeneration studies (and one recent report) indicated that the CN sent bilateral (in guinea pig, Woollard and Harpman, 1939-40; and in chimpanzee, Strominger et al., 1977) or contralateral (in rhesus monkey, Barnes et al., 1943) projections to the IC. Others could not demonstrate a projection from CN to IC (in cat, Papez, 1929; Stotler, 1949, 1953; and in guinea pig, Stotler, 1949). Lesions in these experiments typically destroyed all or most of the CN complex, and the projections described could not be directly related to any one of the three subdivisions of the complex (Lorente de No, 1933; Osen, 1969 a,b).

More recent degeneration studies have involved lesions restricted to one of the three subdivisions of CN, or to cell field(s) within CN subdivisions. This body of work unequivocally defined a projection from all subdivisions of CN to the contralateral ICC, but a projection to the ipsilateral ICC was not always demonstrated. Anteroventral cochlear nucleus (AVCN) projections to ICC have been described as contralateral (in cat, Osen, 1972; van Noort, 1969; Warr, 1969; and in rabbit, Borg, 1973a) or bilateral (in rhesus monkey, Strominger and Strominger, 1971; and in kangaroo rat, Browner and Webster, 1975). In fact, Warr (1966) originally reported a bilateral AVCN projection in cat, but later (Warr, 1969) could not confirm preterminal degeneration in the ipsilateral ICC. Projections from the posteroventral cochlear nucleus (PVCN) to ICC have also been defined as exclusively contralateral (in cat, Osen, 1972; van Noort, 1969; Warr, 1969, 1972; and in rabbit, Borg, 1973a) or bilateral (in kangaroo rat, Browner and Webster, 1975). Finally, following lesions confined to the dorsal cochlear nucleus (DCN), preterminal degeneration has been described in the contralateral ICC (in cat, Osen, 1972; van Noort, 1969; Fernandez and Karapas, 1967; and in rabbit, Borg, 1973a) or in both ICC's (in rhesus monkey, Strominger, 1969, 1973).

2. Projections from the Superior Olivary Complex

The number and small size of nuclei, the complexities of their organization, and the invariable involvement of fibers

of passage have made degeneration studies involving more central nuclei in the auditory system particularly difficult to assess. Early Marchi studies in the cat (Papez, 1929, 1930; Rasmussen, 1946) were equivocal regarding a projection from the superior olivary complex (SOC) to IC, but Barnes et al. (1943) found bilateral projections from the SOC to the IC in the rhesus monkey.

Stotler's (1953) classic degeneration study in cat described specific connections of the nuclei of the SOC, and showed that the MSO and periolivary cell groups sent axons to the ipsilateral IC, while the LSO projected to both IC's. More recently, van Noort (1969) has claimed that the MSO and LSO both project bilaterally to the ICC in the cat. Browner and Webster's (1975) study in the kangaroo rat indicated that the MSO projected to the ipsilateral IC, and that the LSO had bilateral projections.

3. Projections from the Nuclei of the Lateral Lemnisci

Similar problems in the interpretation of data have arisen in the investigations of the ascending connections between the NLL and the IC. Papez' (1929) early work indicated that the NLL sent afferents to both IC's in the cat, but Barnes et al.'s (1943) material in rhesus monkey showed only a contralateral projection via the Commisure of Probst.

Woollard and Harpman (1939-40) defined a projection from DNLL to the contralateral ICC in cats, but were unable to demonstrate any ipsilateral connections. By contrast, Stotler (1953) only found an ipsilateral projection from the VNLL and DNLL to the IC.

More recently, Goldberg and Moore (1967) described a contralateral input to ICC from the DNLL in cat and rhesus monkey; van Noort (1969) confirmed this connection and also demonstrated an ipsilateral projection from VNLL to IC in cat.

C. Brain Stem Afferents to the Central Nucleus: HRP Studies

The introduction of a new technique in neuroanatomical research, the retrograde axonal transport of horseradish peroxidase (HRP) (Kristensson and Olsson, 1971; LaVail and LaVail, 1972), has led to a resolution of many ambiguities and inconsistencies generated by the analysis and interpretation of degeneration material. At present, this HRP data has only been published in abstract form. In his studies on cats and guinea pigs, Adams (1975) reported that ascending projections to the IC arise bilaterally in the DNLL, VNLL, LSO, AVCN, PVCN, DCN, and ipsilaterally in the MSO. Additional projections were found to originate in some periolivary neuron populations and in the contralateral ICC and its external "regions".

Brunso-Bechtold and Thompson (1976) described a similar distribution of HRP-labelled neurons following their injections into the ICC of cats, but they only reported an ipsilateral projection from the VNLL. The same projecting nuclei have been described in HRP studies in the tree shrew (Jones, 1976, 1977) and echo-locating bat (Zook and Casseday, 1976).

In summary, recent HRP experiments have confirmed and extended earlier degeneration studies on the origins of brain stem afferents to ICC. Together, these studies have provided a clear definition of the brain stem projections to the ICC. Very little is known about their functional significance. Experiments reported in this study were directed to a consideration of those issues.

III. Review of the Physiological Literature

Basic physiological investigations of the inferior colliculus have mainly involved two experimental approaches. In one major line of experiments, investigators sought to define some of the principles of the organization of ICC and have demonstrated that there is a precise, continuous three-dimensional representation of the cochlea within that structure. The second group of studies has focused on the response characteristics of ICC neurons, and has employed simple manipulations of a variety of stimulus parameters. In these latter studies, the basic three-dimensional organization of the ICC has been largely ignored. With the exception of two studies (Merzenich and Reid, 1974; FitzPatrick, 1975) relating the cochleotopic (or "tonotopic") organization of the ICC to its laminar organization, there has been virtually no effort made to relate the known structural features to the basic physiology of ICC.

A. Cochleotopic Organization of the Central Nucleus

Some of the data derived from early microelectrode studies of single units in the IC of the cat suggested that a cochleotopic organization might exist, but there was no systematic data to support that concept. For example, Thurlow et al. (1951) noted that the range of frequencies which drove single units in the IC changed as a function of the location within the colliculus, but they could not discern any overall order in those changes. Katsuki et al. (198) described a rough "tonotopic" organization in the IC, with frequencies less than 200 Hz represented caudally, and higher frequencies rostrally. Similarly, Erulkar's (1959) evidence suggested a cochleotopic order, but again lacked the histological control necessary to confirm that order. However, Erulkar did show that

single neurons in the IC could have two "best frequencies" (the frequency at which neurons were driven at lowest threshold), depending on which ear was stimulated. These best frequencies were close to one another, indicating that an IC neuron ultimately derived its input from the same sector of each cochlea.

Rose et al. (1963) were the first to clearly demonstrate the cochleotopic organization of ICC; they supported their results with rigorous histological controls. In electrode penetrations entering the ICC from the dorsolateral aspect and progressing ventro-medially, the best frequencies of isolated neurons increased in an orderly sequence from low to high. Similar results documenting sequential changes in the best frequencies of units (i.e. represented cochlear place) encountered along a single electrode penetration into ICC were later reported in the cat (Aitkin et al., 1970; Aitkin et al., 1975), rabbit (Aitkin et al., 1972), chinchilla (Adams and Teas, 1973), and rat (Clopton and Winfield, 1973). In all of these studies, there was no attempt to relate the representational sequences defined in individual penetrations to the three dimensions of the ICC, or to the laminar organization that had previously been described by Morest (1964a,b).

By combining and analyzing best frequency sequences derived from multiple electrode penetrations through ICC of the cat, Merzenich and Reid (1974) systematically reconstructed, in three dimensions, the cochleotopic organization of ICC and directly related that reconstruction to the anatomical observations of Morest (1964a,b) and Rockel and Jones (1973a). This work demonstrated that sectors of the cochlea are represented within ICC as a stack or series of "isofrequency discs" or "contours" and that the orientation of these discs parallels that of the

ICC laminae. Thus, a sector of the cochlear sensory epithelium is represented within the ICC as a "frequency-band" disc or lamina that spans the ICC from border to border, and the representation of the entire cochlea can be conceptualized as a stack of such discs.

In her combined neuroanatomical-electrophysiological study, FitzPatrick (1975) confirmed this cochleotopic organization in ICC of the squirrel monkey, and more directly related the three-dimensional frequency organization to the anatomically defined cell laminae. These important studies have demonstrated the fundamental relationship between the physiological (i.e. cochleotopic) and anatomical (i.e. laminar) organizations of the ICC. Yet, to date, they represent the sole efforts by physiologists to relate the unique structure of the ICC to its function.

B. Response Classes of Central Nucleus Neurons

Other physiological studies in the IC of the cat have focused on the responses of neurons to a variety of monaural and binaural stimuli. Overall, this body of work has demonstrated that ICC neurons can be (grossly) categorized into three major classes: 1) monaural neurons; 2) binaural neurons sensitive to interaural time differences; and 3) binaural neurons sensitive to interaural intensity differences. Other binaural neurons have also been described that are not sensitive to interaural time or intensity differences.

Some ICC neurons are monaural, i.e., they are influenced solely by input derived from a single cochlea (Erulkar, 1959; Webster and Veale, 1970; Aitkin et al., 1975). Stimulation of the contralateral ear drives most monaural ICC neurons (as well as most binaural units) (Rose et al., 1963; Merzenich and Reid, 1974; Aitkin et al., 1975). The firing pattern of a monaural neuron (and the response of a binaural neuron to monaural stimulation) is ultimately determined by a series of precisely timed excitatory and/or inhibitory synaptic inputs that are generated by stimulation of one ear and converge upon that neuron (Erulkar, 1959; Nelson and Erulkar, 1963; Rose et al., 1963). With monaural stimulation, the discharge rates, firing patterns, and latencies of ICC neurons are functions of the frequency, intensity, duration, and laterality of the applied sound stimulus (Rose et al., 1963).

The large majority of ICC neurons are binaural (Erulkar, 1959; Altman, 1966; Webster and Veale, 1970; Aitkin, et al., 1975). The output of these neurons is a function of the balance of monaural inputs derived from each ear (e.g. Hind et al., 1963; Nelson and Erulkar, 1963). Thus it has been argued that excitatory and inhibitory events from both ears

interact on most single neurons in the ICC, and the temporal patterns and relative intensities of these postsynaptic events determine the binaural discharge rate and firing pattern of the neuron (see e.g. Erulkar, 1959; Nelson and Erulkar, 1963; Hind et al., 1963; Rose et al., 1966).

Many binaural neurons in ICC are sensitive to small interaural time differences (e.g. Hind et al., 1963; Rose et al., 1966; Altman, 1966; Geisler et al., 1969; Benevento and Coleman, 1970; Leiman and Hafter, 1972; Starr and Don, 1972), and if interaural time delays are introduced, the firing rates of these cells can be systematically changed (e.g. Rose et al., 1966; Geisler et al., 1969). Regardless of the frequency or the intensity (at either ear) of the stimulating tone, these time-sensitive ICC neurons have a fixed interaural time delay at which their response rate is maximal or minimal. For this reason, Rose and colleagues termed that interaural time difference a "characteristic delay" (i.e. it is characteristic for each neuron). These "delay-sensitive" ICC neurons have low best frequencies (less than 3000 Hz), and most (but not all) delay-sensitive neurons have "characteristic delays" (Geisler et al., 1969).

Many high best frequency neurons in the ICC are exquisitely sensitive to interaural intensity differences, and the firing rates of these neurons are usually a well-defined function of the interaural intensity differences applied (Geisler et al., 1969; Benevento and Coleman, 1970). Most "interaural intensity-difference" neurons are excited by stimulation of the contralateral ear and inhibited by stimulation of the ipsilateral ear (Rose et al., 1966; Geisler et al., 1969). The auditory system measures interaural intensity differences to encode the location of high frequency sound sources (see Stevens and Newman, 1933); neurons sensitive to those intensity differences are

believed to be involved in that coding process (Rose et al., 1966; Geisler et al., 1969).

This classification of ICC neurons (i.e. monaural cells; binaural cells sensitive to interaural time differences, and binaural cells sensitive to interaural intensity differences) provides a useful (although limited) means of analyzing the physiological organization of the ICC. Responses of ICC neurons have been shown to be basically the same in the alert and anesthetized cat (Bock and Webster, 1974; Bock et al., 1972). The distribution(s) of these neuron classes within the ICC (along with the distribution of other cell classes) has never been assessed. In addition, the distribution(s) of these neural populations has never been related to the overall cochleotopic or laminar organization of the ICC.

As noted above, the ICC receives inputs from a large number of brain stem auditory nuclei. The auditory information that is processed by the CN and VNLL is predominantly monaural (e.g. Rose et al., 1959; Aitkin et al., 1970), while the DNLL, LSO, and MSO process information from both cochleas (e.g. Brugge et al., 1970; Boudreau and Tsuchitani, 1968; Guinan et al., 1972b). All of this information (i.e. all monaural and binaural inputs) converges upon the ICC in an unknown way. Nevertheless, the projections from these nuclei to the ICC maintain and are an integral part of its cochleotopic organization.

It is known that the response properties of neurons in those projecting nuclei are very similar to the response properties of at least many ICC neurons. Thus, nearly all CN neurons are driven only by monaural stimulation (e.g. Rose et al., 1959); many cells in the MSO and DNLL are sensitive to interaural time differences (Brugge et al., 1970; Hall, 1965); and virtually all LSO neurons are sensitive to interaural

intensity differences (e.g. Boudreau and Tsuchitani, 1968). The information carried by the ascending fibers from these nuclei must be processed in an orderly way within the three dimensional cochleotopic framework of ICC. That order should somehow be reflected in the spatial distribution(s) of ICC neurons with specific response characteristics. One of the basic objectives of this work was to study this distribution of ICC inputs and to assess that distribution in relation to the processing of information that takes place at this level of the auditory nervous system.

IV. Methods

A. Physiological Techniques

1. Preparation

Adult cats with no obvious signs of ear infection were initially anesthetized by an intraperitoneal injection of sodium pentobarbital (40 mg/kg), and tracheal and venous cannulae were introduced. A surgical level of anesthesia was maintained throughout the experiment by supplementary injections of barbiturate. A rectal thermometer monitored body temperature, which was maintained at approximately 37° C by a circulating water blanket. After placing the animal in a head holder, a midline scalp incision was made. The skin and muscles were reflected and the pinnae resected to permit insertion of flexible Tygon sound tubes into each transected external auditory meatus.

For dorsal-to-ventral microelectrode approaches, a crainiotomy was performed over occipital cortex, and the dura excised. Surface vessels on the exposed cortex were cauterized (Codman Bipolar Coagulator). With use of a Zeiss operating microscope, the overlying cortex was aspirated by gentle suction until the dorsal surface of the IC could be clearly visualized. A small portion of the bony tentorium cerebelli was removed to completely expose the dorsal collicular surface.

For horizontal penetrations, the crainiotomy was extended further ventrally and laterally. Most of the bony tentorium was removed and about one-half of the cerebellum aspirated. After such an exposure, microelectrodes could be introduced into the lateral or caudal aspect of the IC in a horizontal plane.

Once the appropriate surface of the colliculus was exposed, a photograph was taken. An enlarged (10X) print (with a .5 mm grid

superimposed) was made on which all microelectrode penetrations were recorded by cross reference to the surface vasculature (as viewed through the Zeiss operating microscope).

Single neurons were isolated with electrolytically-etched glass-coated platinum-iridium microelectrodes with platinum-black tips (ca. 3-5 microns in diameter). Electrodes were introduced into the colliculus by use of a hydraulic microdrive (Kopf) controlled by a stepping motor. The microdrive was attached to a micrometer drive on the H bar of a sterotaxic apparatus (Baltimore Instruments). Most often the colliculus was covered by mineral oil warmed to body temperature; on a few occasions, a 3% agar solution (in normal saline) was used to stabilize the preparation. In some of the early experiments, when only dorsal-to-ventral pentrations were made, a plastic cylinder was fixed to the skull by dental acrylic and electrodes were advanced manually by use of a Davies microdrive (Davies, 1956) mounted upon it. In any single experiment, all microelectrode penetrations were made parallel to one another.

Electrode penetrations were often marked by direct current lesions (15 μamps, 10 seconds) to help in reconstruction of microelectrode tracks. At the conclusion of an experiment, the animal was sacrificed by an over-dose of barbiturate, and the cranium was opened widely. The entire head was immersed in formal-saline for 2-4 weeks, when the brain was removed and reimmersed for another 2-4 weeks. Frozen sections were cut parallel to the penetrations in the frontal or saggital plane at 50 microns. All sections were mounted and stained with cresylecht violet. All units reported in this study were localized to the ICC. Reconstructions of electrode tracks were facilitated by reference to penetrations recorded on the photograph.

2. Stimulation and Recording

Tonal stimuli were generated by a General Radio Corp. oscillator (Type 1309 A) and shaped into trapezoidal tone pips with rise-fall times of 5 msec by a pair of electronic switches (Ludwig, 1970). Signals were then fed through two attenuators (Hewlett Packard 350 D) which provided independent control of the stimulus intensity (in 1 dB steps) to each ear. A passive delay network (Ad-Yu Electronics 802 F) was interposed between the oscillator and one tone switch to introduce interaural time (phase) differences in the stimuli delivered to each ear. Stimulus duration and repetition rates were controlled by a series of programmable timers. Stimuli were usually 250 msec in duration, and stimulus frequencies were monitored by a frequency meter (Monsanto Counter-Timer Model 100 B). When noise stimulation was applied (see results), a random noise generator (General Radio Corp. Type 1390 B) replaced the oscillator in this described system. Noise was band-passed from 100 Hz - 20 kHz.

Stimuli were delivered via equal-length flexible Tygon tubes tightly coupled to a matched pair of audiometric drivers (Telex Model 61470-07, 10 Ohms) . The tubes were sealed into each transected external auditory meatus by low melting point wax. The output of each driver was calibrated in 20 Hz steps from 20 Hz to 35 kHz using a probe microphone (¼ inch Bruel and Kjaer condenser microphone) and waveform analyser (General Radio Corp. 1900 A). The frequency response of these speakers was relatively flat up to 13 kHz, but dropped off in higher frequency ranges. All stimulus levels are given in dB attenuation (dBA) re a 1 volt RMS input to the drivers, as monitored on an AC voltmeter(Hewlett Packard 400 E). All experiments were conducted in an IAC sound proof room.

In this experimental series, best frequency (i.e. the frequency at which a neuron responds to the least intense stimulus; in other words, its

threshold frequency) determinations were made with reference to the calibrated speaker curves. Best frequencies (or represented cochlear place, see below) in these experiments were determined using contralateral stimulation. It has already been demonstrated (Erulkar, 1959; Merzenich and Reid, 1974) that best frequencies of ICC neurons to contralateral and ipsilateral monaural stimulation are very similar, if not identical.

Signals from isolated neurons were first led to a high-impedance, unity-gain preamplifier (Winston Electronic Co., Model 1090), and then to a high-gain amplifier (Tektronix Type 3A9) located outside of the IAC room. The spike recording was displayed on an oscilloscope (Tektronix Type 565) and amplified into a loudspeaker; neural activity could then be monitored both aurally and visually. Spikes were discriminated and then totalled on special purpose counters.

For experiments in which the distributions of neuronal response classes in ICC were studied (see Results, section B-1, 2), data were collected in the following manner. A neuron was isolated and its best frequency (represented cochlear place) to contralateral tonal stimulation was determined. Microelectrode depth was logged and spontaneous activity, if present, noted. The neural response (net excitation or net inhibition) and response pattern (onset or sustained; see Results, section B-1) to contralateral and ipsilateral monaural best frequency stimulation were recorded. Binaural interactions, if present, were then assessed. Using best frequency tonal stimulation, the majority of binaural neurons were obviously most sensitive to: 1) interaural time differences; 2) interaural intensity differences; or, 3) the level of the binaural stimulus (but <u>not</u> obviously sensitive to interaural time or intensity differences).

Neurons were categorized into one of these classes (see Results, Section B-1). Neural response and discharge patterns to binaural best frequency stimulation were also recorded. For time-sensitive neurons, interaural time differences which covered the behavioral range ($\pm$ 250 μsec; see Rose et al., 1966) were systematically introduced in 25 or 50 μsec steps; the interaural time difference at which the discharge rate was maximal or minimal was recorded. After obtaining these data, the microelectrode was slowly advanced until another neuron was isolated and the same procedure was repeated.

In another series of experiments, only interaural time-sensitive neurons were studied (see Results, Section B-3). All of these experiments were conducted using dorsal-to-ventral microelectrode approaches. Once a neuron was isolated and the best frequency determined, a series of binaural best frequency tone pips with interaural time differences were introduced that covered the behavioral range in 25 or 50 μsec steps. If the discharge rate of a neuron was a sensitive function of interaural time differences, responses to a variety of stimulus parameters (see below) were tested; neurons whose response rates were insensitive to these time differences were not studied.

If a neuron was sensitive to interaural time differences, five or ten stimulus trials were introduced at each of the defined interaural time difference steps, and the discharges at each stimulus condition totalled. Subsequently, the binaural stimulus was changed to a different level and the procedure repeated. Responses of each neuron were typically determined over a 40-50 dB range of stimulus levels. Noise stimulation and stimulus frequencies above and below each neuron's best frequency were also applied, and the same protocol followed. In this way, the

discharge rates of each isolated neuron were determined as a function of a variety of changing stimulus parameters (i.e. frequency, intensity, and with noise stimulation) at each interaural time difference introduced (i.e. 20 or 25 μsec steps across the behavioral range).

3. Relationship of Cochlear Place to Stimulus Frequency

Greenwood (1974) has developed a frequency-position function* which (empirically) relates distance along the basilar membrane to stimulus frequency. This function incorporates anatomical data (Schuknecht, 1960) and appears to causally relate psychophysical data, cochlear mechanics, and neurophysiological data (see e.g. Greenwood et al., 1976). Stimulus frequency, per se, provides limited information regarding the "real" stimulus (i.e. the traveling wave) which initiates the events that ultimately result in VIIIth nerve activity. However, stimulus frequency and the position of the stimulus on the sensory epithelium (more specifically, the position of the maximum amplitude of the traveling wave envelope) can be simply and directly related by Greenwood's function. In essence, the application of this function is analogous to the use of eccentricity when describing receptive fields of neurons in the visual system. For the auditory system, the stimulus (given as a distance) is referenced to a fixed point (the cochlear apex). Hence, in this study, stimulus frequency will most often be represented as a distance from the cochlear apex, as calculated using Greenwood's function. In the illustrations, frequencies (in kHz) corresponding to the indicated distance (in mm) on

---

* $f=418.6(10^{0.0954x} - 1)$, where f is the stimulus frequency (in Hertz) and x is the cochlear position (in mm from the apex) of maximum amplitude.

the basilar membrane are given by smaller numbers along the same axis. Note that in these illustrations the axis has been truncated at 20 mm (2 mm short of the actual length of the basilar membrane in the cat), because the poor output in the sound system at very high frequencies did not enable us to study neurons representing the most basal (i.e. high frequency) 2 mm of the basilar partition.

B. Anatomical Techniques

A series of neuroanatomical experiments were conducted in cats to define the origins of brain stem afferents to ICC and to directly relate these projections to the anatomical (laminar) and physiological (cochleotopic) organization of the nucleus. In these studies, the retrograde axonal transport of horseradish peroxidase (HRP) was employed to define the origins and topography of ICC inputs. HRP was injected at physiologically defined loci within the ICC. In all of these studies, with the exception of certain procedures described below, the preparation, stimulation, and recording methods were identical to those used in the physiological studies, as described earlier.

1. Preparation

Adult cats weighing 2.5-4 kg were anesthetized and mounted in a head-holder. A midline scalp incision was made and the skin and muscles overlying the left occipital pole of the forebrain were reflected. The IC was directly exposed via a wide craniotomy and ablation of the overlying occipital cortex. The headstage of a Kopf hydraulic microdrive was then mounted over the colliculus. A flexible tube coupled to an audiometric driver was inserted into the contralateral external auditory meatus. Microelectrodes were advanced into the ICC in a dorsorostral to ventrocaudal direction, and the best frequencies (represented cochlear place) of single

units and unit clusters (to contralateral stimulation) were determined with the use of tonal stimuli (as described earlier). After an adequate map of the tonotopic (cochleotopic) organization of ICC was obtained, the microelectrode was replaced by a 10 µl Hamilton syringe with a varnished 28 gauge needle, containing several microliters of a nearly saturated solution of HRP (approximately 40%) in saline.

The microsyringe was lowered into the central nucleus at the same orientation used for microelectrode recording, and evoked multiunit activity was monitored using the tip of the varnished needle as a recording electrode. A good correlation was usually found between the represented cochlear place previously determined for a particular depth and that recorded with the insulated microsyringe needle. Between 0.1 and 0.5 µl of the tracer was injected at given loci and the needle left in position for 15-30 minutes. After removal of the microsyringe, the muscle and skin overlying the cranial opening were sutured and the animal allowed to recover from the anesthetic.

2. Histological Procedures

24-42 hours after the time of injection, cats were anesthetized with sodium pentobarbital and perfused through the heart with 0.9% heparinized saline (37° C) followed by 0.2 M phosphate-buffered (pH 7.6) 2% paraformaldehyde (4° C). The brain was removed, placed in cold fixative for 2-5 hours, then transferred through a graded series of phosphate-buffered sucrose solutions culminating in immersion

in 30% buffered sucrose (4° C) for 8 hours.

Frontal sections from the medial geniculate body to the cochlear nucleus were cut on a freezing microtome in repeating 90μ-30μ-30μ series. Sections were reacted with 3,3'-diaminobenzidine (DAB) solution in Trizma buffer, to which a few drops of 30% H_2O_2 had been added (the method of Graham and Karnovsky, 1966, as modified by Ralston and Sharp, 1973). After 10-20 minutes in DAB, sections were washed with 3 changes of Trizma buffer and mounted on gelatinized slides. The tissue was then dried, dehydrated, cleared, coverslipped, and examined directly for the HRP reaction product.

Neurons of the brain stem auditory nuclei typically developed a diffuse, pale-brown coloration, presumably due to endogenous enzymes which reacted with DAB (Wong-Riley, 1976). Cells containing the dark-brown, granular HRP reaction product were easily distinguished from these lightly-stained, agranular neurons. However, after a section is counterstained and viewed under light microscopy, the stained Nissl substance in endogenously labelled, pale-brown cells can appear similar to HRP granules. In order to avoid possible confusion, all HRP cell counts were therefore made in non-counterstained material. Certain sections were subsequently counterstained with cresylecht violet and the cytoarchitectonic boundaries of the brain stem nuclei (which were usually sharp in non-counterstained material because of the endogenous reaction to DAB) were accurately reconstructed.

In each experiment, the distributions of granule-labelled cells in each nucleus were plotted from thick (90 μ) sections by the combined

use of a Zeiss Photomicroscope II in the transmitted light mode and a Bausch and Lomb microprojector. The location of every labelled neuron was recorded on scale drawings of brain stem auditory nuclei. From these observations and drawings, the numbers of cells containing granules were counted and plotted as a function of their locations within nuclei. Since each thick section in which neurons were counted was separated from the next by two 30 μ sections, no neurons could be counted twice.

3. Interpretative Problems

There are inherent problems in the use of this neuroanatomical procedure that must by recognized and addressed in the interpretation of experimental material. Questions concerning the HRP method include: 1) It has been suggested that a high paraformaldehyde concentration in the fixative might inhibit the demonstration of reaction product (see e.g. Kim and Strick, 1976; Jones and Leavitt, 1974). 2) The method used to develop the reaction product might be important for adequate visualization of the HRP label (de Olmos, 1977). 3) Although it is unlikely that HRP is taken up by fibers of passage (see Nauta et al., 1974; LaVail et al., 1973), the enzyme is incorporated and transported by cut or damaged axons (see Halperin and LaVail, 1975; Adams, 1976). 4) Certain fibers might show a specificity for the incorporation of HRP (see Bunt et al., 1976; Stockel et al., 1974; and Nauta et al., 1974). 5) Finally, it is difficult to estimate the effective size of the actual area of HRP incorporation, and this can lead to the identification of a "false positive" projection (de Olmos, 1977).

The data presented below demonstrate that following HRP injection into physiologically defined loci in ICC, HRP-labelled neurons were localized within all auditory nuclei known to project that nucleus. Some of these projections had previously been defined by anterograde (e.g. Warr, 1969) and retrograde (e.g. Osen, 1972) degeneration techniques, as well as by the HRP method (Adams, 1975; Brunso-Bechtold and Thompson, 1976). In addition, CN cells that were labelled in this experimental series were also found to be labelled in another HRP study (Adams and Warr, 1976) in which O-dianisidine was used to develop the reaction product. The use of paraformaldehyde fixative obviously did not suppress demonstration of reaction product in the material presented below and in other studies (see e.g. Ralston and Sharp, 1973; Wong-Riley, 1974; Bunt et al., 1976). Thus it appears unlikely that specificity of uptake, or the method of fixation or development, limited these experimental observations in any way.

As indicated in the results, many nuclei contained label following large injections, and in the smaller injection cases neurons within only a few nuclei were labelled. After an injection into ICC, arrays of labelled neurons in the projecting brain stem nuclei were restricted to specific locations within those nuclei. In addition, the topography of those arrays of labelled neurons correlated extremely well with the represented cochlear place of the injection site and the known cochleotopic organization of the projecting nuclei. This correlation strongly supports our belief that injections were restricted to given loci in ICC and that HRP was incorporated by the limited

number of axons that terminated at those loci. Because small volume injection cases resulted in very restricted labelling, it would also appear unlikely that this labelling represents fibers of passage or extensive damage to axons coursing across the ICC.

In summary, results of this study have been conservatively analysed with due respect to the recognized limitations of the HRP technique. The strong correlations between physiological data and anatomical results further support the validity of the anatomical data derived in this study.

V. Results

A. Anatomical Studies

1. Origins of Brain Stem Afferents to the Central Nucleus

By use of the retrogade axonal transport of HRP, these experiments have defined the origins of the brain stem auditory afferents to the ICC. In this experimental series, HRP-labelled neurons were localized in over ten brain stem auditory nuclei following injections of the enzyme into the central nucleus. In the largest-volume injection cases (.5 µl; 76-26, 76-28) neurons within all of these major projecting nuclei contained the retrogradely transported label. As described in detail below, neurons in only *a* limited number of these nuclei were labelled with reaction product in smaller-volume injection cases; in each of these smaller-injection experiments, the nuclei in which the HRP-labelled neurons were localized varied from experiment to experiment, depending upon the location of the injection site within the ICC.

The nuclei labelled following the two largest injections were identical, and the projections defined were generally consistent with results in the earlier, brief reports of Adams (1975) and Brunso-Bechtold and Thompson (1976). These results are illustrated by case 76-26. The majority of labelled neurons were located bilaterally in the DNLL and LSO, ipsilaterally in the VNLL and MSO, and contralaterally in the three major divisions of the CN. Scattered HRP-neurons were also observed in the ipsilateral ventral

and lateral periolivary nuclei (PON) and CN (all three dvisions), in the contralateral IC, and (in this case only) bilaterally near the facial nucleus.

Densely labelled neurons were found bilaterally in the DNLL (Figure 5) and ipsilaterally in the VNLL (Figure 6). HRP-labelled neurons in the DNLL were clustered in "islands" and prominently labelled axons of the lateral lemniscus were often seen coursing at right angles to the somas of the labelled neurons on the ipsilateral side (Figure 5-C). Granules of reaction product were most commonly found in fusiform (Figure 5-C) and multipolar (Figure 5-D) neurons, and unlabelled cells lay in close proximity but did not intermingle with each cluster of labelled neurons.

The VNLL apparently consists of two divisions. One of these units is slender and elongated and is vertically oriented along the main body of the ascending fibers of the lateral lemniscus (Figure 6-A). A more ventral division of VNLL is situated medial to the ascending lemniscal fibers and consists of an ovoidal cluster of cells (Figure 6-B). Neuroanatomical (van Noort, 1969; Warr, 1966, 1969) and electrophysiological (Aitkin et al., 1970; Guinan et al., 1972 b) evidence suggests that these two VNLL divisions are functionally different; the arrays of HRP-labelled neurons within each division (following ICC injections) were also very different. HRP-labelled neurons in the vertically oriented dorsal part of "VNLL" were organized in bands that

generally traversed the entire medial-to-lateral dimension of that division (Figure 6-A). Labelled neurons within a band or "streak" were typically bitufted or spindle-shaped, with their dendrites oriented normal to the fibers of the lateral lemniscus (Figure 6-C,D). Unlabelled and labelled neurons were intermingled within any given band. By contrast, HRP-neurons within the more ventral division of the nucleus were restricted to a single, dense cluster, and there, labelled neurons were generally multipolar or star-shaped (Figure 6-B,E).

HRP-labelled neurons were found within the ipsilateral MSO and PON and, bilaterally, in the LSO (Figure 7). Sections stained with cresylecht violet indicated that along the region of labelling most, if not all, of the neurons in each nucleus were labelled with HRP granules. The distribution of HRP-labelled neurons in those (and other) nuclei systematically changed as a function of the best frequency of the injection site (see below). No label was ever found in the neurons of the medial nucleus of the trapezoid body (MNTB) or in the contralateral MSO.

Neurons in all three subdivisions of both CN complexes contained HRP granules, but far heavier labelling was evident in the contralateral CN. In the contralateral DCN, fusiform cells of the middle laminae were heavily labelled (Figure 8-B); other neurons in the deep lamina including a few giant cells (Figure 8-A) were also labelled. No reaction product was observed in neurons within the superficial lamina. In the contralateral

PVCN, octopus cells (Figure 8-F) and multipolar cells (Figure 8-D) contained granules of reaction product; many marginal and globular cells (Figure 8-E) were also labelled. In the rostral aspect of the contralateral AVCN, including the large spherical cell field and the lateral cap area of Osen (1969 a,b), many neurons were labelled. However, only small cells were labelled with HRP reaction product (Figure 8-C); the easily characterized large and small spherical cells in AVCN apparently were not labelled.

In addition to these major projections, small numbers of labelled neurons were found in the ipsilateral ventral and lateral periolivary cell groups (Figure 7-F). As indicated above, scattered HRP-neurons were also seen in the three divisions of the ipsilateral CN complex. A small number of labelled neurons were observed in the contralateral ICC, scattered widely throughout its mass. Finally, a small group of neurons situated immediately ventral to the medial division of the facial motor nucleus and at the lateral margin of the pyramidal track contained HRP reaction product (Figure 8-G). These labelled neurons appeared to be located within the nucleus reticularis paragiganticocellularis lateralis of Taber (1961). The HRP-neurons were located bilaterally, and were only observed in this case (76-26).

In summary, these HRP-studies have defined the various origins of the brain stem auditory afferents to the ICC. Results of this anatomical study have clarified some of the inconsistencies

reported in earlier degeneration studies. They are generally consistent with results of other HRP studies in the cat. Thus, major brain stem auditory projections to the ICC originate bilaterally in the DNLL and LSO, contralaterally in the CN, and ipsilaterally in the VNLL and MSO. Other, less prominent, projections arise in the ipsilateral PON and CN, and from the contralateral IC.

2. Topography of Brain Stem Projections to the Central Nucleus

The topography of these defined brain stem projections could be directly related to the known physiological (i.e. cochleotopic) organization of the ICC and brain stem auditory nuclei. Within the major projecting nuclei (particularly evident in the MSO, LSO, and the contralateral CN), the location of the HRP-labelled neurons systematically shifted as a function of the represented cochlear place (best frequency) at the injection site. This is clearly demonstrated by two illustrated large volume injection cases (76-26, 76-28), since all of the major projecting nuclei were labelled in these cases, and the injection sites represented apical (76-26 at 2 kHz, or 8.0 mm from the cochlear apex) and more basal (76-28 at 9 kHz, or 14.2 mm from the cochlear apex) sectors of the cochlea.

Following the injection at the 2 kHz representational locus in the dorsal aspect of ICC (76-26), labelled neurons were located in the dorsal-medial tip of the ipsilateral MSO and, bilaterally, in the dorsal-lateral tip of the LSO (Figure 9-top half). After an injection into the 9 kHz representational locus, more ventral

in the ICC (76-28), the cluster of HRP-labelled neurons in these nuclei were displaced to a more ventro-lateral position in the MSO and to a more ventral position in the LSO (Figure 9-bottom half). Both the locations of HRP-labelled neurons within the MSO and LSO and the recorded best frequencies at the injection sites correspond closely with the known tonotopic organization of these structures (see Guinan et al., 1972 b). Note that a smaller cluster of HRP-cells is situated more ventrally in the MSO and LSO of 76-26, presumably a result of the spread of HRP to a more ventral (i.e. higher frequency) region of the ICC.

For all injection cases in which the MSO and LSO were labelled by the retrograde tracer, the HRP cells were distributed along the entire rostral-caudal extent of the nucleus (see histograms, Figure 9), forming a slab-like array of neurons. The width of this array (in frontal section) within each nucleus varied in different cases as a function of the volume of the tracer injected, but the length of the projecting "slab" covered the rostral-caudal extent of the nucleus, regardless of the size of the injection. Larger injections resulted in a fairly wide array of labelled neurons (Figure 9, 76-26, 76-28); the array was much narrower with smaller injections. In the smallest volume injection case (76-4, 0.1 µl) in which neurons in the MSO and LSO were labelled, only a very few HRP-labelled neurons were present in each 90 µ section, but they were evenly distributed along the entire length of each nucleus (Figure 10). Results in all other cases were

consistent with these topographical findings.

In the contralateral CN, the distribution of the tracer could also be directly related to the represented cochlear place at the injection site. Figure 11 compares the patterns of HRP-labelled neurons following the largest low best frequency injection (76-26, 2 kHz, 8.0 mm) and the largest high best frequency injection (76-28, 9 kHz, 14.2 mm). The low best frequency injection (76-26) led to transport of HRP by neurons (primarily fusiform cells and a few giant cells) localized ventro-caudally in DCN (Figure 11, section 2) and in multipolar cells (Figure 11, sections 5,9) of PVCN. Many globular cells and some marginal cells were also labelled (Figure 11, section 18). In the AVCN, small neurons containing HRP granules were scattered throughout the rostral portion of the nucleus (Figure 11, section 25), including the area described as the large spherical cell field by Osen (1969 a,b).

The higher best frequency injection of 76-28 (Figure 11, lower row) led to labelling more rostrally and dorsally in DCN, and again the reaction product was most prominent in the fusiform cells of the middle lamina (Figure 11, sections 3,7,10). In PVCN, HRP granules were present in small cells and in multipolar cells situated further rostrally and dorsally (Figure 11, sections 7,10) than in 76-26. As in the latter experiment, a contingent of labelled neurons occurred as a swathe across AVCN at a mid-rostral-to-caudal level (Figure 11, section 19), identifiable in this and other high frequency injections as the small spherical

cell area (Osen, 1969 a,b). As in the case of the more rostral AVCN labelling of 76-26, only a fraction of the small cells in this area were labelled (labelled neurons did not appear to be the small spherical cells of this field). Note that the 9 kHz best frequency injection of 76-28 did not lead to uptake in the rostral aspect of AVCN, except at its dorso-rostral tip (Figure 11, lower section 25). Cells in this region were also labelled in other experiments and were presumably analogous to the peripheral cap of marginal cells observed by Osen (1969 a,b) and Merzenich (unpublished observations).

The topography of these connections, most apparent in the fusiform cell layer in the DCN, conforms with the defined tonotopic organization of the CN complex (Rose et al., 1959). Thus, for example, a strip of fusiform cells located relatively caudally and ventrally projected to relatively dorsal (low best frequency) regions of ICC, while a more dorsal and rostral strip projected to more ventral (higher best frequency) regions of the ICC. Results in all other cases were consistent with these findings.

The topographical relationship between the distributions of labelled neurons and the best frequencies at the injection sites were not nearly as apparent in the NLL. The complex and irregular appearance of the clumps of cells composing DNLL made exact comparisons between the regions containing HRP cells in different experiments difficult. However, in general, for lower-frequency injections labelled cells were concentrated in the

more dorsal aspect of the cellular islands (e.g. 76-26); while in higher-frequency ICC injection cases, labelled cells were observed more ventrally in DNLL (e.g. 76-28). This is consistent with the described tonotopic organization of DNLL (Aitkin et al., 1970).

Cells in the lateral streak of VNLL (Figure 6-A,C,D) were labelled in bands, and although the thickness of the bands varied from experiment to experiment, it was virtually impossible to determine the topographic relationship between cells in this portion of VNLL and the injection site. By contrast, the rounded mass of cells at the ventral extremity of the VNLL consisted of a single, relatively uniform cluster of neurons (Figure 6-B,E). Although there was clearly a shift in the main concentration of labelled cells from experiment to experiment, the irregular boundaries of the ventral part of VNLL made any topographical relationships with injection sites difficult to define.

Thus, the topography of the major projections from brain stem auditory nuclei (and particularly those of projections from the SOC and CN complex) to the ICC can be directly related to the anatomical (i.e. laminar) organization of ICC. In addition, the topography of these projections clearly demonstrate the precise relationship between the known physiological (i.e. cochleotopic) organization of the ICC and these various projecting brain stem structures.

3. Segregation of Brain Stem Afferents to the Central Nucleus

As demonstrated above, all brain stem auditory nuclei known to project to the ICC were labelled following the larger HRP injections. In each of the smaller volume cases, neurons in only some of these nuclei were labelled. These smaller injections were often made at sites in ICC representing similar sectors of the cochlea, but the distributions of HRP-neurons in the brain stem (i.e. the nuclei which were labelled by the tracer) were never the same. Data from these injections indicate that afferent inputs to the ICC from different brain stem auditory nuclei are segregated to at least a large extent within the ICC, and that regions of areas within ICC that represent the same cochlear place can receive input from different auditory brain stem nuclei.

Two of these smaller injection cases (76-4, 0.1 µl, 15.4 mm; 76-10, 0.25 µl, 16.4 mm) clearly demonstrate this segregation of ascending afferents to ICC. These injections were both made in high frequency regions of ICC, yet were sufficiently far apart to make it unlikely (given the nearly parallel orientation of the afferent fibers and the injection needle) that major overlap occurred between ascending axonal groups that incorporated and transported HRP. The injection of 76-10 was introduced in the extreme posterior aspect of ICC; while the injection site of 76-4 was located centrally in the nucleus. HRP-labelling following

the injection in 76-4 was restricted solely to neurons in the ipsilateral MSO, LSO, and PON. In each 90 micron section only 1-4 neurons were labelled in each nucleus; neurons clearly contained reaction product, and were restricted to the ventral tip of MSO and medio-ventral aspect of LSO (see Figure 10). The topography of the projection in this experiment was thus similar to that of 76-28 (Figure 9), although numbers of labelled cells were far lower. No neurons were labelled within the CN or NLL on either side.

By contrast, over 75% of labelled neurons in experiment 76-10 were within the principle divisions of the contralateral CN (Figure 12). There was also labelling of a small number of neurons in the ipsilateral VNLL and PON. In this case, no neurons were labelled in the MSO, LSO or DNLL of either side. Results from these experiments are compared to four other injection cases in Figure 13. For each case, the number of labelled neurons in each nucleus is plotted as a percentage of the total number of HRP-labelled neurons recorded in each experiment (N's in Figure 13). Only neurons in the thick (90 micron) sections were counted. As illustrated, the labelled nuclei and the proportion of HRP-labelled neurons distributed within each major projecting nucleus were very similar following the two larges volume injections (76-26, 76-28; Figure 13-C,D) but the results of other (smaller) recorded injection cases differed in detail from these larger volume cases and from each other (Figure 13-A,B,E,F).

For example, in 76-10 over 75% of the labelled neurons were localized to the contralateral CN, while in 75-6, less than 5% of the total number of HRP cells were found in the contralateral CN. Over 35% of the labelled neurons were in the contralateral CN in 75-8, and the CN contained no HRP cells in 76-4. In fact, over this experimental series, no single nucleus invariably contained labelled neurons. Thus, no single nucleus can project to all parts of the ICC.

These results provide anatomical evidence for a segregation of the ascending inputs from brain stem auditory nuclei within the ICC. Larger injections presumably resulted in incorporation and transport of HRP by axons terminating over a large area in ICC, and therefore HRP-labelled neurons were found in all brain stem auditory nuclei projecting to ICC. Following smaller injections, HRP was presumably incorporated by terminals ending in relatively restricted regions of ICC, and therefore labelling was restricted to a limited number of projecting nuclei. As demonstrated earlier, regardless of the size of the injection and the number of nuclei labelled, the topography of the defined projections corresponded with the known cochleotopic organization of the brain stem auditory nuclei. Thus it would appear that there is a segregation of afferent inputs in the ICC, and that this segregation constitutes another feature of the anatomical organization (in addition to the laminar organization) of the nucleus.

B. Physiological Studies

An initial objective of these experiments was to determine the basic distributions of neurons with different response properties within the ICC, and to relate their distributions to the three-dimensional cochleotopic organization of the nucleus. These basic data (reported below in sections 1 and 2) were derived in a series of experiments in cats in which response properties were defined for large numbers of neurons studied within the ICC in each individual experiment. In these studies, single neurons were isolated in horizontal or dorso-ventral microelectrode penetrations that passed through the nucleus.

1. Response Classes and Discharge Patterns of Central Nucleus Neurons

Some of the data from these experiments is summarized in Figure 14, in which the number of monaural and binaural ICC neurons studied is shown as a function of the location along the cochlea (distance from the cochlear apex) that they represent (see methods). The distribution of all binaural and monaural neurons studied in this series is represented in Figure 14-F. The paucity of neurons representing cochlear sectors further than 16 and less than 4 mm from the apex is probably a consequence of experimental limitations. That is, anatomical-surgical restrictions prevented recording from a greater number of neurons in the most ventral aspect (i.e. the region of representation of the cochlear base or of high frequencies) of the ICC when a horizontal approach to the ICC was used. Penetrations intended to survey the most dorsal part (i.e. the region of representation of the cochlear apex, or low frequencies) of ICC often skirted the nucleus. This skewed distribution should not be interpreted to indicate, then, that there are substantially fewer neurons in ICC

representing these regions of the basilar partition. In fact, there is direct experimental evidence (Merzenich and Reid, 1974) that neurons representing sectors of the basal cochlea actually occupy a larger volume of the ICC than do those representing more apical cochlear sectors.

The distribution of monaural and binaural ICC neurons representing different cochlear loci, is illustrated in Figure 14-A and E. Of the 546 ICC neurons studied in this experimental series, 179 (33%) were excited or inhibited* solely by stimulation of one ear and were therefore classified as monaural. Responses of 364 (67%) ICC neurons were influenced by inputs derived from both ears, and were therefore classified as binaural. Three other ICC units were spontaneously active, and were unaffected by the applied auditory stimulation.

It was found that binaural ICC neurons could be sharply delineated into three major classes by their responses to best frequency tones: 1) neurons whose firing rate varied as a function of interaural time differences of ± 250 μsec or less (the behaviorally relevant range in the cat; see Rose et al., 1966); 2) neurons whose firing rates varied as a sensitive function of interaural intensity differences; and 3) neurons whose firing rates primarily varied as a simple function of the intensity of stimuli delivered to either or both ears, but were not noticeably sensitive to interaural time or intensity differences.

---

* It is well known that stimulation of one ear can generate both excitatory and inhibitory inputs that impinge upon the same ICC neuron (e.g. Rose et al., 1966; Nelson and Erulkar, 1963). The experiments reported here were directed toward assessing the overall activity of a population(s) of ICC neurons and hence descriptions of single unit responses refer to the net excitation or inhibition of a neuron observed under the defined stimulus conditions. No attempts were made to quantify the excitatory and/or inhibitory synaptic inputs that resulted in that net excitation or inhibition.

The distribution of these three classes of binaural neurons (as a function of the cochleotopic organization of the ICC) is shown in Figure 14-B, C, and D. Note that "intensity-sensitive" binaural neurons were relatively evenly distributed as a function of represented cochlear place (Figure 14-D). Interaural time-sensitive neurons primarily represented the most apical 8 mm of the basilar partition (Figure 14-B). By contrast, most (146/177, 82%) interaural intensity-sensitive neurons derived their input from cochlear position more basal than the 8 mm position (Figure 5—C).

The excitatory inputs to ICC neurons delivered from each of the two ears are summarized in Figure 15. Most excitatory inputs which drove ICC neurons were ultimatley derived from the contralateral ear (Figure 15-B). Nearly all monaural neurons, and nearly all binaural neurons sensitive to interaural intensity differences were excited by stimulation of the contralateral ear (Figure 15-A, D). In the vast majority (174/177, 98%) of neurons sensitive to interaural intensity differences, the contralateral input was excitatory and the ipsilateral input inhibitory. By contrast, the ipsilateral ear more frequently excited binaural ICC neurons whose firing rates were functions of interaural time differences or those binaural neurons that were not sensitive to differences of interaural time or intensity. While the great majority (93/108, 86%) of time-sensitive ICC neurons were excited by contralateral stimulation, about one-half (47/108, 44%) were also driven by ipsilateral monaural stimulation (Figure 15-C). As will be discussed in detail below, most (87/108, 81%) of the interaural time-sensitive cells fired maximally with the contralateral stimulus leading. Nearly all ICC neurons (70/79, 89%) with "intensity" response functions (i.e., neurons that were not sensitive to

differences in interaural time or intensity) were driven by contralateral stimulation. A majority (49/79, 62%) of these neurons were also excited by tonal stimulation of the ipsilateral ear (Figure 15-E). In 73 of the 79 "intensity" sensitive cells studied, the discharge rate to binaural stimulation typically represented either a summation or a facilitation of the responses to stimulation of either ear alone. The remaining six units categorized in this class were spontaneously active and were inhibited by monaural stimulation of either ear, and by binaural stimulation.

The discharge patterns of 532 ICC neurons in these response "classes" were categorized (using supra threshold best frequency tone pips) as onset, i.e. cells that responded at the stimulus onset with a single spike or a brief burst of spikes, or sustained, i.e. cells that responded throughout most or all of the stimulus duration. "Onset" neurons responded only at the stimulus onset regardless of the frequency, intensity, or laterality of the applied stimulus. Discharge patterns of "sustained" ICC neurons changed as a function of the stimulus parameters, but were sustained under the defined stimulus conditions. Similar findings have been reported in ICC studies in the cat (Rose et al., 1963) and kangaroo rat (Stillman, 1971b).

Distributions of "onset" and "sustained" subclasses are plotted as a function of represented locations along the basilar partition in Figure 16. While the majority (334/532, 63%) of ICC neurons responded to monaural or binaural best frequency tones with sustained discharges (Figure 16-F), 198 units discharged only at the stimulus onset (Figure 16-A). Note that each "response class" of ICC neurons contained units that could be categorized as "onset" or "sustained". The distributions (re the cochleotopic order of ICC) of onset and sustained responses to monaural neurons (Figure 16-B, C) and of binaural "intensity-sensitive"

neurons (Figure 16-E, J) are very similar, and relatively even over the cochlear distances represented along the abscissa. By contrast, most (86/108, 80%) interaural time-sensitive neurons and two-thirds (118/177, 67%) of the interaural intensity-difference cells fired with sustained discharge patterns to binaural best frequency tones (Figure 16-C, D, H, I).

2. Segregation of Neural Response Classes with the Central Nucleus

Within ICC, neurons in the same response class are usually found in close proximity to one another. Although exceptions are common, for neurons representing any given sector of the basilar membrane within ICC, response classes typically change as a function of location within the nucleus. This is particularly evident in horizontal microelectrode penetrations and provides strong physiological evidence that: 1) afferent inputs that drive neurons of given response classes are segregated within ICC; and 2) the segregation of ICC neurons of different response classes constitutes an additional (as yet unappreciated) feature of the physiological organization of the nucleus.

Figure 17 illustrates two representative cases taken from this series of experiments. In penetrations 1 and 3 of experiment 76-41 and penetrations 1 and 2 of experiment 76-46, neurons isolated represented a restricted sector of the basilar membrane, indicating the electrodes must have passed approximately parallel to the ICC laminae. In penetration 1 of 76-41, the response properties of 16 ICC neurons were categorized. During this penetration, 12 units in a row were isolated that were sensitive to interaural time differences (filled triangles, left-most graph). Each time-sensitive unit was driven by monaural contralateral and ipsilateral stimulation (c.f. Figure 15-C), and responded with a

sustained discharge pattern (c.f. Figure 16-C, H). Eight of these twelve time-sensitive neurons discharged maximally when the ipsilateral stimulus was leading; three units fired best when the contralateral stimulus was delivered first; and one unit responded maximally when no interaural time differences were introduced. It is remarkable that in this entire experimental series, only thirteen time-sensitive neurons (of a total of 108) were studied that discharged maximally when the ipsilateral stimulus was leading, and eight of those neurons were isolated in this penetration, within 1500 microns of one another.

A sequence of ten time-sensitive neurons was also encountered over approximately 1500 microns in penetration 1 of 76-46. All interaural time-sensitive units isolated in penetration 1 of 76-46 responded maximally to ipsilateral time delays, and eight of those ten units responded at the onset of the binaural stimulus. Again, note that only 22 time-sensitive neurons were isolated in this experimental series that discharged at the stimulus onset, and over one-third of them were encountered in this single penetration (see Figure 16-C, H).

Neurons studied in penetration 3 of 76-41 and penetration 2 of 76-46 derived their input from approximately the same sector of the basilar membrane (about 15-16 mm from the cochlear apex). There was no obvious segregation or grouping of response classes in the first seven neurons isolated in penetration 3 of 76-41. Neurons with binaural (filled symbols, Figure 17) and monaural (open circles) properties were intermingled, and one spontaneously active unit (asterisk) was unaffected by auditory stimuli. However, eight of the next nine neurons isolated successively in this penetration were sensitive to interaural intensity differences. All eight were driven by the contralateral ear and inhibited by the

ipsilateral ear (c.f. Figure 15-D), and five responded at the stimulus onset (c.f. Figure 16-D, I). In penetration 2 of 76-46, eleven neurons sensitive to interaural intensity differences were isolated consecutively; again, all were driven by the contralateral ear and inhibited by the ipsilateral ear. The first eight of these interaural intensity-sensitive neurons discharged throughout the duration of the stimulating tone, while the three most rostral studied binaural neurons responded only at the stimulus onset.

Penetration 2 of 76-41 did not parallel ICC laminae, and neurons examined in this microelectrode track represented cochlear loci covering approximately a 4 mm segment of the basilar partition. The first eight units studied were isolated within 500 microns of one another. All were sensitive to interaural intensity differences, and each was driven by the contralateral ear and inhibited by the ipsilateral ear (c.f. Figure 15-D). Seven of those eight interaural "intensity-difference" neurons fired throughout the duration of the stimulus (c.f. Figure 7-D, I). A variety of response functions and discharge patterns were seen in the neurons examined from that point on, and although no obvious order was present, most neurons were influenced by binaural interactions.

Most neurons isolated in the caudal aspect of ICC in three horizontal penetrations in experiment 76-55 were monaural (Figure 18). Penetration 1 covered approximately 3000 microns along the rostral-caudal dimension of ICC, and twelve of the eighteen ICC neurons isolated were monaural, and fired only at the onset of a contralateral stimulus (c.f. Figure 16-B, G). All other neurons studied in this microelectrode track also responded only at the stimulus onset, with the exception of one spontaneously active unit that was unaffected by auditory stimulation (asterisk).

In penetration 2, twelve of the first fourteen neurons isolated over the caudal 2800 microns of the ICC were only driven by contralateral monaural stimulation. Response patterns of these monaural units were evenly distributed between onset and sustained discharges, and were not obviously grouped. More rostrally, sixteen neurons were isolated, thirteen of which were binaural. The responses of ten of these binaural units was a function of interaural intensity differences, but their response patterns (onset or sustained) were not clustered in any discernible order. The three other binaural units (indicated by filled squares) were all spontaneously active, and inhibited by stimulation of either or both ears. These neurons were located within 350 microns of one another and appeared to be located in the rostroventral process (RVP) of the ICC (van Noort, 1969; FitzPatrick; 1975).

In penetration 3 of 76-55 (Figure 18), all neurons isolated in the more posterior aspect of ICC were also monaural and driven by the contralateral ear. Along this monaural sequence of the microelectrode track, four onset neurons were examined over approximately 700 microns, and the seven sustained monaural units were encountered over the next 700 microns (c.f. Figure 16-B, G). Response properties and discharge patterns of neurons isolated along the remainder of this penetration were mixed.

The response classes of ICC neurons also appeared to be grouped or clustered together along the lateral-to-medial dimension of the nucleus. Figure 19 summarizes data obtained from an experiment in which the electrode was introduced into the lateral surface of the IC in a horizontal plane. Here the represented cochlear place of studied neurons is plotted as a function of distance from the lateral surface. In each penetration the cochlear place represented by each isolated neuron gradually moved

toward the apex, and then reversed and continued to progress more basally. The general shape of each curve is compatible with the orientation of the ICC laminae in the cat as defined by Golgi studies (Rockel and Jones, 1973a), and if each curve in Figure 19 is inverted, their shape and orientation closely approximate the contours of ICC laminae (c.f. Figures 5 and 22, Rockel and Jones, 1973a).

Note that although in each penetration a similar sequence of neurons were isolated that represented nearly identical cochlear positions relative to the lateral-medial distance in the ICC, the classes of neurons studied in these two penetrations were quite different. In penetration 1, twelve of the first 15 neurons studied were sensitive to interaural time differences (filled triangles). Nearly all (11/12) of these delay-sensitive cells fired in a sustained pattern to best frequency tone pips (c.f. Figure 16-C, H). Ten of the next eleven neurons isolated were sensitive to interaural intensity differences (filled circles); their response patterns were evenly distributed between onset and sustained. In penetration 2, the response properties of neurons representing the most apical 8 mm of the cochlea were mixed. Firing rates of eight of the nine neurons isolated within the most medial 1700 microns of this penetration were functions of binaural intensity levels; none of these eight neurons were sensitive to interaural time or intensity differences. Seven of the eight responded only at the onset of the stimulating tone (c.f. Figure 16-E, J) and showed binaural facilitation; all were driven by monaural stimulation of either ear (c.f. Figure 15-E).

Figure 20 illustrates data obtained from an experiment in which the response functions and patterns of ICC neurons were studied using the more "conventional" dorsal-to-ventral microelectrode approach. The

response functions of the twelve units isolated over the first 2000 microns of penetration 1 were mixed. Six units studied over the next 800 microns were sensitive to interaural intensity differences (filled circles). Each discharged in a sustained pattern to the best frequency tone. Most (18/21) neurons isolated in this penetration responded with a sustained firing pattern, regardless of their other response characteristics (c.f. Figure 16). Penetration 2 of 76-33 passed across the most medial aspect of ICC, and most (16/23) neurons isolated along this electrode track were monaural. This was particularly evident in the deeper aspect of ICC where thirteen of the most ventral fourteen units isolated were monaural and driven by the contralateral ear with a sustained discharge pattern (c.f. Figure 16-B, G). The discharges of a large majority (21/23) of neurons studied in this penetration were sustained.

In summary, data obtained from experiments in which large numbers of isolated neurons were studied within each ICC demonstrate that neurons of different "classes" are typically segregated from one another within ICC and suggest that neurons of the same "class" in close proximity to one another derive their synaptic inputs from similar sources. These data indicate, then, that the segregation of neurons of different response "classes" within ICC constitutes another basic feature of the physiological organization of that nucleus that is superimposed upon the fundamental (cochleotopic) order of ICC.

3. Response Properties and Distribution of Central Nucleus Neurons Sensitive to Interaural Time Differences

In 19 other single unit experiments in cats, and attempt was made to determine if there is some form of spatial representation of the low

frequency sound field (i.e. some internal organization of neurons sensitive to behaviorally relevant differences in interaural time) within ICC. Rose et al. (1966) originally described neurons in the ICC of the cat that discharged maximally or minimally at a fixed interaural time difference. This specific interaural time difference (or "characteristic delay") did not change as a function of the intensity, frequency, or spectrum (with noise stimulation) of the applied acoustic waveform (Rose et al., 1966; Geisler et al., 1969). By virtue of their sensitivity to a fixed interaural time delay, Rose and colleagues suggested that neurons with characteristic delays could conceivably be used to encode the location of a low frequency sound source. These and other studies on time-sensitive neurons in the cat ICC often employed interaural time differences well outside of the physiological range for that animal (e.g. Benevento and Coleman, 1970; Altman, 1966).

Interaural time-sensitive ICC neurons must in some way encode sound location within the low frequency sound field. Yet, to date, no information exists to suggest how this encoding is accomplished spatially or how time-sensitive neurons with different characteristic delays are distributed within the ICC. In order to determine, then, if the location of a low frequency sound source is represented spatially within ICC, the maximum discharge rates that occurred <u>within the physiological range of interaural time delays</u> (i.e. $\pm$ 250 μsec for the cat; see Rose et al., 1966) was recorded from a large population of ICC neurons with characteristic delays, and the interaural time differences at those maximal discharge rates were related to the cochleotopic organization of that nucleus.

It should be noted that during this experimental series, a number of penetrations in ICC were made in which no time-sensitive neurons were

isolated. In these penetrations, the microelectrode isolated many neurons representing the apical cochlea (i.e. their best frequencies were below 2500 Hz), yet their responses were not functions of interaural time differences in the physiological range. Thus, characteristic delay neurons appear to be restricted to a region(s) of the low frequency laminae within ICC, and are not distributed throughout the dorsal (i.e. low frequency) aspect of the nucleus.

Responses of one ICC neuron representative of the interaural delay-sensitive population(s) are plotted as a function of interaural time differences in the physiological range in Figure 21. Neural responses (Figure 21-A) have been converted to a percentage of the maximum neural response observed within the behavioral range of interaural time delays at each intensity level (Figure 21-B). Neuron 74-48-9 is representative of the great majority of delay-sensitive ICC cells; it fired continuously to binaural stimulation, and to monaural stimulation. Response functions at each intensity level, when normalized to a percentage of the maximum discharge rate at that level, are remarkably similar. Maximum neural discharge rate at any given loudness level occurred with an interaural time difference of about 225-250 μsec, with the contralateral ear leading.

The characteristic delays of many isolated neurons (see below) were near the extreme limit or outside the behavioral range. In the following illustrations revealing discharge properties of these neurons as a function of interaural time differences, discharge rates are plotted as a percentage of the number of neural discharges that occurred at the maximum possible physiologic time delays (i.e. $\pm$ 250 μsec). It should be noted that all time-sensitive ICC neurons studied discharged strongly to binaural stimuli within the behavioral range of interaural time differences.

The responses of neurons with characteristic delays typifying the population(s) of ICC units examined are summarized in the next seven illustrations. Most, but not all, ICC neurons sensitive to interaural time differences have characteristic delays (Geisler et al., 1969; Stillman, 1971b). Thus a variety of stimuli were applied to the neurons described to document each characteristic delay. Regardless of the frequency, spectrum, or intensity of the applied binaural stimuli, these neurons responded best at a particular interaural time difference within the behavioral range. Figures 22 and 23 illustrate four examples in which the stimulus was located at a more apical (Figures 22-A; 23-A, B) or basal (Figure 22-B) position along the cochlea, relative to the cochlear place corresponding to the neuron's best frequency. Figures 24 and 25 demonstrate responses of four other ICC neurons to tonal (best frequency) and noise stimulation. Neural response functions of three of these illustrated units (Figures 24-A, B; 25-A) formed well-defined peaks in the physiologic range of time delays, and unit 74-94-10 (Figure 25-B) responded maximally when the contralateral stimulus was leading by 250 μsec. Stimuli were typically delivered over a 40-50 dB range in this experimental series, as illustrated by the responses of four ICC neurons to a wide range of stimulus intensities (Figures 26, 27). To simulate the behavioral situation, nearly all binaural stimuli were of equal loudness (see Wiener et al., 1965; Leiman and Hafter, 1972).

Thus the population of neurons reported here had well defined characteristic delays. Each responded vigorously to a particular interaural time delay (or restricted range of time differences) within the behavioral range of the cat. Response functions of each neuron (when normalized to the maximum discharge rate observed under each of a

variety of stimulus conditions) were remarkably uniform within the range of behaviorally relevant interaural time differences.

The interaural time delays at which maximum neural responses were observed covered the entire behavioral range of the cat and could be generated by sources covering much of the low frequency sound field. In Figure 28, response functions of six units which fired maximally to interaural time delays that would result from contralateral (Figure 28-A, B), ipsilateral (Figure 28-D, E), and midline (Figure 28-C, F) free sound field sources are illustrated. Many neurons in this studied population only responded over a restricted portion of the behaviorally relevant range of interaural time differences (e.g. Figure 28-A, B, F).

If it is assumed that the distance between the tympanic membranes of a hypothetical (and admittedly large) cat is 8.75 cm., then a sound directly off of one ear (i.e. 90° off of the medial sagittal plane) would take approximately 250 μsec to reach the opposite eardrum. The free sound field of this hypothetical cat can be divided into 22.5° sectors along the azimuth, and interaural time differences that would be generated by sound stimuli at each of these positions calculated. In this way, the distribution of characteristic delays derived from the studied population of ICC neurons can be comapared with interaural time delays that are "physiologic" for this "cat".*

Figure 29 plots the distribution of ICC neurons with characteristic delays as a function of interaural time differences (Figure 29-A) and of 22.5° sectors of this hypothetical free sound field (Figure 29-B).

---

* These results should not be generalized to other real cats. Obviously, a sound source at one location in the free sound field will generate different interaural time delays for different cats, depending on the distance between their tympanic membranes.

Neurons included in each bin fired maximally within the range of interaural time differences sound sources in that sector of the sound field could generate. If a neuron's response function had a broadly defined maximum, the midpoint of the curve was estimated and the neuron was placed in the appropriate bin.

The large majority (120/158) of ICC neurons with characteristic delays fire maximally when a sound source is located in the contralateral sound field (i.e. when the contralateral input is leading). Over 40% (67/158) of studied ICC neurons responded best to interaural time delays equal to or greater than a contralateral time lead of 225 μsec. Many neurons in this category had characteristic delays outside of the physiologic range of most cats, but all responded vigorously at the extreme edge of the behavioral range. Other ICC neurons that preferred contralateral time leads were evenly distributed across that half of the represented sound field. Only a small number of these ICC neurons responded best to ipsilateral time leads, and most fired maximally to ipsilateral time leads that could be generated by sound sources located near the midline (i.e. up to 22.5^{o} off of the midline in this half of the sound field).

Interaural time-sensitive neurons were found within ICC that represented the most apical 9 mm of the cochlea (i.e. with best frequencies below about 2600 Hz), and their distribtuion is plotted as a function of preferred interaural time difference in Figure 30. The preferred interaural time differences of neurons representing any given sector along that length of the basilar partition covered at least most of the physiologic range of delays that correspond to sound sources located in the central and contralateral portions of the sound field. For example, the large majority of neurons driven best by frequencies representing the

6-7 mm sector (from the apex) of the basilar membrane discharged maximally with the contralateral stimulus leading.

In this series of experiments, neurons isolated in close proximity to one another in dorsal to ventral microelectrode penetrations often fired maximally to similar interaural time delays within the physiological range. Although exceptions were seen, saltatory jumps from contralateral to ipsilateral time delays (and vice versa) were not common. Thus, neurons located in nearby positions within ICC would be driven at maximal or near-maximal rates by sound sources located in similar positions in the sound field. Figure 31 illustrates data obtained from four representative penetrations made in 2 experiments in this series. Each isolated neuron's represented cochlear place is plotted versus the interaural time delays at which maximum neural discharges occurred. In penetration 1 of experiment 74-90, the characteristic delays of seven of the eight neurons studied exceeded or were close to the maximum physiologic time difference. In penetration 2, characteristic delays of the first three neurons also approached or exceeded the physiological maximum, but the most ventral two units discharged best to 150 and 125 μsec contralateral time leads. The characteristic delays of nine neurons isolated in penetration 1 of 75-18 appeared to shift in an orderly sequence from maximum contralateral time leads to ipsilateral time leads. In penetration 2, the first two neurons responded best to contralateral time leads, and the next four characteristic delay neurons fired maximally when no interaural time differences were introduced.

In summary, the response properties of a large population of time-sensitive ICC neurons have been documented and related to the cochleotopic organization of that structure. These results have demonstrated that:

1) there is a region(s) in the dorsal aspect (i.e. low frequency) of ICC where no time-sensitive neurons are present; 2) in the region(s) where time-sensitive neurons predominate, delay-sensitive neurons respond vigorously and maximally to particular interaural time delays within the behavioral range; 3) the great majority of these neurons respond best to time differences that could represent the contralateral and middle sectors of the free sound field; and 4) as a general rule, characteristic delay neurons in close proximity to one another prefer (i.e. discharge maximally) similar interaural time differences, although exceptions are common.

Discussion

These described results have included data obtained from a large number of neuroanatomical and neurophysiological experiments conducted in the central nucleus of the inferior colliculus of the cat. The anatomical studies defined the origins and some of the spatial features of the organization of the brain stem afferents to ICC. The physiological studies have led to some understanding of how ICC neurons with different response properties are distributed within the nucleus. These different neural populations must ultimately receive their inputs from the brain stem nuclei defined in these anatomical studies. Thus, the two sets of data can be directly related. Some of the implications regarding the processing of auditory information inherent in this interrelationship shall be discussed.

A. Cochlear Nucleus Projections to the ICC; Distributions of Monaural Neurons in the ICC

These anatomical studies have demonstrated that neurons within all three subdivisions of the contralateral CN provide a large number of afferents to the ICC, and that the topography of those projections is directly related to the laminar (cochleotopic) organization of ICC. Furthermore, seven of the nine morphologically distinct "classes" of CN cells (Osen, 1969a,b) appear to project to the ICC. The overwhelming majority of CN neurons, irrespective of their morphological classification, are monaural. During these physiological studies in ICC, 179 monaural neurons were studied. 178 of those neurons responded only to contralateral stimulation. In addition, microelectrode penetrations

through ICC typically isolated groups or clusters of monaural neurons with similar discharge patterns. These clusters of monaural neurons tended to be localized in the central, posterior aspect of ICC, or in the far medial aspect of the nucleus.

Restricted HRP injections into the posterior aspect of ICC (e.g. illustrated case 76-10) resulted in labelling that was primarily concentrated in the contralateral CN. Jones (1976, 1977) has found similar HRP-labelling patterns in the brain stem after injection into ICC of the tree shrew. Following injections of a high concentration of H^3-proline in the guinea pig, Silverman et al. (1977) found autoradiographic grains concentrated in a vertical streak in the central aspect of the contralateral ICC. Thus, these neurophysiological and neuronanatomical results are strongly correlated. They indicate that monaural synaptic inputs largely predominate and are at least partially restricted to particular regions of the ICC, and that the contralateral CN is the major source of the brain stem synaptic input to those regions.

The HRP studies reported here indicate that the contralateral CN projections are situated in close proximity to one another and probably converge on a region(s) within ICC. However, at least a portion of the DCN projection remains segregated from other contralateral CN projections, although overlap probably occurs.

In her anterograde degeneration studies in the cat, Osen (1972) noted that lesions restricted to VCN never resulted in degeneration in the rostroventral process (RVP) of the contralateral ICC. However, lesions restricted to DCN caused preterminal degeneration in the same areas as the VCN lesions and in the RVP. Osen suggested that the VCN and DCN projections to the contralateral ICC overlapped, except for the

DCN input to the RVP. The anatomical results presented here appear to be compatible with Osen's, but since no HRP injections were made into RVP, they cannot provide additional insight regarding these differential CN projections to ICC. However, these physiological results have provided some preliminary evidence regarding the response properties of neurons situated within the RVP of ICC. Microelectrode penetrations in this region of ICC isolated spontaneously active neurons that were inhibited by stimulation of either ear. Similar electrophysiological results have been obtained in the RVP of the squirrel monkey (FitzPatrick, 1975). The anatomical and electrophysiological distinctions between the RVP and the rest of the ICC suggest that it constitutes a functional subdivision of the nucleus.

The HRP studies reported here and by Adams (1976) have defined the CN cell types that project to the ICC, and have clarified some questions raised by Osen's (1972) earlier study. Following destruction of the ICC, Osen observed no chromatolysis in the large and small spherical cells of the contralateral AVCN. She suggested that these neurons might send collaterals to SOC and ICC, and therefore little if any chromatolysis would take place following IC lesions. Our results have demonstrated that small neurons located within the large and small spherical cell fields project to ICC, but the spherical cells do not.

Although a small number of scattered HRP-labelled neurons were localized to the ipsilateral CN in a number of the experiments reported above, physiological recordings from over five-hundred and forty ICC neurons isolated only <u>one</u> monaural unit that was driven solely by the ipsilateral ear. These results suggest that neurons in the CN complex supply the sole synaptic inputs to very few individual neurons in the

ipsilateral ICC (which would be reflected by the presence of monaural cells driven by the ipsilateral ear). Inputs from these ipsilateral CN neurons may be principally involved in relatively minor (because of their low numbers), modulatory interactions within ICC.

B. NLL Projections to the ICC; Response Properties of ICC and NLL Neurons

These anatomical results have shown that the NLL provide a major share of the input to ICC. With one illustrated exception (76-4), VNLL alone contributed a significant proportion (averaging 30%) of projecting neurons to ICC injection loci. Following these injections, the DNLL was easily distinguished from the ventral nucleus by virtue of its bilateral projections and its highly distinctive cytoarchitecture. The HRP labelling patterns could not be as easily related to the represented cochlear place of the ICC injection site as in other major projecting nuclei. However, low best frequency ICC injections typically labelled neurons in the dorsal aspect of the DNLL, and following higher best frequency ICC injections, neurons were clustered in the ventral aspect of DNLL; these results are in agreement with the defined tonotopic organization of that structure (Aitkin et al., 1970).

Degeneration studies have indicated that DNLL is an important target for ascending axons from the SOC (Stotler, 1953; van Noort, 1969; Browner and Webster, 1975), which is primarily a binaural nuclear complex (Guinan et al., 1972b; Boudreau and Tsuchitani, 1968). DNLL receives only a small projection from the CN complex (Warr, 1966, 1969, 1972; Fernandez and Karapas, 1967; van Noort, 1969; Strominger and Strominger, 1971), which is primarily monaural. Microelectrode studies

have demonstrated that the great majority of neurons in the DNLL are binaural (Aitkin et al., 1970; Brugge et al., 1970); thus the physiological results are consistent with the anatomical data. The results presented above clearly demonstrate that DNLL provides major inputs to both ICC's. The large majority of these synaptic inputs to ICC neurons must be transmitting binaural information to the ICC neurons on which they synapse.

In the smallest volume HRP injection cases, no neurons were labelled in either DNLL. In three illustrated experimental cases (75-8, 76-28, 76-26), both DNLL's contained reaction product. Within the DNLL of another illustrated case (75-6), HRP-neurons were only found on the contralateral side. These anatomical results reveal that the two DNLL do not project throughout the entire ICC, and suggest that at least some of the projections from each DNLL remain segregated from one another within ICC, although overlap between the two DNLL projections might occur.

Aitkin et al. (1970) reported that nearly 90% of DNLL neurons were binaural, and responded with sustained discharge patterns to best frequency tones. Low best frequency DNLL neurons were commonly sensitive to interaural time differences. Neurons with higher best frequencies were typically sensitive to interaural intensity differences; these neurons were driven by the contralateral ear and inhibited by the ipsilateral ear. Two similar, distinct populations of neurons (i.e. sustained-firing, low best frequency neurons sensitive to interaural time differences, and sustained-firing high best frequency neurons sensitive to interaural intensity differences that were driven by the contralateral ear and inhibited by the ipsilateral ear) were observed within ICC in the present study (Figure 16-H, I). However, these HRP injections into ICC were not small or restricted enough to enable any

correllations to be made between the DNLL projections to ICC and the recording sites within ICC at which groups of neurons with these specific response properties were found.

During the entire experimental series surveying the distributions of neurons of different response "classes" in ICC, virtually no neurons sensitive to interaural time or intensity differences were observed with response properties corresponding to those of contralateral DNLL neurons. In contrast, neurons with response properties mimicking ipsilateral DNLL neurons were common (Figure 16-H, I). These neurophysiological results suggest, then, that the inputs from contralateral DNLL neurons responding to interaural time or intensity differences are combined with inputs from other brain stem sources on ICC neurons; thus the contralateral "DNLL-like" response are apparently masked in this neural processing. It is also conceivable that this population of contralateral DNLL neurons does not project to the ICC (but some other subpopulation does); however, HRP-labelling patterns make this possibility unlikely. Note that in one illustrated HRP-injection case (75-6), the contralateral DNLL (and not the ipsilateral DNLL) was labelled by HRP. This suggests that the contralateral DNLL projection might overlap some of the projections from the other brain stem nuclei that were labelled following this injection.

In contrast to DNLL, the VNLL is less homogenous in structure, connections, and electrophysiology. In these anatomical studies, two different labelling patterns were observed within VNLL following HRP injections into ICC. In the vertically oriented lateral streak, "bands" of HRP-labelled neurons were horizontally distributed across the lateral lemniscus. More ventrally, HRP-neurons were always clustered

within a well-defined ovoidal group of neurons.

Warr (1966, 1972) has described bands of degeneration with a similar orientation and distribution following VCN lesions. In addition, fibers that terminate within the lateral streak of VNLL leave the main fiber tracks of the lateral lemniscus at right angles (Warr, 1969, 1972; Fernandez and Karapas, 1967; van Noort, 1969); thus the orientation of these ascending inputs to the lateral streak of VNLL appear to parallel the orientation of the HRP-labelled neurons described in these studies.

van Noort (1969) has claimed that the SOC (primarily a binaural complex) supplies afferent fibers of the lateral streak of VNLL, but not the ventral cluster of neurons. This ventral group of neurons receives most of its projections from the contralateral PVCN and the ipsilateral AVCN (Warr, 1966, 1969; van Noort, 1969; Strominger and Strominger, 1971; Strominger, 1973). Aitkin and colleagues (1970) have demonstrated that most neurons in the lateral streak are binaural, and that most neurons in the ventral cluster are monaural. These physiological data are also consistent with the anatomical evidence. In view of the differences in structure, connections, and electrophysiology, it appears that these divisions of "VNLL" should be regarded as distinct auditory brain stem nuclei. van Noort (1969) and Guinan et al. (1972) have also suggested that VNLL might consist of two distinct nuclei or subnuclei. When these earlier anatomical and physiological data are assessed in relation to the projections defined in this study, it would appear that the ventral cluster of the VNLL primarily delivers monaural auditory information to ICC, while neurons in the more dorsal, lateral streak of VNLL primarily deliver binaural information.

The monaural neurons in VNLL are driven by the contralateral ear

(Aitkin et al., 1970; Guinan et al., 1972b), as are monaural neurons in the ICC. In a number of the HRP cases reported, HRP-labelled neurons were localized in both the three divisions of the contralateral CN and the ipsilateral VNLL. However, in one other experiment a large number of labelled neurons were found in VNLL, while only a very small number were localized to the contralateral DCN. Although far from conclusive, these results suggest that projections from VNLL are at least partially segregated from projections from the contralateral CN with ICC, but that they are in close proximity to one another and possibly overlap. Thus it is conceivable that monaural regions in ICC might derive their brain stem inputs from four major sources (i.e. the contralateral AVCN, PVCN, DCN, and the ipsilateral VNLL). As indicated above, this would be compatible with the neurophysiological data obtained in the ICC.

C. SOC Projections to the ICC; Response Properties of ICC and SOC Neurons

The anatomical data presented above have demonstrated that the ipsilateral MSO and LSO and contralateral LSO send major projections to ICC. LSO is a binaural nucleus; virtually all of its neurons are driven by the ipsilateral ear and inhibited by the contralateral ear (and hence are sensitive to interaural intensity differences), and discharge in sustained firing patterns to tonal stimulation (Tsuchitani and Boudreau, 1967; Boudreau and Tsuchitani, 1968). Neurons in the MSO are also predominantly binaural, are driven by monaural stimulation of either ear, and respond in sustained firing patterns to tonal stimulation (Guinan et al., 1972a,b; Goldberg and Brown, 1969). The discharge rates of many of these neurons is a sensitive function of interaural time

differences (Hall, 1965; Goldberg and Brown, 1969).

In the study reported here, a large population of ICC neurons with response characteristics similar to ipsilateral MSO and contralateral LSO neurons were isolated within ICC in close proximity to one another (e.g. penetrations 1 and 2 of 76-41, Figure 17). Neuroanatomical evidence demonstrates that the SOC does not project to the entire ICC and that at least some portion of the projections of each MSO and LSO remain segregated within ICC (e.g. see Figure 13-B, C, F), although overlap between any or all might occur. Furthermore, there does appear to be an area within ICC that receives input solely from the ipsilateral SOC.

As indicated above, many ICC neurons have response properties similar to ipsilateral MSO and contralateral LSO neurons. However, virtually no ICC neurons respond as if they were driven solely by the ipsilateral LSO (i.e. ipsilateral excitation, contralateral inhibition). The fact that few if any ICC neurons have "ipsilateral LSO-like" responses provides preliminary evidence that this ipsilateral LSO input plays some modulatory role in the processing of auditory information within ICC.

These neurophysiological results have also demonstrated that the overwhelming majority of ICC neurons sensitive to interaural time differences had best frequencies below 2 kHz, while most interaural intensity difference neurons had best frequencies greater than 2 kHz. Microelectrode studies in the SOC have shown that there is a disproportionately large representation of the higher frequencies in the LSO (Boudreau and Tsuchitani, 1968, 1970; Guinan et al., 1972b) and a greater

representation of the lower frequencies in the MSO (Guinan et al. 1972b; Goldberg and Brown, 1968). Anatomical evidence (Osen, 1969) has also indicated that the MSO might primarily represent more apical (low best frequency) sectors of the cochlea.

The neurophysiological data presented above have demonstrated that there appear to be two distinct populations, or "classes", of ICC neurons that predominantly represent different sectors of the cochlea. Time-sensitive ICC neurons predominantly represent the most apical 8 mm of the cochlea, while interaural intensity-sensitive neurons tend to have best frequencies representing more basal cochlear positions (Figure 14-B, C). This uneven distribution within ICC almost certainly reflects the disproportionate representation of high and low frequencies within the LSO and MSO.

Finally, it should be noted that in a single ICC injection case (76-26), HRP-labelled neurons were located bilaterally near the ventral aspect of the medial division of the facial motor nucleus. This group of neurons appeared to be located within the nucleus reticularis paragiganticocellularis lateralis of Taber (1961). Warr (1972) has described a projection to this nucleus from the contralateral VCN, and van Noort (1969) has also reported a projection from the contralateral AVCN to an area just medial to the VIIth nucleus which may correspond to this structure. Motorneurons innervating the muscles of the middle ear and pinnae are located in the medial division of the VIIth nucleus; motorneurons in the most medial aspect of the medial division innervate the stapedius muscle, and form a part of the neural system controlling the middle ear reflex (Borg, 1973b). Although preliminary, the evidence presented here suggests that some ICC neurons may also be involved in

the control of middle ear reflexes or of pinna movement.

D. The Encoding of Low Frequency Sound Location (Interaural Time Differences) in the MSO and ICC

Results from experiments in which a specific population of low best frequency time-sensitive ICC neurons were examined have provided evidence indicating that the neural representation of the low frequency sound field is spatially restricted within ICC. In addition, these data have demonstrated that the large majority of those neurons discharge maximally when the contralateral stimulus is leading, suggesting that this neural population encodes the location of sound sources in the contralateral free sound field.

A variety of physiological (e.g. Goldberg and Brown, 1969; Moushegian et al., 1975), comparative and anatomical (e.g. Stotler, 1953; Harrison, 1974; Masterton, 1974; Masterton et al., 1975), and ablation-behavioral studies (e.g. Masterton et al., 1967; Moore et al., 1974; Casseday and Neff, 1975) have indicated that the MSO is directly involved in sound localization and that the first order encoding of interaural time differences takes place at this nucleus. Models of the binaural interactions requisite for sound localization have also focused on the MSO (e.g. Jeffress, 1948; van Bergeijk, 1962).

Like other nuclei in the auditory system, the MSO is tonotopically organized. In the cat, low frequency units are localized in the dorsal-medial extreme of the MSO, and there is an orderly progression of best frequencies out to the ventro-lateral tip (Guinan et al., 1972b). Thus the frequency organization of the MSO is oriented in a dorso-medial to ventro-lateral direction when viewed in the frontal plane, and this

organization is preserved over the approximately 3.5 mm rostral-caudal extent of the nucleus. A place theory of sound localization (e.g. Jeffress, 1948) implies that different interaural time delays (i.e. sound sources in different locations in auditory space) would be represented by different foci of neural activity within the MSO. Therefore, the encoding of interaural time delays might somehow be superimposed upon or overlay the basic tonotopic organization of the nucleus. For example, different interaural time delays might be encoded by the "coincidence" of impinging inputs (derived from each ear) upon MSO neurons, and thus different interaural time delays (i.e. their neural representation) might be systematically organized along the rostrocaudal dimension of the MSO. Such an organization would, in effect, create a spatial representation of the low frequency sound field within the MSO and has been proposed by a number of authors (most recently for nucleus laminaris in the chicken, the avian homolog of the MSO; see Parks and Rubel, 1975).

Neuroanatomical evidence presented above indicates that the ipsilateral SOC projects to a restricted area(s) of ICC, and that within this region, MSO and LSO Projections are at least partially segregated from one another. Neurophysiological data have shown that low best frequency interaural time-sensitive neurons (i.e. neurons with response properties similar to MSO neurons) are clustered within ICC, and that the characteristic delays of ICC neurons in close proximity to one another appear to be organized in an orderly (but somewhat imprecise) pattern.

Recordings from a large population of ICC neurons whose firing rates were strong functions of interaural time delays in the physiological range have demonstrated that about 80% of these neurons discharge maximally to contralateral time leads; data derived from recordings in the ICC of the alert cat are consistent with these findings (Bock and

Webster, 1974b). The characteristic delays of these studied neurons included all interaural time differences that could be generated by sound sources located over the entire contralateral auditory field. The presence of additional units preferring contralateral delays (ipsilateral leads) indicates that a portion of the ipsilateral sound field (near the midline) might also be represented within the ICC. Ablation of the brachium of the IC disrupts localization in the contralateral sound field (Strominger and Osterreich, 1970), and thus behavioral evidence is compatible with these neurophysiological results.

The distribution and response functions of delay sensitive ICC neurons reported in these studies indicates that a low frequency sound source in a given location would selectively excite a population of neurons in the ICC; a sound source in another location would be represented by activity in another set of ICC neurons that might or might not overlap the original population, depending on the degree of separation of the sound sources. As previously emphasized by Stillman (1971a) and Moushegian et al. (1971), and as demonstrated above (e.g. Figure 28), the slopes of the response functions of characteristic-delay neurons are often steeply rising with contralateral time leads and the peaks are often broad. It is unlikely that these neurons could be responsible for the neural representation of one very small region in the free sound field, and thus a strict place theory(i.e. one neuron encoding one location) obviously cannot hold in the ICC.

Stillman (1971a,b) and Moushegian et al. (1971) have suggested that the characteristic delay, per se, of an ICC neurons does not encode the location of a low frequency sound source by "place", but that the discharge rate or discharge pattern of ICC neurons with characteristic

delays might be involved in that coding process. More recent evidence in the ICC of the alert cat (Bock and Webster, 1974) indicates that ICC neurons fire maximally to sound sources in a "preferred location" of the sound field (i.e. to "preferred" interaural time or intensity differences), and supports the concept of a "place" code for sound localization. Our data, both neuroanatomical and neurophysiological, indicates that both suppositions are probably correct in part. That is, the discharge rate of a population of neurons with characteristic delays and the locations of those neurons within ICC probably both account for the encoding of sound location. In addition, data reported here also demonstrate that delay-sensitive neurons are restricted to a certain region(s) within ICC.

It should be noted that most low best frequency DNLL neurons are sensitive to interaural time differences (Brugge et al., 1970), and thus these DNLL neurons are processing information derived from both ears. As demonstrated above, the DNLL provides a large number of afferent inputs to ICC. Rose et al.(1966) have provided physiological evidence suggesting that the activity of phase-locked time-sensitive ICC neurons probably represents binaural interactions that take place at the level of the ICC neuron itself, and that the activity of ICC neurons that are sensitive to interaural time differences but are not phase-locked to the stimulating tones probably reflect binaural processing that occurs at a lower level (Rose et al., 1966), presumably at the MSO or DNLL. The techniques utilized in these physiological experiments cannot distinguish between these populations of neurons. However, neuroanatomical evidence does indicate that at least a portion of the projections from the ipsilateral DNLL and MSO remain segregated within ICC.

The physiological observation that the precise temporal processing of information derived from each ear can take place at the level of the ICC neuron is interesting in view of our anatomical finding that spherical cells in the AVCN do not project to ICC. Spherical cells are strickingly phase-locked to the stimulus waveform (Lavine, 1971), and presumably these time-sensitive, phase-locked ICC neurons derive their well synchronized inputs from other monaural sources in the CN (possibly the globular cells).

E. Role of the ICC in the Processing of Auditory Information

These results have provided neuroanatomical and neurophysiological evidence for the segregation of some brain stem inputs to the central nucleus of the IC. The brain stem nuclei that provide these afferent inputs to ICC neurons often display unique response properties, and presumably they encode different aspects of auditory sensation. A particular aspect of auditory sensation (i.e. low frequency sound localization) appears to be encoded within a restricted region(s) of ICC. Monaural ICC neurons also appear to be predominant in a particular region(s) of ICC. Thus, some aspects of auditory sensation appear to be encoded or represented separately within the nucleus.

The response characteristics of auditory neurons can often be related to the auditory sensation(s) they might encode. For example, neurons excited by one ear and inhibited by the other ear must be primarily involved in the coding of interaural intensity differences and not interaural intensity levels (e.g. Boudreau and Tsuchitani, 1968; Goldberg and Brown, 1968, 1969); the "class" of interaural intensity-difference neurons cited above corresponds to this population. In

contrast, neurons that are driven by each ear and show a facilitation or summation of the monaural response can encode a wide range of binaural intensity levels, but not intensity differences (e.g. Goldberg and Brown, 1968, 1969); the large majority of neurons in the described "intensity sensitive class" respond in this manner. Finally, low best frequency time-sensitive neurons are probably involved in low frequency sound localization (e.g. Rose et al., 1966); most neurons in the described "interaural time-sensitive class" correspond to this population.

The physiological data presented above has demonstrated that neurons of each of these "classes" are clustered within ICC, and has thus provided direct physiological evidence that different aspects of auditory sensation might be represented separately within ICC. A body of psychophysical data also suggest that at least certain aspects of auditory sensation must be encoded separately within the auditory nervous system. For example, two neural systems must be involved in the time-intensity trading ratios often studied in lateralization and localization experiments (Whitworth and Jeffress, 1961; Hafter and Jeffress, 1968; Hafter and Carrier, 1972). These psychophysical studies may or may not be directly related to the data presented above, but they do support the concept of the separate representation of at least some aspects of sensation within the auditory system.

Anatomical evidence by others indicates that the ICC is not a homogeneous structure. For example, the unlaminated dorsal-medial division is mostly populated by multipolar cells (e.g. Rockel and Jones, 1973a; FitzPatrick, 1975; Ryugo and Killackey, 1977), and receives most of its afferents from the auditory cortex (e.g. Rasmussen, 1964; Rockel and Jones, 1973a,c). A ventro-lateral collection of large neurons

(Rockel and Jones, 1973a; see Figures 2 and 3) can be distinguished from the rest of ICC on cytoarchitectural grounds, and the distinct brain stem inputs to the rostroventral process (Osen, 1972) can serve to distinguish that region from the rest of ICC. These anatomical differences suggest that different parts or regions of ICC might subserve different auditory functions.

On the basis of his Golgi studies in young cats, Morest (1966; personal communication) has distinguished three major subdivisions (pars lateralis, medialis, and centralis) in his conceptualization of the central nucleus, each with a distinctive neuropil. Jones (1977) has subdivided the central nucleus of the tree shrew on the basis of cytoarchitectural evidence, and recent studies on the endogenous peroxidatic activity of ICC neurons (Wong-Riley and Merzenich, unpublished observations) also suggests that the ICC might consist of a number of subdivision.

One of the criteria Morest (1966) used to subdivide the central nucleus was the diameter of the lemniscal afferents that innervate each "subdivision". For example, his pars lateralis receives 3-4 μ fibers from the lateral lemniscus and pars medialis receives 1-2 μ fibers from the medial lateral lemniscus. (It is interesting to note that distinct fiber bundles in the trapezoid body representing projections from different CN cell groups can also be classified by the diameter of axons and by the characteristic responses of the fibers in each bundle (Brownell, 1975)).

In these described results, groups of neurons with different response properties and discharge patterns were isolated in horizontal microelectrode penetration crossing the lateral-to-medial dimension of ICC (e.g. Figure 19). These microelectrode penetrations traversed the

the three ICC subdivisions distinguished by Morest (1966), and conceivably the changes in response properties and discharge patterns observed might be related to the location of these isolated neurons within these subdivisions. In addition, Morest (194a) has reported that lesions of the lateral lemniscus result in alternating streaks of course and fine fiber degeneration within the central nucleus (in the three subdivisions he described) and has suggested that these streaks might represent crossed and uncrossed lemniscal projections to the central nucleus. The anatomical and physiological data reported here might also be related to this earlier finding.

Thus it appears that the large laminated division of the ICC of the cat cannot be regarded as a uniform, homogenous structure on anatomical or physiological grounds. Evidence presented here and in these other cited studies indicates that the ICC must be considered as consisting of a number of subdivisions. These subdivisions must be integrated within the laminar, cochleotopic organization of the ICC, and thus constitute another basic feature of the anatomical and physiological organization of the nucleus.

Finally, the described neuroanatomical and neurophysiological evidence suggest that auditory information is processed in at least two distinct ways within the ICC. The segregation of brain stem afferents and of response properties within ICC (each presumably carrying different aspects of auditory sensation) indicates that certain aspects of auditory perception must be processed in parallel in ICC. This parellel processing of information may be related to the proposed subdivisions of the central nucleus (Morest, 1966) and is probably directly related to the segregation of brain stem afferents described here. Thus, this study

has provided important evidence regarding the spatial organization of higher auditory centers.

Other neuroanatomical and neurophysiological data reported here indicate that some integration of the auditory information carried by certain brain stem afferents must take place within ICC. This is particularly evident in regard to the afferent inputs supplied to ICC by the ipsilateral LSO and contralateral DNLL. Since LSO and DNLL neurons project to both ICC's and virtually no ICC neurons respond with ipsilateral "LSO-like" or contralateral "DNLL-like" response properties, the auditory information supplied by the ipsilateral LSO and contralateral DNLL projections must be involved in some integrative process. ICC neurons can receive both excitatory and inhibitory inputs that are derived from each ear (e.g. Nelson and Erulkar, 1963; Hind et al., 1963); the studies reported here indicate that the ipsilateral LSO and contralateral DNLL (and possibly the ipsilateral CN) provide some of the inputs that must be integrated at the level of the ICC.

In summary, these studies have provided some neuroanatomical and quantitative neurophysiological data relevant to the definition of the functional organization of the ICC. Results from these experimetns have demonstrated: 1) the origins of the auditory brain stem afferents to ICC and the topography of these projections in relation to the cochleotopic organization of ICC; 2) the segregation of at least some of those brain stem projections to ICC; 3) the segregation of at least some of those brain stem projections to ICC: 3) the segregation of response properties of ICC neurons; 4) that the response properties of ICC neurons in close proximity to one another are often similar to the

response properties of neurons within one of the brain stem nuclei that project to ICC; 5) that a large population of ICC neurons sensitive to interaural time differences in the behavioral range appears to constitute a neural representation of the contralateral (and perhaps part of the ipsilateral) sound field; 6) that the ICC appears to encode some aspects of auditory sensation (e.g. sound localization) separately within ICC; 7) that the ICC processes some auditory information in parallel and other information by integration; and 8) that the laminated division of the ICC probably consists of anatomically, physiologically, and functionally distinct subdivisions.

LITERATURE CITED

Adams, J.C. 1975. Ascending and descending projections to the inferior colliculus. Society for Neuroscience Abstracts I: 37.

Adams, J.C. 1976. Types of cells in the cochlear nucleus that project to the inferior colliculus in the cat. Proceedings of American Anatomical Society p. 340.

Adams, J.C. and D.C. Teas. 1973. Organization of the posterior colliculus. J. Acoust. Soc. Amer. 53: 361.

Adams, J.C. and W.B. Warr. 1976. Origins of axons in the cat's acoustic striae determined by injection of horseradish peroxidase into severed tracts. J. Comp. Neurol. 170: 107-122.

Aitkin, L.M., D.J. Anderson and J.F. Brugge. 1970. Tonotopic organization and discharge characteristics of single neurons in nuclei of the lateral lemniscus of the cat. J. Neurophysiol. 33: 421-440.

Aitkin, L.M., S. Fryman, D.W. Blake and W.R. Webster. 1972. Responses of neurons in the rabbit inferior colliculus. I. Frequency-specificity and topographic arrangement. Brain Res. 47: 77-90.

Aitkin, L.M., W.R. Webster, J.L. Veale and D.C. Crosby. 1975. Inferior colliculus. I. Comparison of response properties of neurons in central, pericentral and external nuclei of adult cat. J. Neurophysiol. 38: 1196-1207.

Altman, Y.A. 1966. Reaction of the neurons of the Corpus Quadrigeminum of the cat with change in the time intervals between binaurally

presented signals. Biofizika 11: 488-497.

Barnes, W.T., H.W. Magoun and S.W. Ranson. 1943. The ascending auditory pathway in the brain stem of the monkey. J. Comp. Neurol. 79: 129-152.

Benevento, L.A. and P.D. Coleman. 1970. Responses of single cells in cat inferior colliculus to binaural click stimuli combinations of intensity levels, time differences and intensity differences. Brain Res. 17: 387-405.

Bock, G.R. and W.R. Webster. 1974a. Spontaneous activity of single units in the inferior colliculus of anesthetized and unanesthetized cats. Brain Res. 76: 150-154.

Bock, G.R. and W.R. Webster. 1974b. Coding of spatial location by single units in the inferior colliculus of the alert cat. Exp. Brain Res. 21: 387-398.

Bock, G.R., W.R. Webster and L.M. Aitkin. 1972. Discharge patterns of single units in inferior colliculus of the alert cat. J. Neurophysiol. 35: 265-277.

Borg, E. 1973a. A neuroanatomical study of the brainstem auditory system of the rabbit. Part 1. Ascending Connections. Acta Morph. Neerl. - Scand. 11: 31-48.

Borg, E. 1973b. On the neuronal organization of the acoustic middle ear reflex. A physiological and anatomical study. Brain Res. 49: 101-123.

Boudreau, J.C. and C. Tsuchitani. 1968. Binaural interaction in the cat superior olive S segment. J. Neurophysiol. 31: 442-454.

Boudreau, J.C. and C. Tsuchitani. 1970. Cat superior olive S-segment cell discharge to tonal stimulation. In: Contributions to Sensory Physiology, edited by W.D. Neff. New York: Academic, Vol. 4: 143-213.

Brownell, W.E. 1975. Organization of the cat trapezoid body and the discharge characteristics of its fibers. Brain Res. 94: 413-433.

Browner, R.H. and D.B. Webster. 1975. Projections of the trapezoid body and the superior olive complex of the kangaroo rat (Dipodymys merriami). Brain Behav. Evol. 11: 322-354.

Brugge, J.F., D.J. Anderson and L.M. Aitkin. 1970. Responses of neurons in the dorsal nucleus of the lateral lemniscus of the cat to binaural tonal stimulation. J. Neurophysiol. 33: 441-458.

Brunso-Bechtold, J.K. and G.C. Thompson. 1976. Auditory hind brain projections to the inferior colliculus as demonstrated by horseradish peroxidase in the cat. Proceedings of the American Anatomical Society, p. 365.

Bunt, A.H., R.H. Haschke, R.D. Lund and D.F. Calkins. 1976. Factors affecting retrograde axonal transport of horseradish peroxidase in the visual system. Brain Res. 102: 152-155.

Casseday, J.H. and W.D. Neff. 1975. Auditory localization: Role of auditory pathways in brain stem of the cat. J. Neurophysiol. 38: 842-858.

Clopton, B.M. and J.A. Winfield. 1973. Tonotopic organization

in the inferior colliculus of the rat. Brain Res. 56: 355-358.

Davies, P.W. 1956. Chamber for microelectrode studies in the cerebral cortex. Science 124: 179.

de Olmos, J. 1977. An improved HRP tract tracing technique. In press.

Erulkar, S.D. 1959. The responses of single units of the inferior colliculus of the cat to acoustic stimulation. Proceed. Roy. Soc. B. 150: 336-355.

Fernandez, C. and F. Karapas. 1976. The course and termination of the striae of Monakow and Held in the cat. J. Comp. Neurol. 131: 371-386.

Fitzpatrick, K.A. 1975. Cellular architecture and topographic organization of the inferior colliculus of the squirrel monkey. J. Comp. Neurol. 164: 185-208.

Fullerton, B.C. 1975. The organization of the inferior colliculus of the rhesus monkey. Anat. Rec. 181: 359.

Geisler, C.D., W.S. Rhode and D.W. Hazelton. 1969. Responses of inferior colliculus neurons in the cat to binaural acoustic stimuli having wide-band spectra. J. Neurophysiol. 32: 960-974.

Geniec, P. and D.K. Morest. 1971. The neuronal architecture of the human posterior colliculus. Acta Oto-Laryngologica, Suppl. 295.

Goldberg, J.M. and P.B. Brown. 1968. Functional organization of the dog superior olivary complex: An anatomical and electrophysiological study. J. Neurophysiol. 31: 639-656.

Goldberg, J.M. and P.B. Brown. 1969. Response of binaural neurons of dog superior olivary complex to dichotic tonal stimuli: Some physiological mechanisms of sound localization. J. Neurophysiol. 32: 613-636.

Goldberg, J.M. and R.Y. Moore. 1967. Ascending projections of the lateral lemniscus in the cat and monkey. J. Comp. Neurol. 129: 143-156.

Graham, R.C. and M.J. Karnovsky. 1966. The early stages of absorption of injected horseradish peroxidase in the proximal tubules of the mouse kidney: Ultrastructural cytochemistry by a new technique. J. Histochem. Cytochem. 14: 291-302.

Greenwood, D.D. 1974. Critical bandwidth in man and in some other species in relation to the travelling wave envelope. In: Sensation and Measurement, edited by H.R. Moskowitz, B. Scharf and J.C. Stevens. Dordrecht: Reidel. p. 231-239.

Greenwood, D.D., M.M. Merzenich and G.L. Roth. 1976. Some preliminary observations on the interrelations between two-tone suppression and combination-tone driving in the anteroventral cochlear nucleus of the cat. J. Acoust. Soc. Amer. 59: 607-633.

Guinan, J.J. Jr., S.S. Guinan and B.E. Norris. 1972a. Single auditory units in the superior olivary complex. I: Responses to sounds and classifications based on physiological properties. Intern. J. Neuroscience 4: 101-120.

Guinan, J.J. Jr., B.E. Norris and S.S. Guinan. 1972b. Single auditory units in the superior olivary complex. II: Locations

of unit categories and tonotopic organization. Intern. J. Neuroscience 4: 147-166.

Hafter, E.R. and S.C. Carrier. 1972. Binaural interaction in low-frequency stimuli: The inability to trade time and intensity completely. J. Acoust. Soc. Amer. 51: 1852-1862.

Hafter, E.R. and L.A. Jeffress. 1968. Two-image lateralization of tones and clicks. J. Acoust. Soc. Amer. 44: 563-569.

Hall, J.L. 1965. Binaural interaction in the accessory superior-olivary nucleus of the cat. J. Acoust. Soc. Amer. 37: 814-823.

Halperin, J.J. and J.H. LaVail. 1975. A study of the dynamics of retrograde transport and accumulation of horseradish peroxidase neurons. Brain Res. 100: 253-269.

Harrison, J.M. 1974. The auditory system of the medulla and localization. Fed. Proceed. 33: 1901-1903.

Hind, J.E., J.M. Goldberg, D.D. Greenwood and J.E. Rose. 1963. Some discharge characteristics of single neurons in the inferior colliculus of the cat. II. Timing of the discharges and observations on binaural stimulation. J. Neurophysiol. 26: 321-341.

Jeffress, L.A. 1948. A place theory of sound localization. J. Comp. and Physiol. Psych. 41: 35-39.

Jeffress, L.A. and D. McFadden. 1971. Differences of interaural phase and level in detection and lateralization. J. Acoust. Soc. Amer. 49: 1169-1179.

Jones, D.R. 1976. Ascending auditory pathways to inferior colliculus in the tree shrew. Society for Neuroscience Abstracts II: 20.

Jones, D.R. 1977. Personal communication.

Jones, E.G. and R.Y. Leavitt. 1974. Retrograde axonal transport and the demonstration of non-specific projections to the cerebral cortex and striatum from thalamic intralaminar nuclei in the rat, cat and monkey. J. Comp. Neurol. 154: 349-378.

Katsuki, Y., T. Sumi, H. Ochiyama and T. Watanabe. 1958. Electric responses of auditory neurons in cat to sound stimulation. J. Neurophysiol. 21: 569-588.

Kim, C.C. and P.L. Strick. 1976. Critical factors involved in the demonstration of horseradish peroxidase retrograde transport. Brain Res. 103: 356-361.

Kristensson, K. and Y. Olsson. 1971. Uptake and retrograde axonal transport of peroxidase in hypoglossal neurones. Acta Neuropath. 19: 1-9.

LaVail, J.H. and M.M. LaVail. 1972. Retrograde axonal transport in the central nervous system. Science 176: 1416-1417.

LaVail, J.H., K.R. Winston and A. Tish. 1973. A method based on retrograde axonal transport of protein for identification of cell bodies of origin of axons terminating within the CNS. Brain Res. 58: 470-477.

Lavine, R.A. 1971. Phase-locking in response of single neurons in cochlear nuclear complex of the cat to low-frequency tonal stimuli. J. Neurophysiol. 34: 467-483.

Leiman, A.L. and E.R. Hafter. 1972. Responses of inferior colliculus neurons to free field auditory stimuli. Exper. Neurol. 35: 431-449.

Lorente de No, R. 1933. Anatomy of the eighth nerve. The central projections of the nerve endings of the internal ear. Laryngoscope (St. Louis) 43: 1-38.

Ludwig, H. 1970. An integrated circuit switch for auditory research. Med. biol. Engng. 8: 319-322.

Masterton, R.B. 1974. Adaptation for sound localization in the ear and brainstem of mammals. Fed. Proceed. 33: 1904-1910.

Masterton, R.B., J.A. Jane and I.T. Diamond. 1967. Role of brain stem auditory structures in sound localization. I. Trapezoid body, superior olive, and lateral lemniscus. J. Neurophysiol. 30: 341-359.

Masterton, B., G.C. Thompson, J.K. Bechtold and M.J. RoBards. 1975. Neuroanatomical basis of binaural phase-difference analysis for sound localization: A comparative study. J. Comp. Physiol. Psych. 89: 379-386.

Merzenich, M.M. and M.D. Reid. 1974. Representation of the cochlea within the inferior colliculus of the cat. Brain Res. 77: 397-415.

Moore, C.N., J.H. Casseday and W.D. Neff. 1974. Sound localization: The role of the commissural pathways of the auditory system of the cat. Brain Res. 82: 13-26.

Morest, D.K. 1964a. The laminar structure of the inferior colliculus of the cat. Anat Rec. 148: 314.

Morest, D.K. 1964b. The probable significance of synaptic and dendritic patterns of the thalamic and midbrain auditory system. Anat. Rec. 148: 390-391.

Morest, D.K. 1966. The non-critical neuronal architecture of the inferior colliculus of the cat. Anat. Rec. 154: 477.

Morest, D.K. 1977. Personal communication.

Moushegian, G., R.D. Stillman and A.L. Rupert. 1971. Characteristic delays in superior olive and inferior colliculus. In: Physiology of the Auditory System, edited by M.B. Sachs, Baltimore: Nat. Ed. Consult., Inc. p. 245-263.

Moushegian, G., A.L. Rupert and J.S. Gidda. 1975. Functional characteristics of superior olivary neurons to binaural stimuli. J. Neurophysiol. 38: 1037-1048.

Nauta, H.J.W., M.B. Pritz and R.J. Lasek. 1974. Afferents to the rat caudoputamen studied with horseradish peroxidase. An evaluation of a retrograde neuroanatomical research method. Brain Res. 67: 219-238.

Nelson, P.G. and S.D. Erulkar. 1963. Synaptic mechanisms of excitation and inhibition in the central auditory pathway. J. Neurophysiol. 26: 908-923.

Oliver, D. 1977. Personal communication.

Osen, K.K. 1969a. The intrinsic organization of the cochlear nuclei in the cat. Acta-Otolaryngologica 67: 352-359.

Osen, K.K. 1969b. Cytoarchitecture of the cochlear nuclei in the cat. J. Comp. Neurol. 136: 453-484.

Osen, K.K. 1972. Projection of the cochlear nuclei on the inferior colliculus in the cat. J. Comp. Neurol. 144: 355-372.

Papez, J.W. 1929. Central acoustic tract in cat and man. Anat. Rec. 42: 60.

Papez, J.W. 1930. Superior olivary nucleus. Its fiber connections. Arch. Neurol. and Psychiat. 24: 1-20.

Parks, T.N. and E.W. Rubel. 1975. Organization and development of brain stem auditory nuclei of the chicken: organization of projections from N.magnocellularis to N.laminaris. J. Comp. Neurol. 164: 435-448.

Ralston, H.J. III and P.V. Sharp. 1973. The identification of thalamocortical relay cells in the adult cat by means of retrograde axonal transport or horseradish peroxidase. Brain Res. 62: 273-278.

Ramon y Cajal, S. 1911. Histologie du systeme nerveux de l'homme et des vertebres. Consejo Superior de Investigaciones Cientificas Instituto Ramen y Cajal, Madrid, 1955.

Rasmussen, G.L. 1946. The olivary peduncle and other fiber projections of the superior olivary complex. J. Comp. Neurol. 84-85: 141-219.

Rasmussen, G.L. 1964. Anatomic relationships of the ascending and descending auditory systems. In: Neurological Aspects of Auditory and Vestibular Disorders, edited by W.S. Fields and B.R. Alford, Springfield: Thomas, p. 1-19.

Rockel, A.J. and E.G. Jones. 1973a. The neuronal organization of the inferior colliculus of the adult cat. I. The central nucleus. J. Comp. Neurol. 147: 11-60.

Rockel, A.J. and E.G. Jones. 1973b. The neuronal organization of the inferior colliculus of the adult cat. II. The pericentral nucleus. J. Comp. Neurol. 149: 301-334.

Rockel, A.J. and E.G. Jones. 1973c. Observations on the fine structure of the central nucleus of the inferior colliculus of the cat. J. Comp. Neurol. 147: 61-92.

Rose, J.E., R. Galambos and J.R. Hughes. 1959. Microelectrode studies of the cochlear nuclei of the cat. Bull. Johns Hopk. Hosp. 104: 211-251.

Rose, J.E., D.O. Greenwood, J.M. Goldberg and J.E. Hind. 1963. Some discharge characteristics of single neurons in the inferior colliculus of the cat. I. Tonotopic organization, relation of spike-counts to tone intensity, and firing patterns of single elements. J. Neurophysiol. 26: 294-320.

Rose, J.E., N.B. Gross, C.D. Geisler and J.E. Hind. 1966. Some neural mechanisms in the inferior colliculus of the cat which may be relevant to localization of a sound source. J. Neurophysiol. 29: 288-314.

Ryugo, D.K. and H.P. Killackey. 1977. The central auditory system of the rat. I. The inferior colliculus. In press.

Schuknecht, H.F. 1960. Neuroanatomical correlates of auditory sensitivity and pitch discrimination in the cat. In: Neural Mechanisms of the Auditory and Vestibular Systems, edited by G.L. Rasmussen and W.F. Windle, Springfield: Thomas, p. 76-90.

Silverman, M.S., A.E. Hendrickson and B.M. Clopton. 1977. Mapping of the tonotopic organization of the auditory system by uptake of radioactive metabolites. Abstract submitted for publication.

Starr. A. and M. Don. 1972. Responses of squirrel monkey (Samiri sciureus) Medial Geniculate Units to binaural click stimuli. J. Neurophysiol. 35: 501-517.

Stevens, S.S. and E.B. Newman. 1936. The localization of actual sources of sound. Amer. J. Psychol. 48: 297-306.

Stillman, R.D. 1971a. Characteristic delay neurons in the inferior colliculus of the kangaroo rat. Exp. Neurol. 32: 404-412.

Stillman, R.D. 1971b. Pattern responses of low-frequency inferior colliculus neurons. Exp. Neurol. 33: 432-440.

Stöckel, K., V. Paravicini and H. Thoenen. 1974. Specificity of the retrograde axonal transport of nerve growth factor. Brain Res. 76: 413-421.

Stotler, W.A. 1949. The projection of the cochlear nerve on the acoustic relay nuclei of the medulla. Anat. Rec. 103: 561.

Stotler, W.A. 1953. An experimental study of the cells and connections of the superior olivary complex of the cat. J. Comp. Neurol. 98: 401-432.

Strominger, N.L. 1969. Projections of the dorsal cochlear nucleus in the rhesus monkey. Anat. Rec. 163: 271.

Strominger, N.L. 1973. The origins, course, and distribution of the dorsal and intermediate acoustic striae in the rhesus monkey. J. Comp. Neurol. 147: 209-234.

Strominger, N.L., L.R. Nelson and W.J. Dougherty. 1977. Second order auditory pathways in the chimpanzee. J. Comp. Neurol. 172: 349-366.

Strominger, N.L. and R.E. Oesterreich. 1970. Localization of sound after section of the brachium of the inferior colliculus. J. Comp. Neurol. 138: 1-18.

Strominger, N.L. and A.I. Strominger. 1971 Ascending brain stem projections of the anteroventral cochlear nucleus in the rhesus monkey. J. Comp. Neurol. 143: 217-241.

Taber, E. 1961. The cytoarchitecture of the brain stem of the cat. I. Brain stem nuclei of the cat. J. Comp. Neurol. 116: 27-69.

Thurlow, W.R., N.B. Gross, E.H. Kemp and K. Lowy. 1951. Microelectrode studies of neural auditory activity of cat. I. Inferior colliculus. J. Neurophysiol. 14: 289-304.

Tsuchitani, C. and J.C. Boudreau. 1967. Encoding of stimulus frequency and intensity by cat superior olive S-segment cells. J. Acoust. Soc. Amer. 42: 794-805.

van Bergeijk, W.A. 1962. Variation on a theme of BéKésy: A model of binaural interaction. J. Acoust. Soc. Amer. 34: 1431-1437.

van Noort, J. 1969. The structure and connections of the inferior colliculus. van Gorcum, Assen.

Warr, W.B. 1966. Fiber degeneration following lesions in the anteroventral cochlear nucleus of the cat. Exp. Neurol. 14: 453-474.

Warr, W.B. 1969. Fiber degeneration following lesions in the posteroventral cochlear nucleus of the cat. Exp. Neurol. 23: 140-155.

Warr, W.B. 1972. Fiber degeneration following lesions in the multipolar and globular cell areas in the ventral cochlear nucleus of the cat. Brain Res. 40: 247-270.

Webster, D.B., R.F. Ackerman and G.C. Longa. 1968. Central auditory system of the kangaroo rat, Dipodomys merriami. J. Comp. Neurol. 133:477-494.

Webster, W.R. and J.L. Veale. 1970. Binaural response patterns in the inferior colliculus. Proceed. Austral. Physiol. Pharmacol. Soc. 1: 60-61.

Whitworth,R.H. and L.A. Jeffress. 1961. Time vs. intensity in the localization of tones. J. Acoust. Soc. Amer. 33: 925-929.

Wiener, F.M., R.R. Pfeiffer and A.S.N. Backus. 1965. On the sound pressure transformation by the head and auditory meatus of the cat. Acta Oto-laryng. 61: 255-269.

Wong-Riley, M.T.T. 1974. Demonstration of geniculocortical and callosal projection neurons in the squirrel monkey by means of retrograde axonal transport of horseradish peroxidase. Brain Res. 79: 267-272.

Wong-Riley, M.T.T. 1976. Endogenous peroxidatic activity in brain stem neurons as demonstrated by their staining with diaminobenzidine in normal squirrel monkeys. Brain Res. 108: 257-277.

Woollard, H.H. and J.A. Harpman. 1939-1940. The connexions of the inferior colliculus and of the dorsal nucleus of the lateral lemniscus. J. Anat., Lond. 74: 441-458.

Zook, J.M. and J.H. Casseday. 1976. Projections to the inferior colliculus in the echolocating bat. Society for Neuroscience Abstracts II: 29.

Figure 1. Schematic representation of the three major divisions of the inferior colliculus as viewed in the frontal (A), sagittal (B), and horizontal (C) planes. Section A-1 is the most rostral in the frontal plane, B-1 is the more medial in the sagittal plane. Abbreviations shown here: CN - Central Nucleus; EN - External Nucleus; Pc - Pericentral Nucleus (solid diagonal lines); SC - Superior Colliculus; PSC - Posterior Superior Colliculus; LL - Lateral Lemniscus; NLL - Dorsal Nucleus of the Lateral Lemniscus; CfN - Cuneiform Nucleus; CG - Central Grey Matter; and BC - Brachium Conjunctivum. Abbreviations used in the text and in the following illustrations: ICC - Central Nucleus; ICP - Pericentral Nucleus; and ICX - External Nucleus. The dotted lines indicate the approximate orientation of the laminae within the ventro-lateral division of the central nucleus. The approximate border of the unlaminated, dorsal-medial division of the central nucleus is indicated by crosses. Reproduced from Rockel and Jones (1973b).

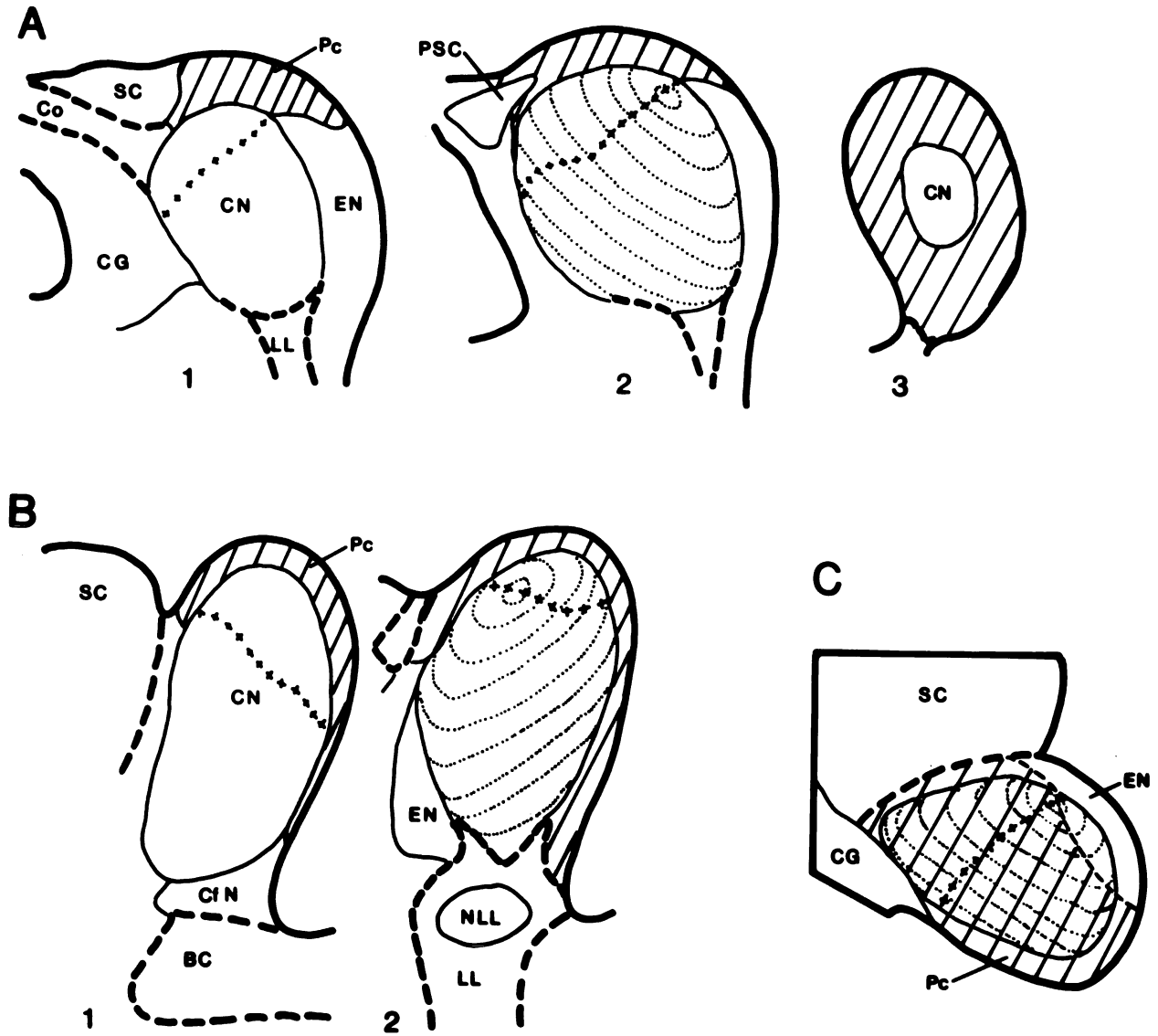
A
Pc
SC
Co
CN
EN
CG
LL
1
PSC
2
CN
3
B
Pc
SC
CN
CfN
BC
1
EN
NLL
LL
2
C
SC
EN
CG
Pc

Figure 2. See legend below illustration. M is medial; L is lateral. Reproduced from Rockel and Jones (1973a).

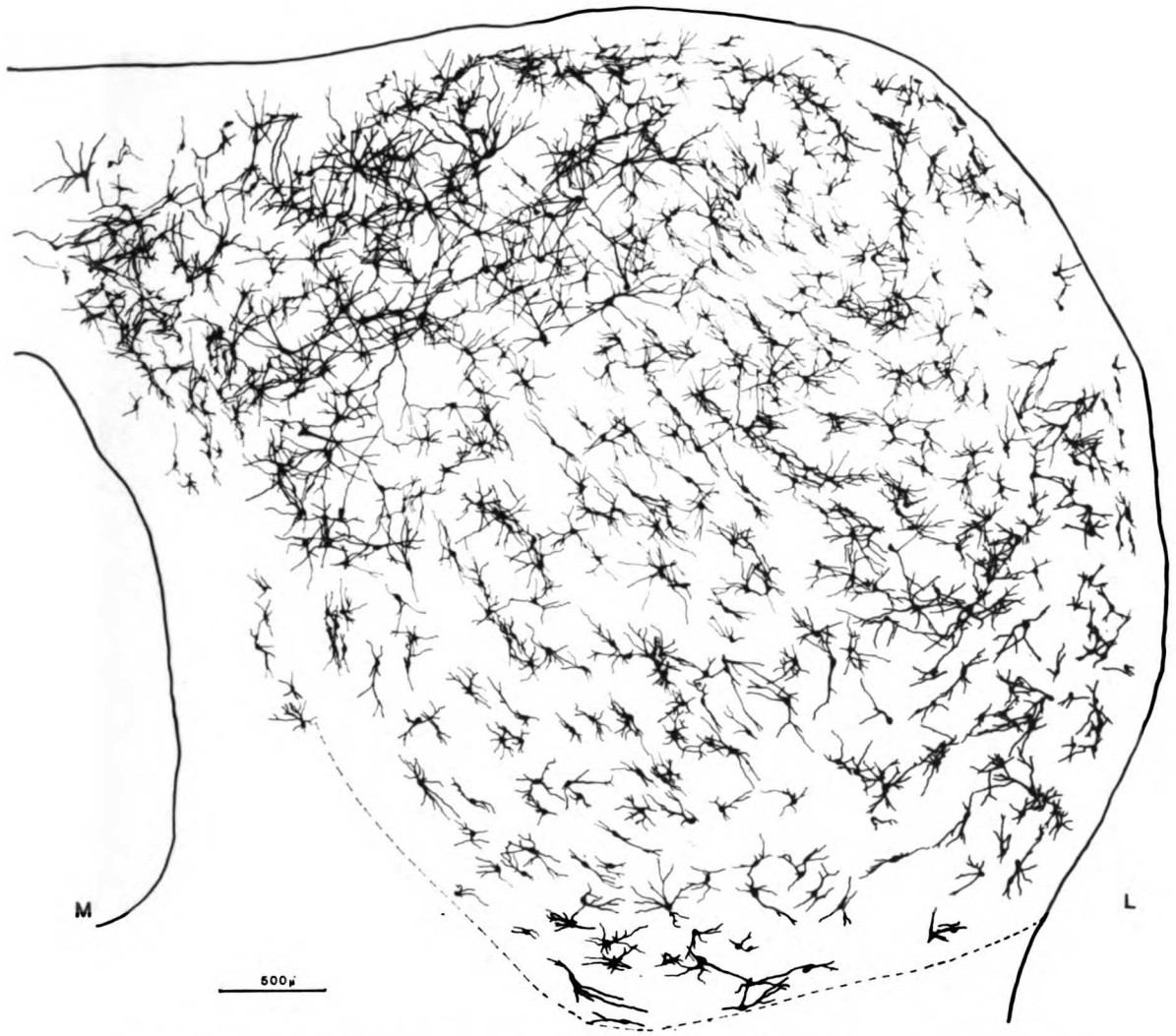

Fig. 1 Camera lucida drawing of a Golgi impregnated coronal section of the inferior colliculus. Most of the cells present have been drawn. Note the laminated form of the central parts of the central nucleus and the concentrations of large cells in the dorsomedial and ventrolateral aspects.

Figure 3. See legend below illustration. A is anterior; P is posterior. Reproduced from Rockel and Jones (1973a).

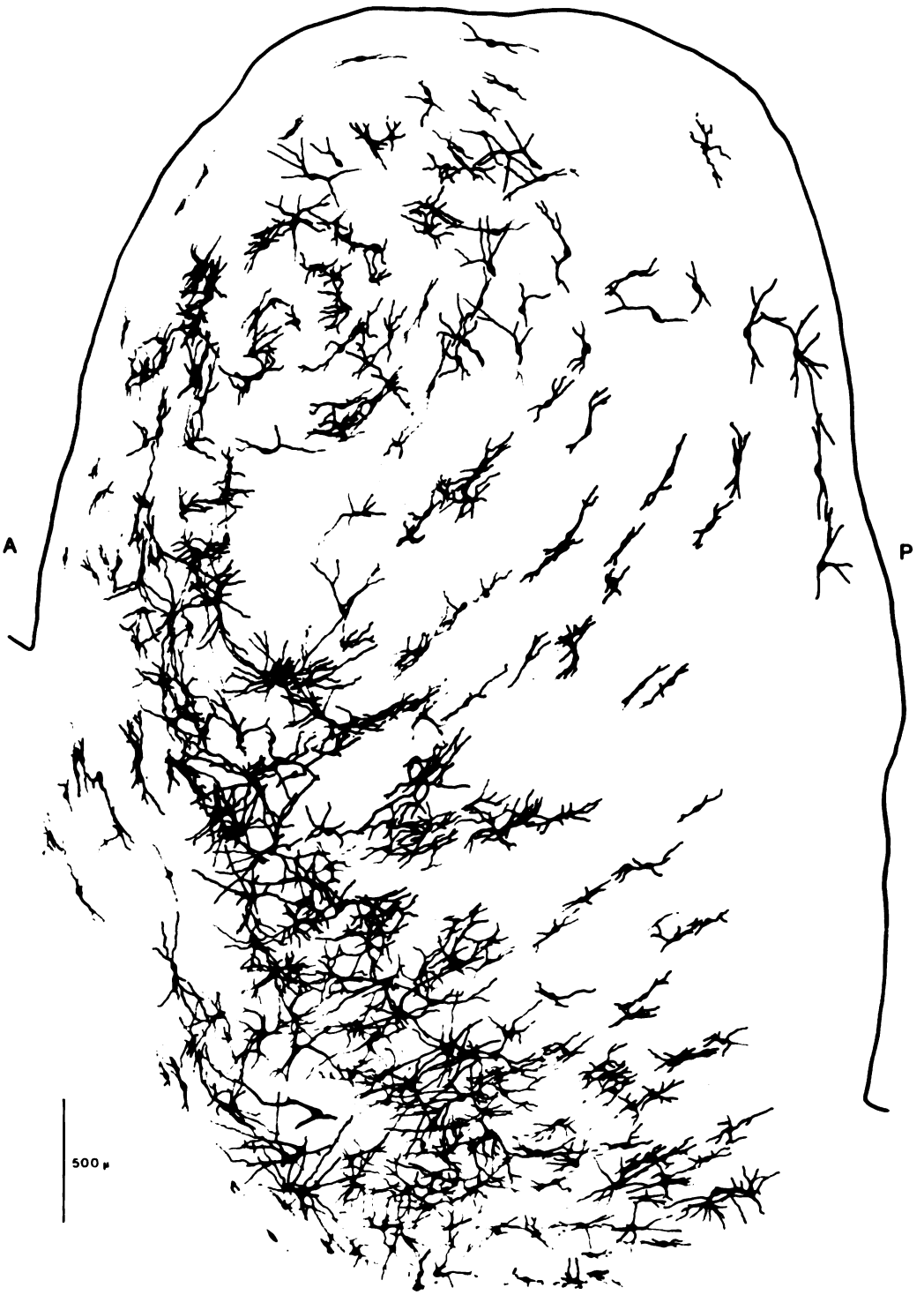

Fig. 3 Camera lucida drawing of a sagittal section. Note the lamination of the central nucleus and the region of large cells at its anterior and ventral aspect.

Figure 4. See legend below illustrations. A is anterior; P is posterior. Reproduced from Rockel and Jones (1973a).

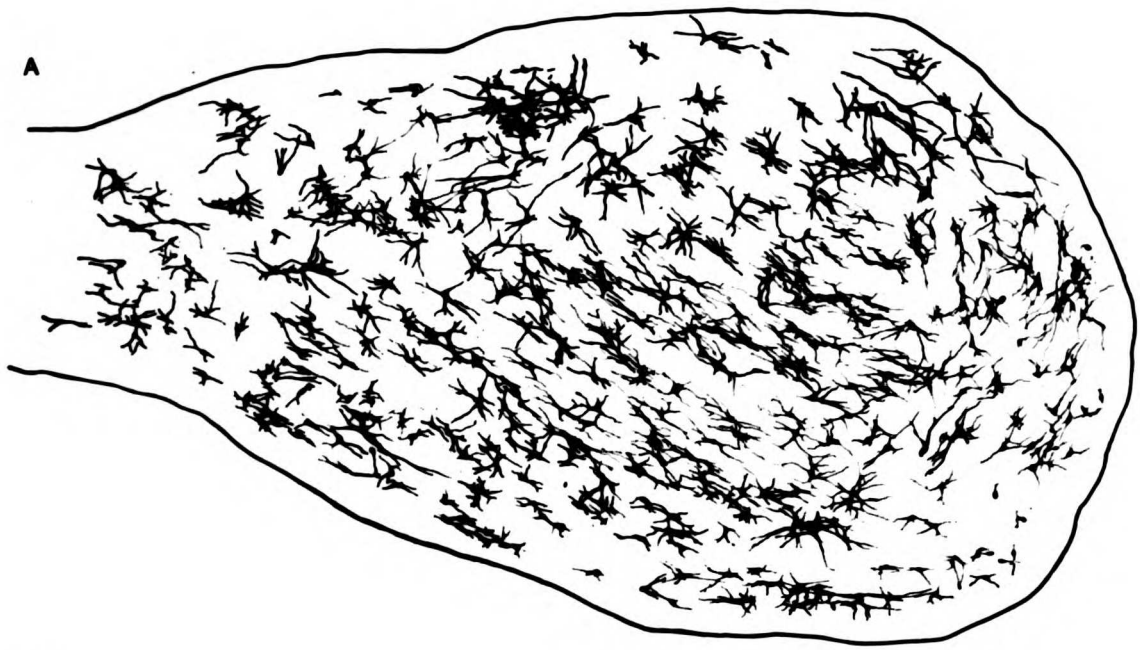

Fig. 2A Camera lucida drawing of a horizontal section. Note the laminated form of the central nucleus and the small region of large cells at its anteromedial aspect.

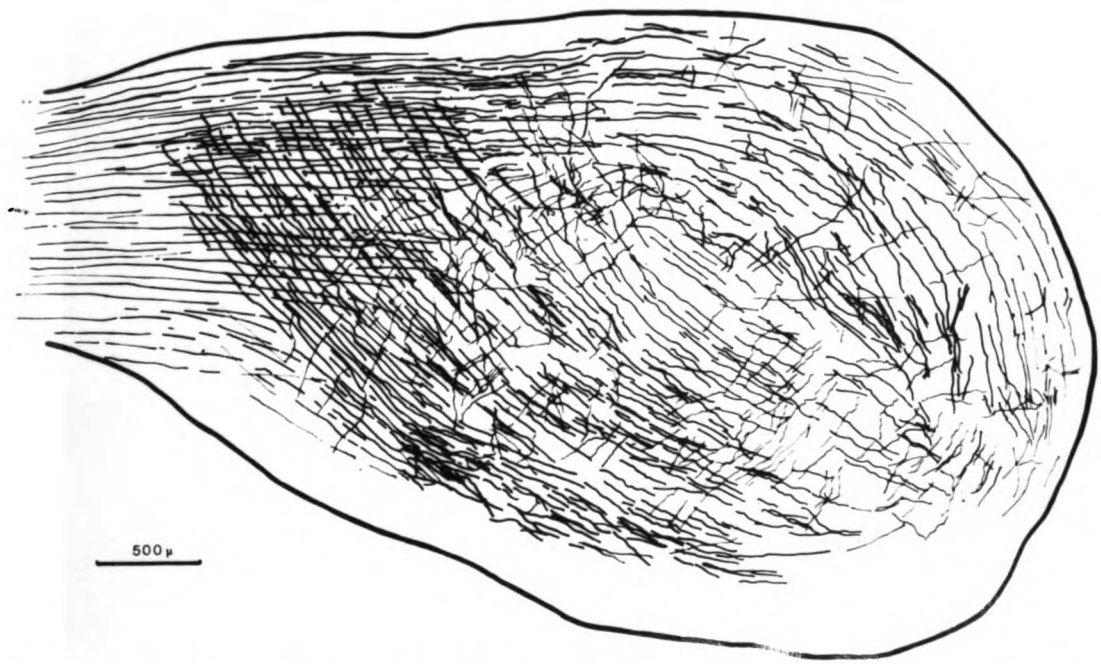

Fig. 2B Camera lucida drawing of the same section as figure 2A but in which some of the longer axons readily visible at this low magnification have been drawn. Note the manner in which the axons follow the same laminar pattern as seen in figure 2A.

Figure 5. HRP-labelled neurons in the ipsilateral (A,C) and contralateral (B,D) Dorsal Nuclei of the Lateral Lemnisci. Neuron in C was localized to a 30 μ section adjacent to the 90 μ section shown in A. Note that the orientation of the neuron's soma is perpendicular to the HRP-labelled lateral lemniscal axons coursing through the ipsilateral DNLL. Neurons in D were taken from the 90 μ section shown in B (arrowhead). Calibration bars are 500 μ for A and B, 50 μ for A and B, 50 μ for C and D. Case 76-26.

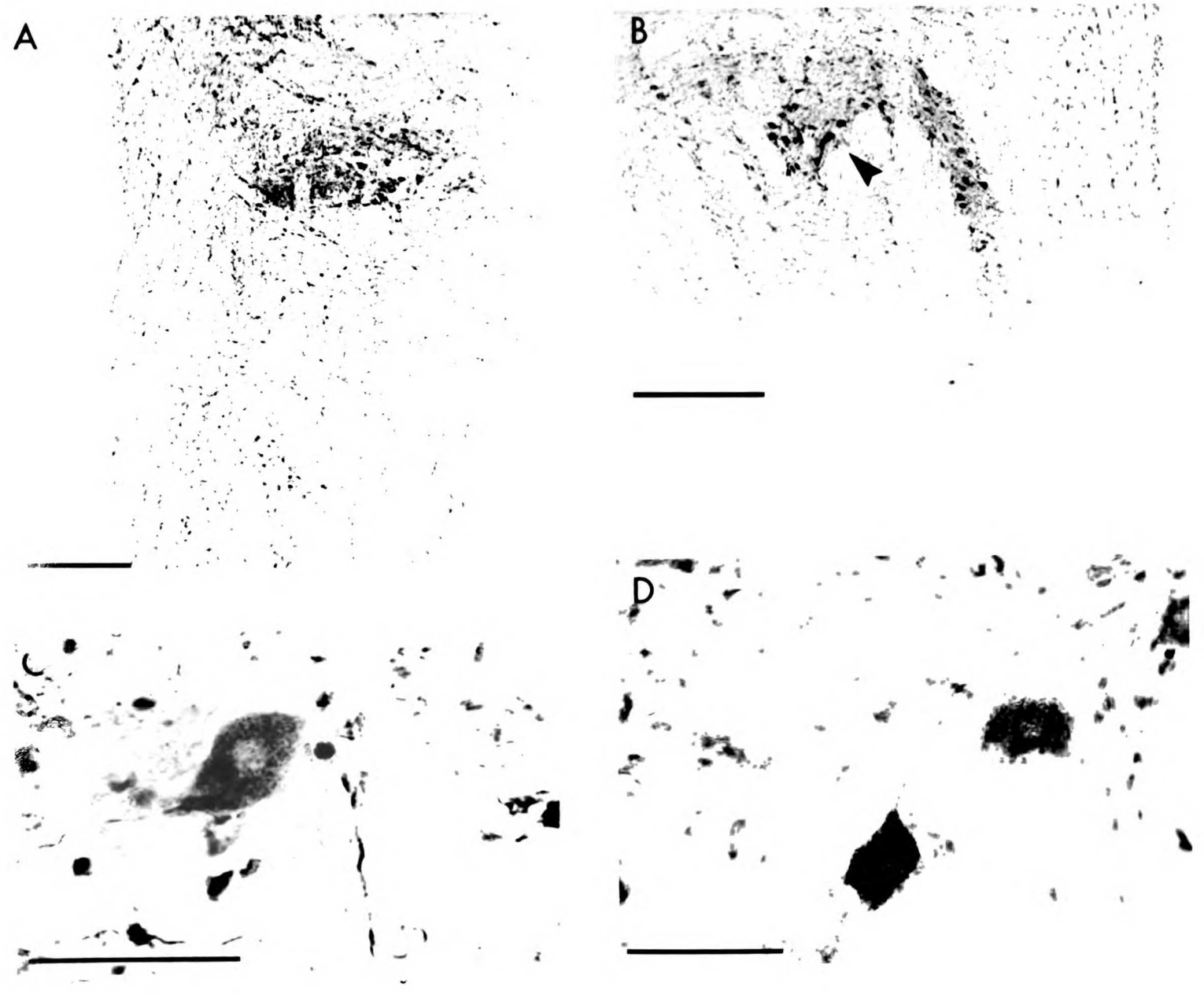
A
B
D

Figure 6. HRP-labelled neurons in the ipsilateral Ventral Nucleus of the Lateral Lemniscus. Note the "bands" of labelled neurons (small arrowheads in A) that cross the lateral to medial dimensions of the lateral "streak" of VNLL. C and D are neurons located in the most dorsal (C) and ventral (D) bands (large arrowheads in A). Neurons labelled in the more ventral division of VNLL were clustered in its more medial aspects (B). Note the diffuse, endogenous staining that serves to delimit the borders of the nucleus in this unstained section. Neurons in E were taken from the 90 μ section shown in B. Calibration bars are 500 μ for A and B, 50 μ for C, D, and E. Case 76-26.

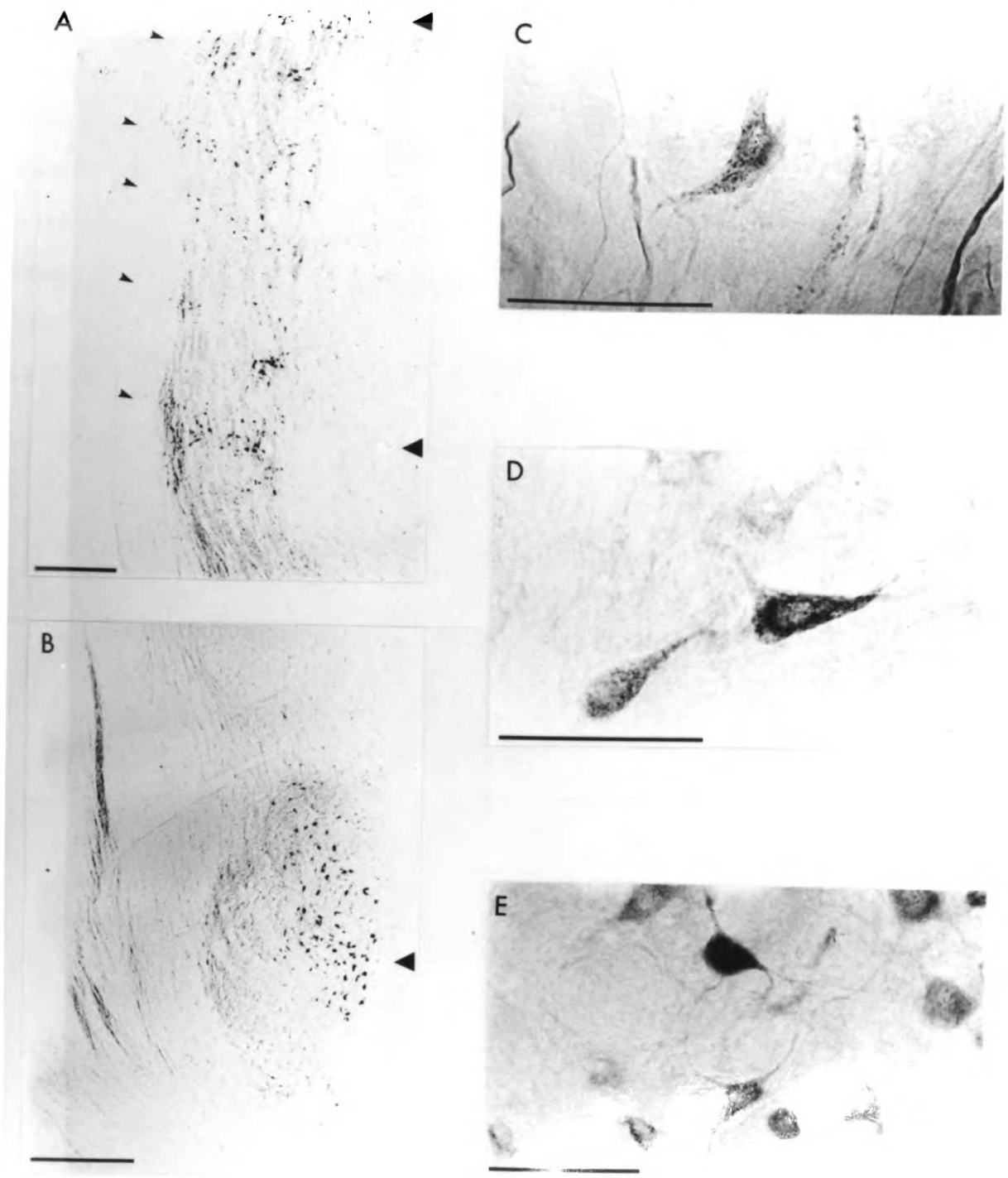
A
B
C
D
E

Figure 7. HRP-labelled neurons in the ipsilateral Superior Olivary Complex (A, C, E, F) and contralateral Lateral Superior Olive (B, D). Note how the HRP-labelled neurons are clustered within different aspects of each nuclues. C and E are taken from the ipsilateral LSO and MSO respectively (arrowheads in A). Neuron in D was localized to the contralateral LSO in a section 150 μ caudal to the section shown in B. Neuron in F was localized to the ipsilateral lateral periolivary nucleus in a section 300 μ rostral to A. Calibration bars are 500 μ for A and B; 50 μ for C, D, and E; and 50 μ for F. Case 76-26.

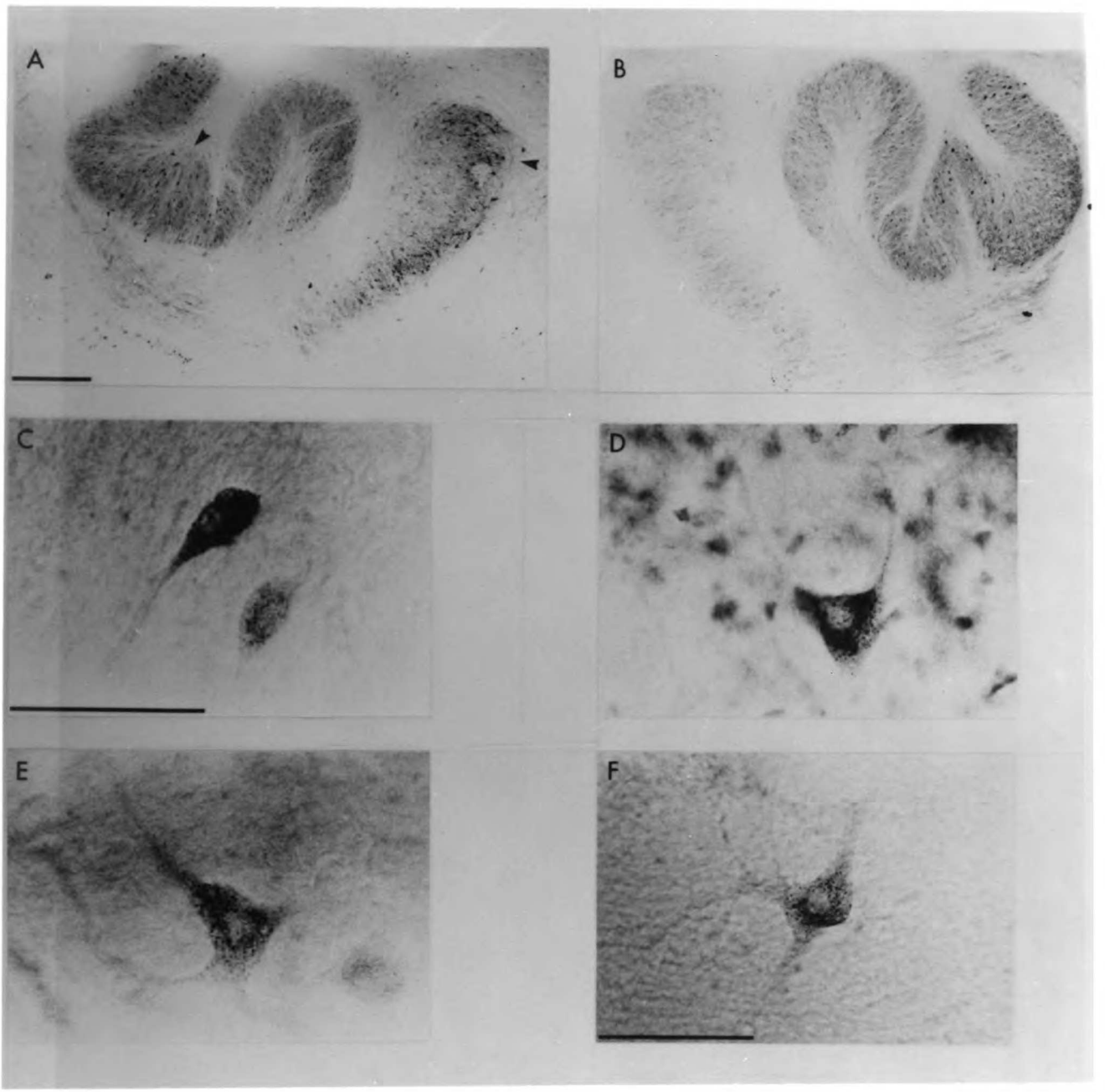
A
B
C
D
E
F

Figure 8. HRP-neurons in the contralateral cochlear nuclear complex (A-F) and near the contralateral facial nucleus (G). HRP-granules were found in giant (A) and fusiform (B) neurons of the DCN, in small neurons (C) in the large spherical cell field of AVCN, and in multipolar (D), globular (E), and octopus (F) neurons of the PVCN. HRP-neurons near the medial aspect of the facial nucleus (G) appeared to be situated within the nucleus reticularis paragiganticocellularis lateralis of Taber (1961). Calibration bar is 50 μ. Case 76-26.

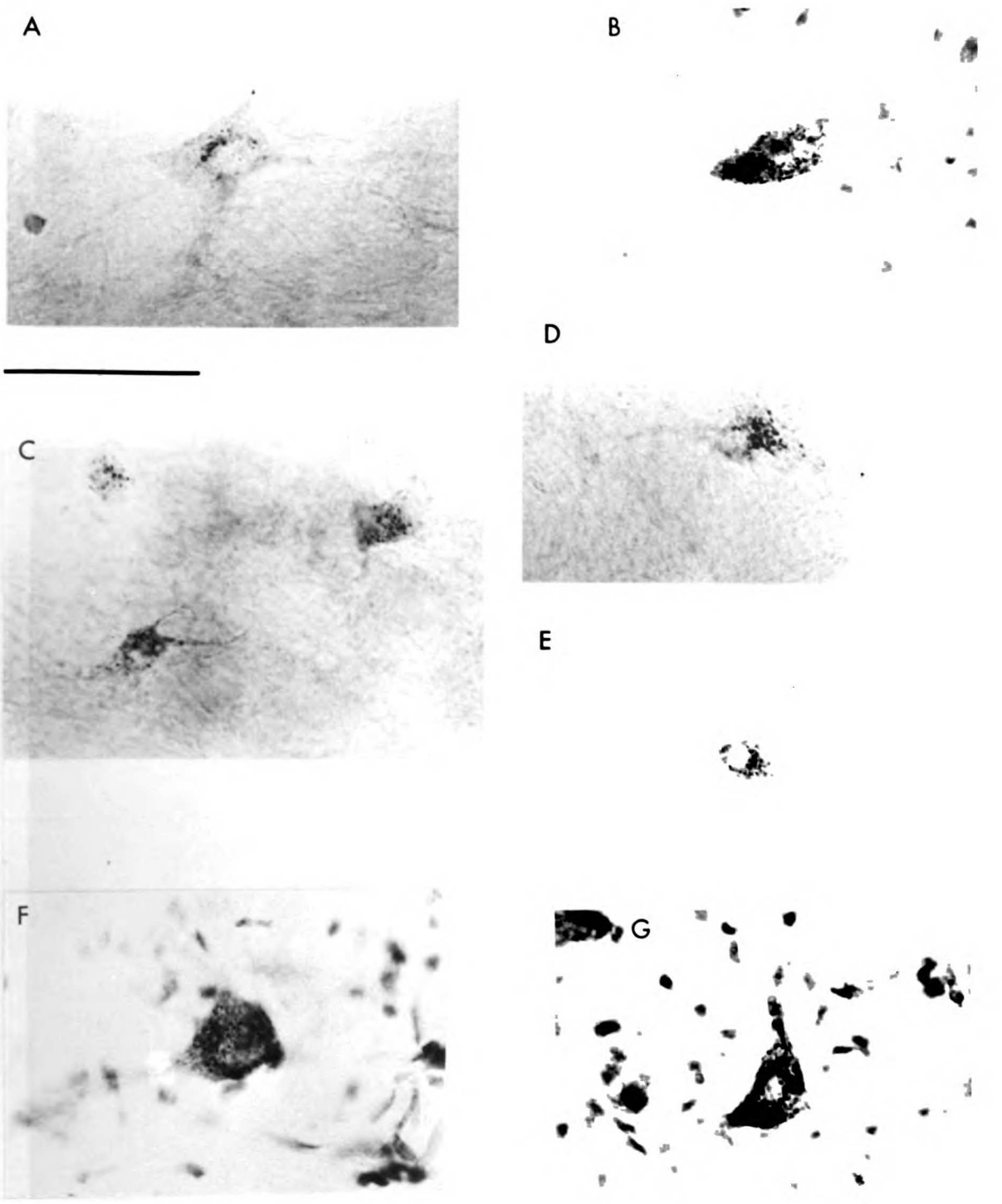
A
B
D
C
E
F
G

Figure 9. Right hand side: outline drawings of 90 μ frontal sections through the ipsilateral (I) MSO and both ipsilateral (I) and contralateral (C) LSO's for cases 76-26 and 76-28. Each dot in this and other similar illustrations represents a single HRP-labelled neuron. Best frequency at the ICC injection site was 2 kHz for case 76-26, 9 kHz for case 76-28. Left hand side: histograms of the number of labelled neurons in each 90 μ section (ordinate) as a function of the location of the section along the rostral (R) to caudal (C) extent of the superior olivary nuclei, in mm (abscissa). Arrowheads above each histogram correspond to the locations of each outline drawing to the right of that histogram. Note that the number of neurons counted does not include HRP-labelled neurons present in the interleaved 30 μ sections.

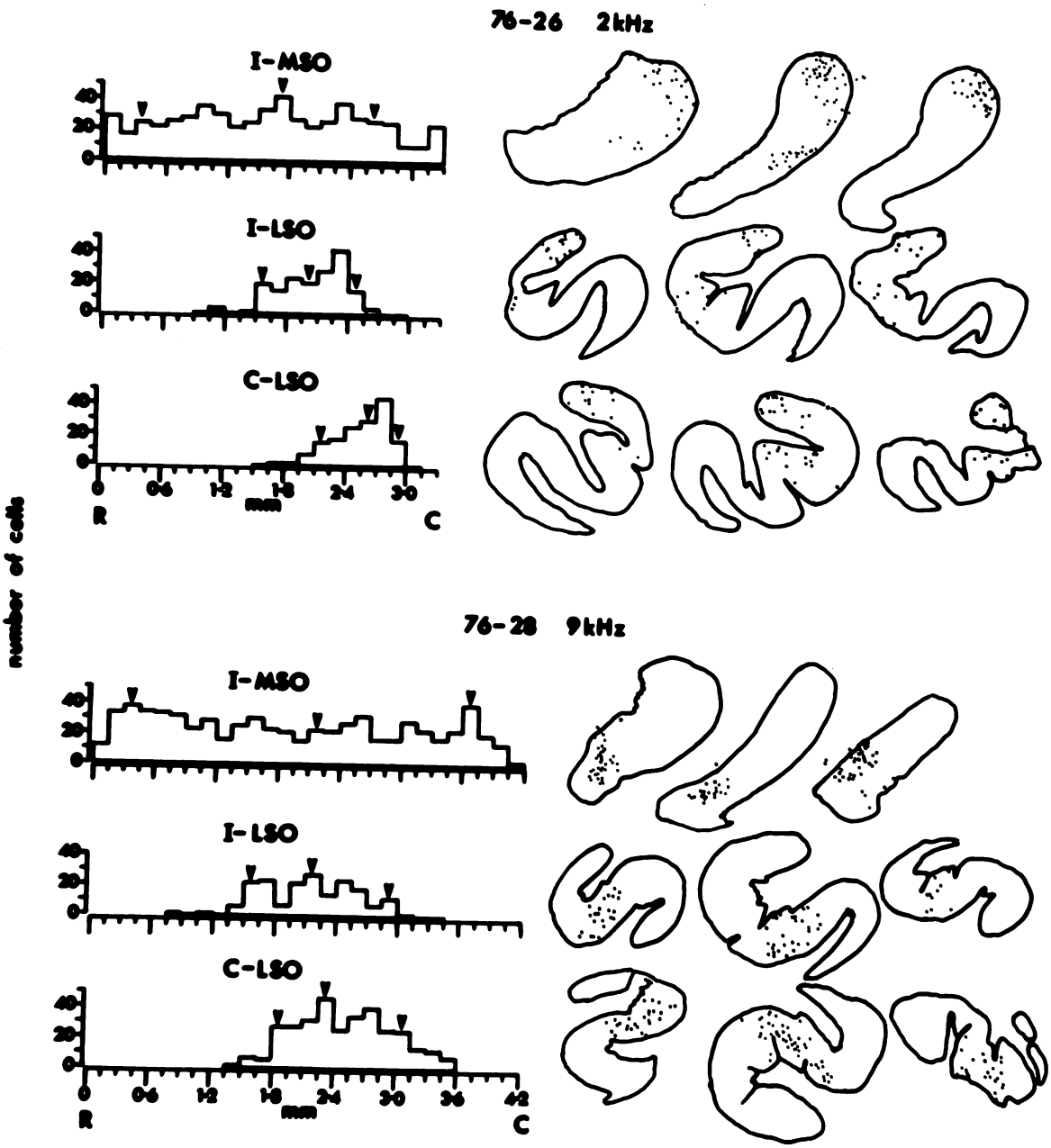
76-26 2kHz
I-MSO
I-LSO
C-LSO
number of cells
R
C
mm
76-28 9kHz
I-MSO
I-LSO
C-LSO
R
C
mm

Figure 10. Rostral (1) to caudal (14) outline drawings of HRP-labelling patterns in the ipsilateral MSO and LSO of case 76-4 following a small volume injection (0.1 µl) at a 15 kHz representational locus in ICC. This and all following outline drawings were taken from 90 µ sections. Section separation is given by the section number multiplied by 150 µ.

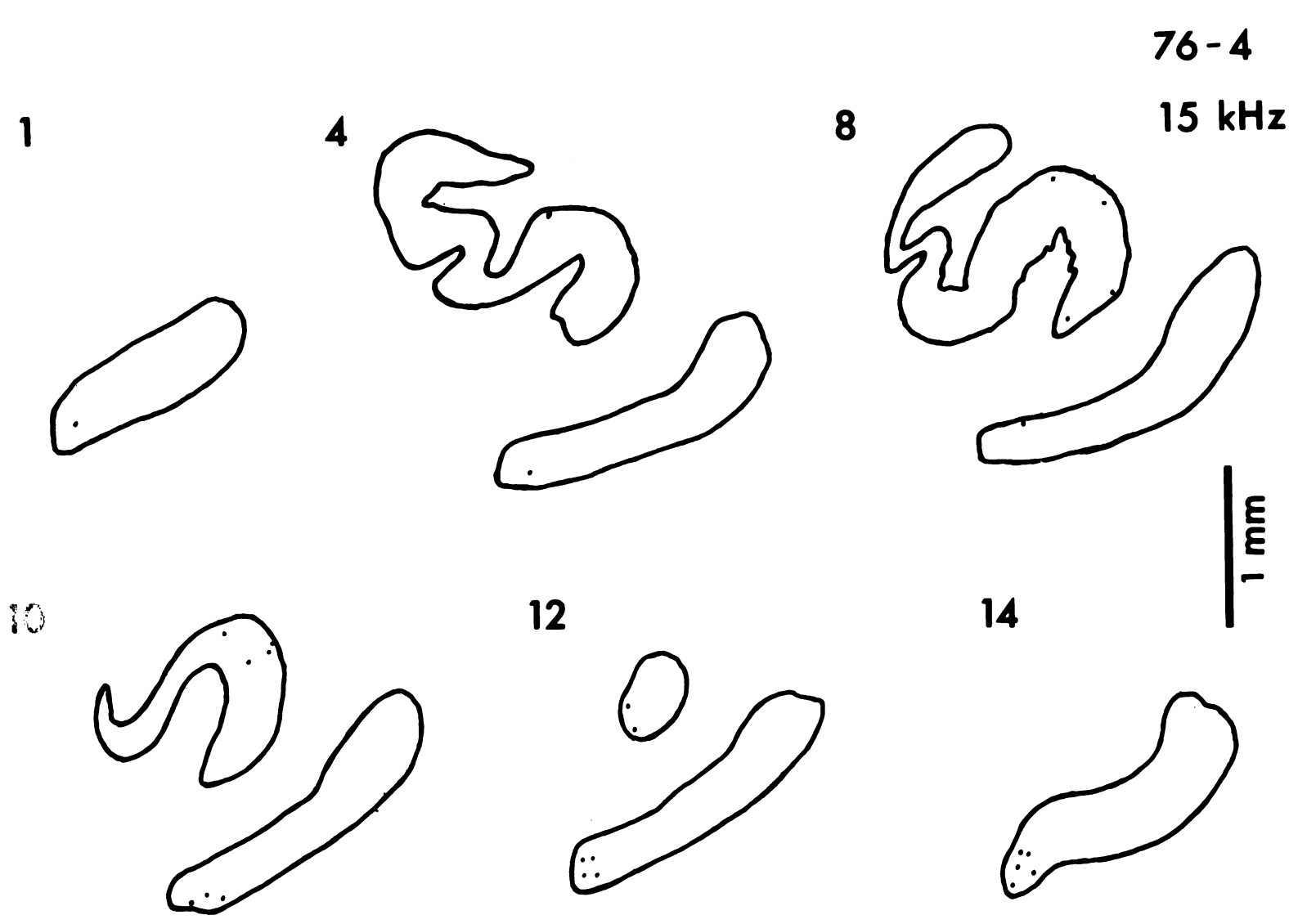
76-4
15 kHz
1
4
8
1 mm
10
12
14

Figure 11. Outline drawings of frontal sections through the contralateral cochlear nuclei of cases 76-26 (upper row) and 76-28 (lower row), arranged from caudal to rostral (left to right). Section separation given by the number multiplied by 150 μ.

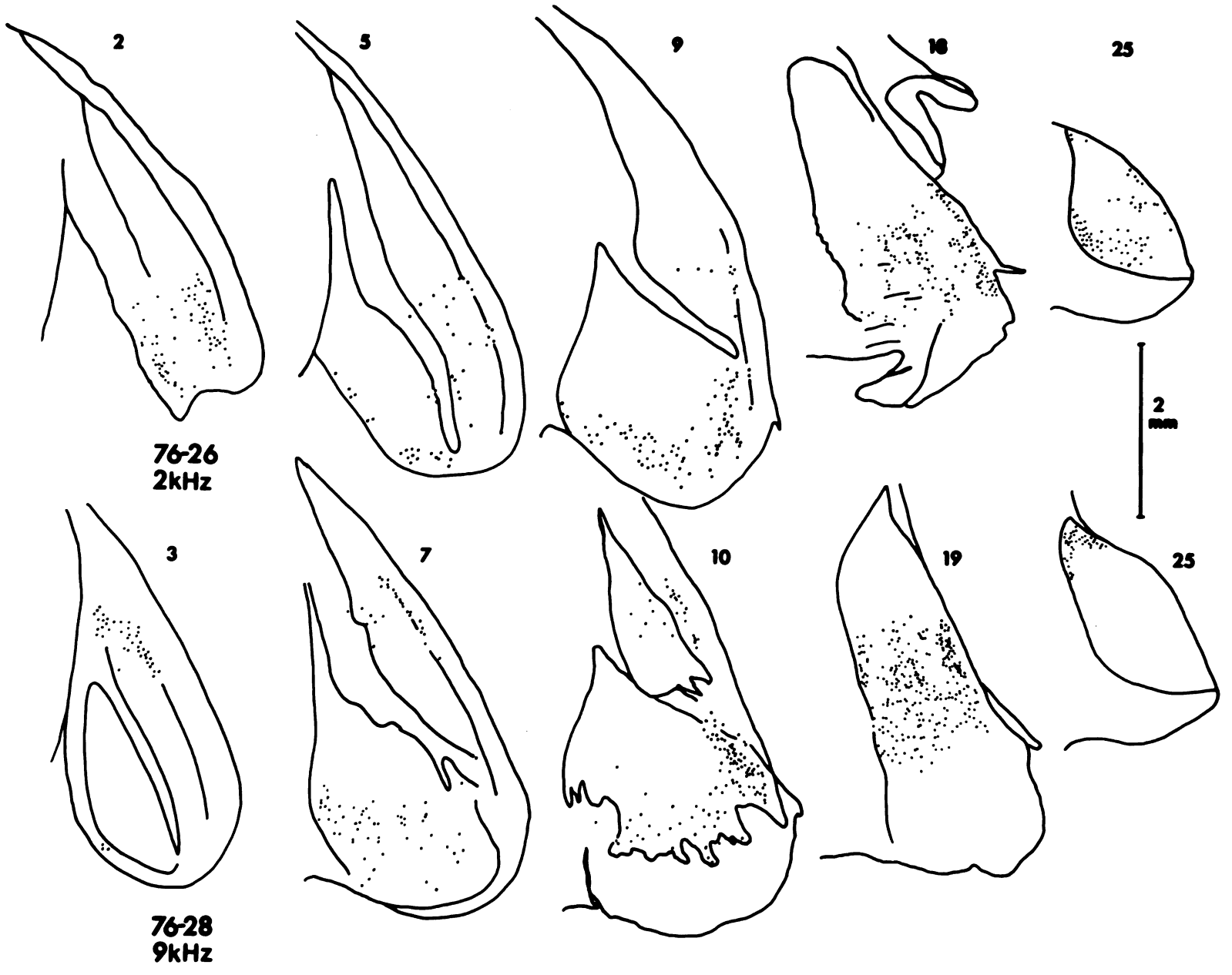
2
5
9
18
25
76-26
2kHz
2
mm
3
7
10
19
25
76-28
9kHz

Figure 12. Outline drawings of the contralateral cochlear nucleus of case 76-10, including DCN (1-6), PVCN (2-7), and AVCN (7-10). Numbers indicate section separation in 300 μ steps. Best frequency at the injection locus was 12 kHz.

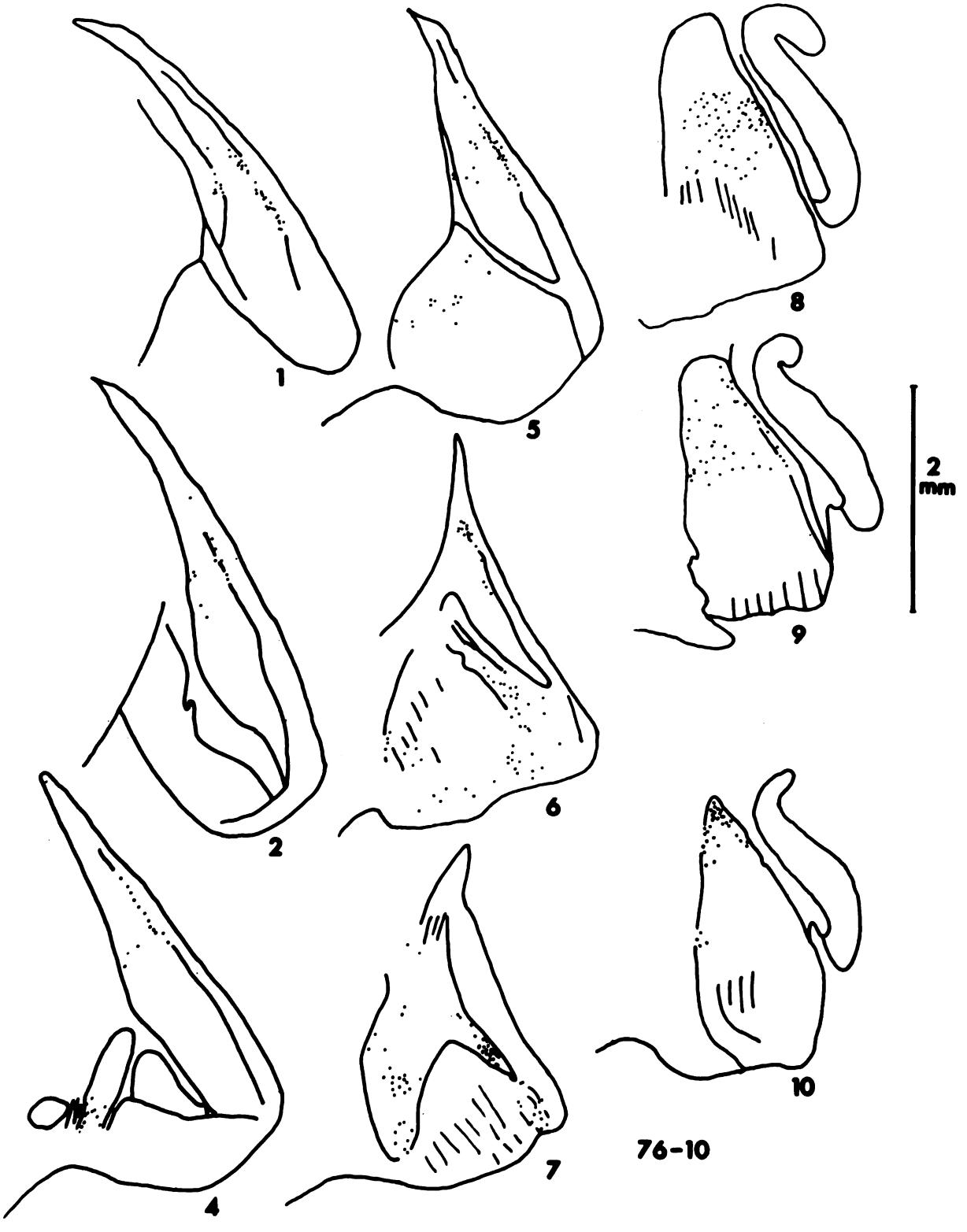
1
5
8
2
mm
2
6
9
4
7
10
76-10

Figure 13. Histograms of the numbers of HRP-labelled neurons in each nucleus (abscissa) expressed as a percentage of total number (N) counted in each of 6 experiments. Note that percentages and total numbers were taken from neurons counted in the 90 μ (but not the interleaved 30 μ) sections. In each case, the experiment number, injection volume, and best frequency (in kHz) at the injection site in ICC are identified. See text for abbreviations.

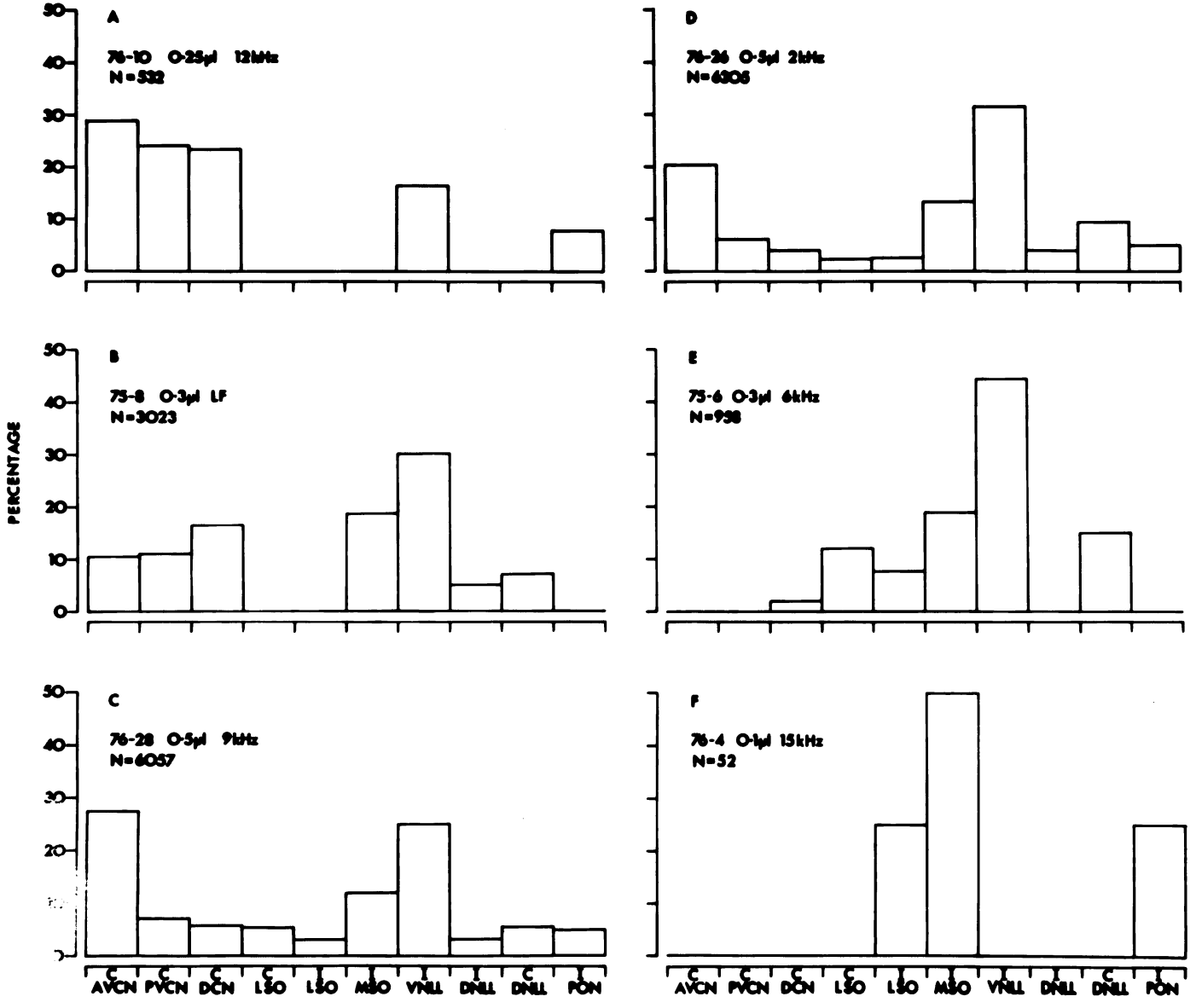
A
76-10 0·25µl 12kHz
N=532
B
75-8 0·3µl LF
N=3023
C
76-28 0·5µl 9kHz
N=6057
D
76-26 0·5µl 2kHz
N=6306
E
75-6 0·3µl 6kHz
N=958
F
76-4 0·1µl 15kHz
N=52
PERCENTAGE
0
10
20
30
40
50
C AVCN
C PVCN
C DCN
C LSO
I LSO
I MSO
I VNLL
I DNLL
C DNLL
I PON

Figure 14. Numbers of ICC neurons (ordinate) in each response "class" plotted as a function of their represented cochlear place (abscissa), in 4 mm bins. Best frequencies (in kHz) that correspond to the represented cochlear place are listed in these and other figures along the same axis.

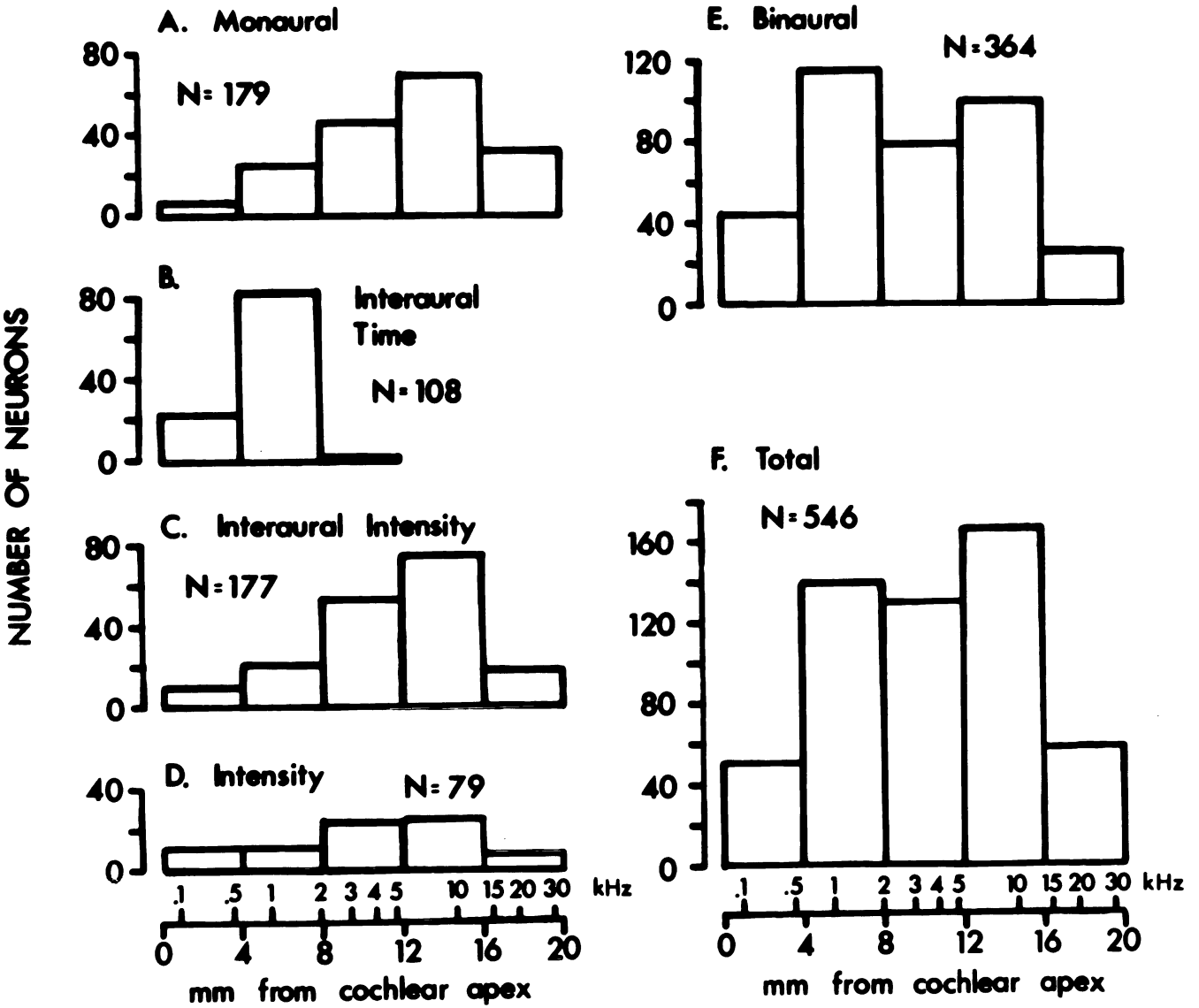
A. Monaural
N= 179
B.
Interaural Time
N= 108
C. Interaural Intensity
N= 177
D. Intensity
N= 79
E. Binaural
N= 364
F. Total
N= 546
NUMBER OF NEURONS
0
40
80
120
160
.1 .5 1 2 3 4 5 10 15 20 30 kHz
0 4 8 12 16 20
mm from cochlear apex

Figure 15. Numbers of ICC neurons in each response "class" driven by monaural stimulation of either the contralateral ("Contra") or ipsilateral ("Ipsi") ear.

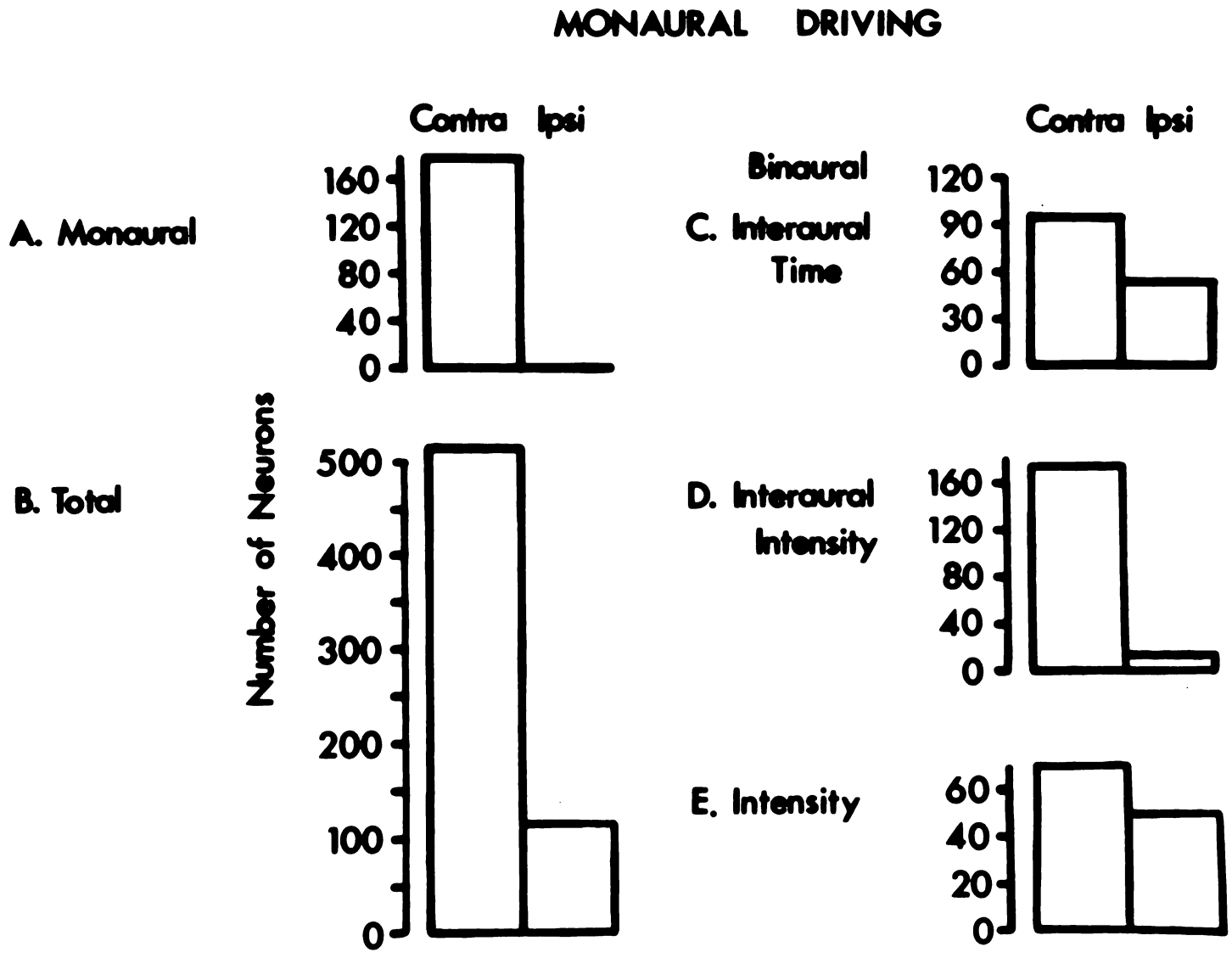
MONAURAL DRIVING
Contra
Ipsi
A. Monaural
160
120
80
40
0
B. Total
Number of Neurons
500
400
300
200
100
0
Binaural
C. Interaural Time
120
90
60
30
0
D. Interaural Intensity
160
120
80
40
0
E. Intensity
60
40
20
0

Figure 16. Numbers of ICC neurons in each response "class" that discharged with "onset" or "sustained" patterns (see text) to best frequency tonal stimulation, plotted as a function of their represented cochlear place.

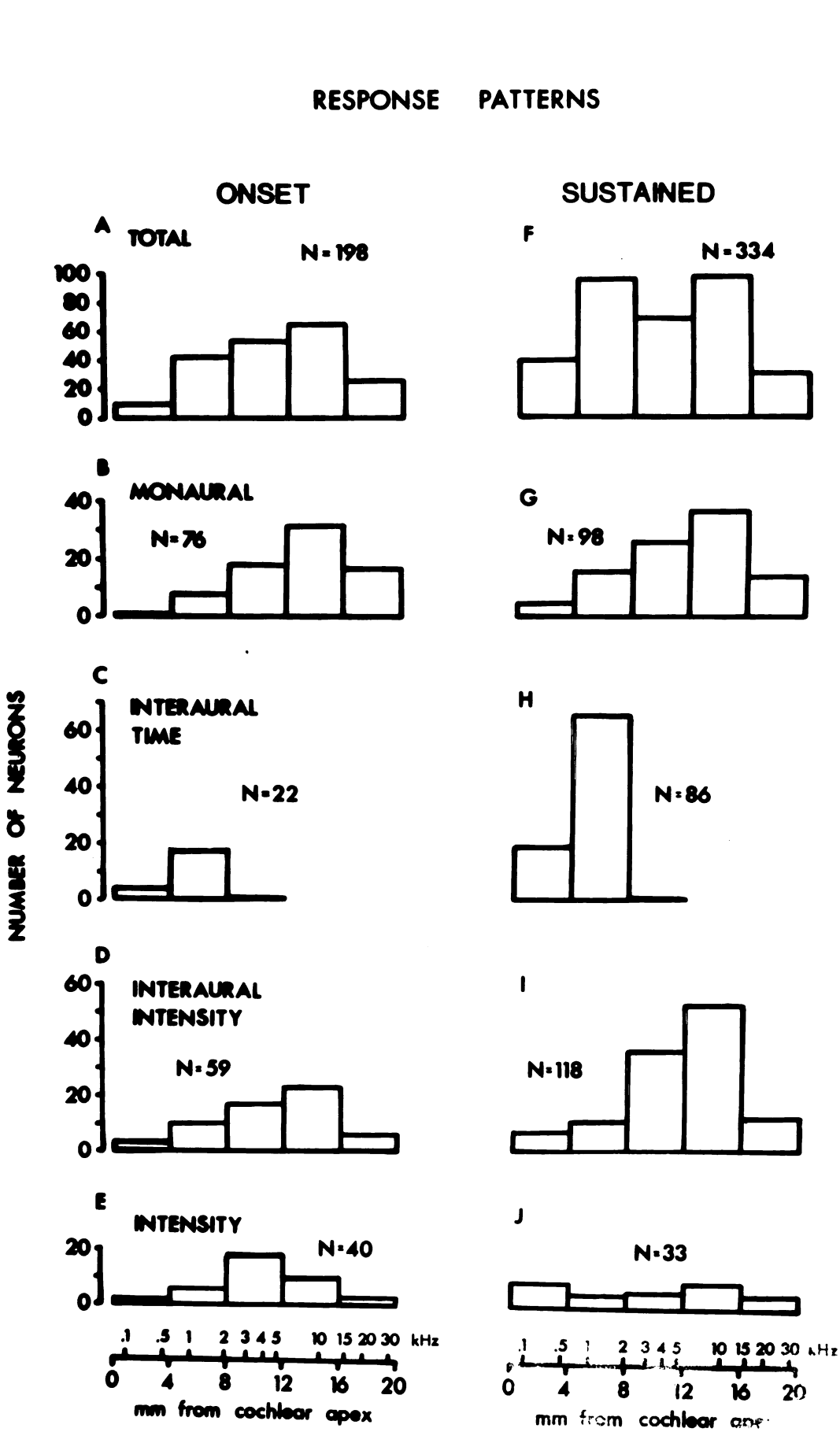
RESPONSE PATTERNS
ONSET
SUSTAINED
A
TOTAL
N = 198
F
N = 334
100
80
60
40
20
0
B
MONAURAL
N = 76
G
N = 98
40
20
0
C
INTERAURAL TIME
N = 22
H
N = 86
60
40
20
0
NUMBER OF NEURONS
D
INTERAURAL INTENSITY
N = 59
I
N = 118
60
40
20
0
E
INTENSITY
N = 40
J
N = 33
20
0
.1 .5 1 2 3 4 5 10 15 20 30 kHz
0 4 8 12 16 20
mm from cochlear apex

Figure 17. Lower illustrations plot the represented cochlear place of each isolated neuron as a function of the neuron's location (in mm) relative to the caudal (C) surface of the IC (abscissa). R is rostral. In Figures 17-20, open circles represent monaural neurons and closed symbols represent binaural neurons. Closed symbols represent the following binaural response "classes": circles = interaural intensity-difference neurons; triangles = interaural time-sensitive neurons; squares = binaural intensity-sensitive neurons; stars = binaural neurons that could not be categorized in any of these other response "classes".
Upper tracings are taken from sagittal sections cut in the approximate plane of the electrode penetrations through the ICC and stained with cresylecht-violet. Caudal is to the right. The dorsal nucleus of the lateral lemniscus (DNLL) is located immediately ventral to ICC. The rostral and ventral limits of ICC are distinct in Nissl-stained material because of the large number of unstained fibers that surround the nucleus at these borders, and are indicated here as solid lines. The dorsal and caudal extent of ICC is not well defined in this histological material and is therefore indicated by dashed lines; the dorsocaudal boundry of ICC could not be accurately defined, and is not demarcated. Penetrations represented by solid lines through ICC in this and in following illustrations were reconstructed in the section drawn; penetrations represented by dashed lines were parallel to the section outlined. In experiment 76-41, penetrations

1 and 2 were 1000 μ and 750 μ lateral to Penetration 3, respectively. In 76-46, Penetration 2 was approximately 1150 μ medial to Penetration 1. Small dots (see e.g. Penetration 3 of 76-41) in these and other drawings outline microlesions made during these experiments to aid in reconstruction of electrode tracks.

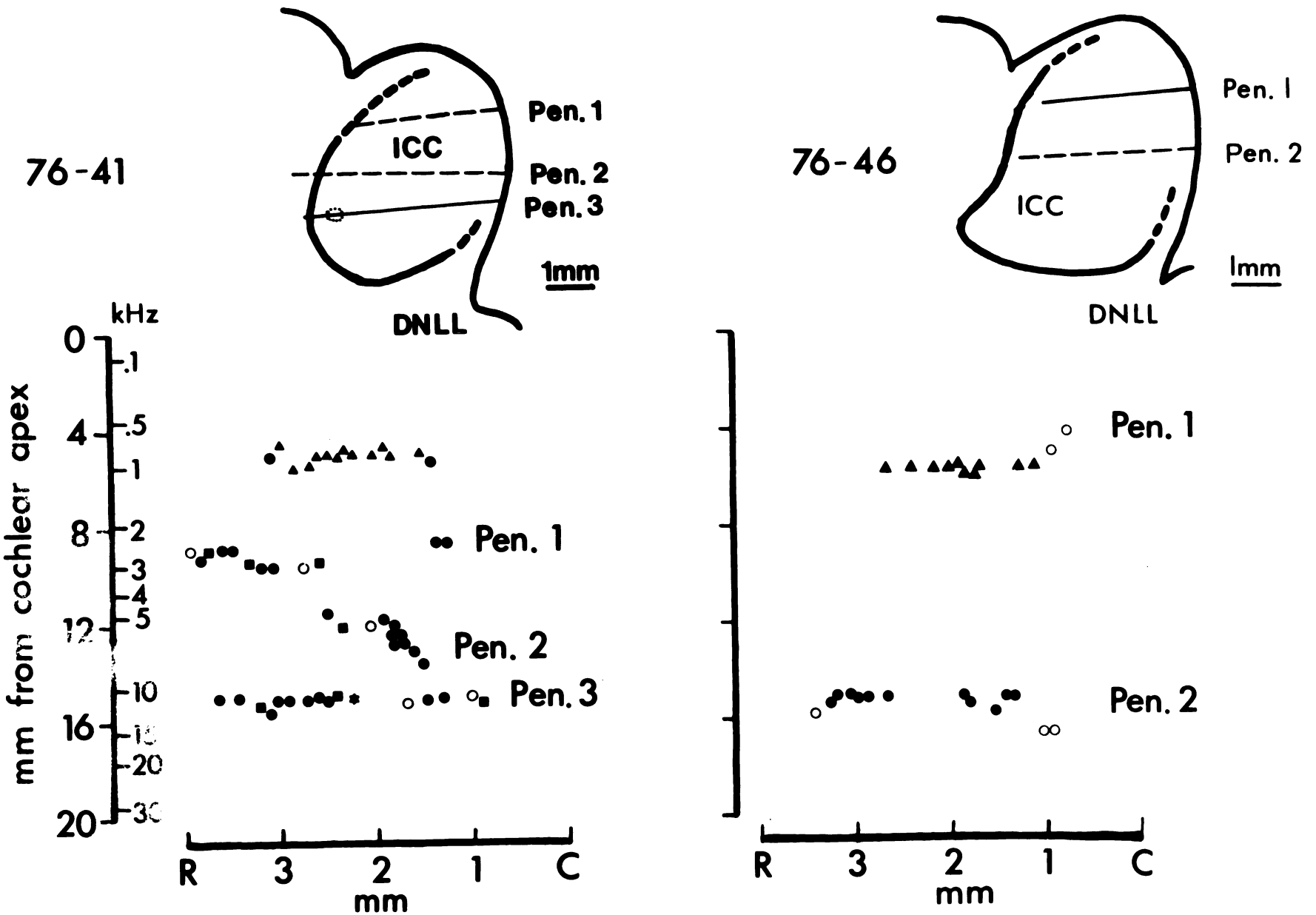
76-41
ICC
Pen. 1
Pen. 2
Pen. 3
1mm
DNLL
kHz
0
.1
4
.5
1
8
2
3
4
12
5
10
16
20
30
mm from cochlear apex
Pen. 1
Pen. 2
Pen. 3
R
3
2
1
C
mm
76-46
ICC
Pen. 1
Pen. 2
1mm
DNLL
Pen. 1
Pen. 2
R
3
2
1
C
mm

Figure 18. Represented cochlear place of ICC neurons isolated within three horizontal penetrations in experiment 76-55, plotted as a function of their location (in mm) from the caudal surface of the IC. Penetrations 1 and 3 were 1100 μ medial and 900 μ lateral to penetration 2, respectively.

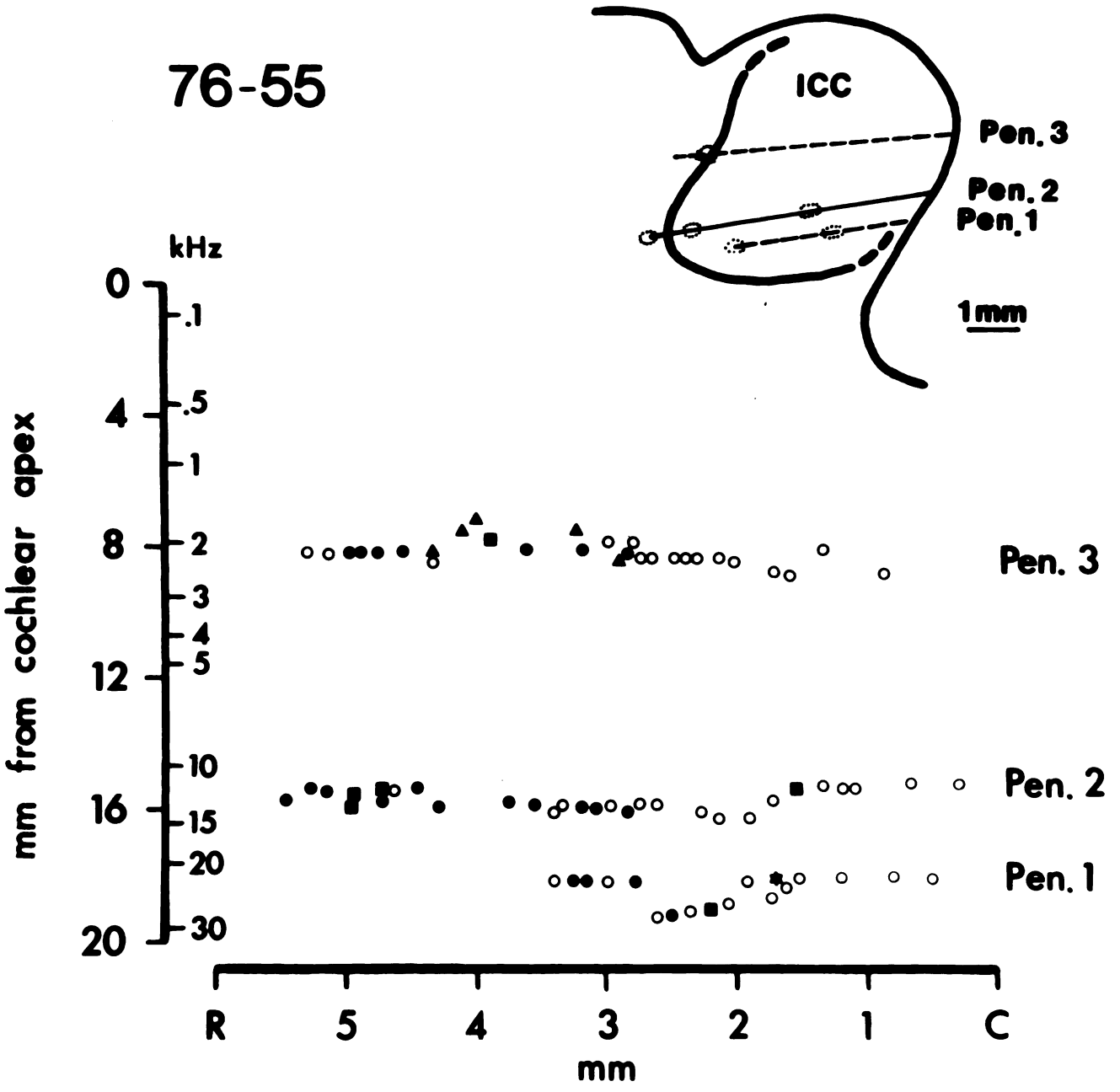
76-55
ICC
Pen. 3
Pen. 2
Pen. 1
1mm
kHz
0
.1
4
.5
1
8
2
3
4
12
5
10
16
15
20
20
30
mm from cochlear apex
Pen. 3
Pen. 2
Pen. 1
R
5
4
3
2
1
C
mm

Figure 19. Represented cochlear place of ICC neurons isolated within two penetrations in experiment 76-49, plotted as a function of their location (in mm) from the lateral surface of the IC. Penetration 2 was 350 μ rostral to penetration 1. Abbreviations: IC Comm. = IC Commissure; PAG - Periaqueductal Grey.

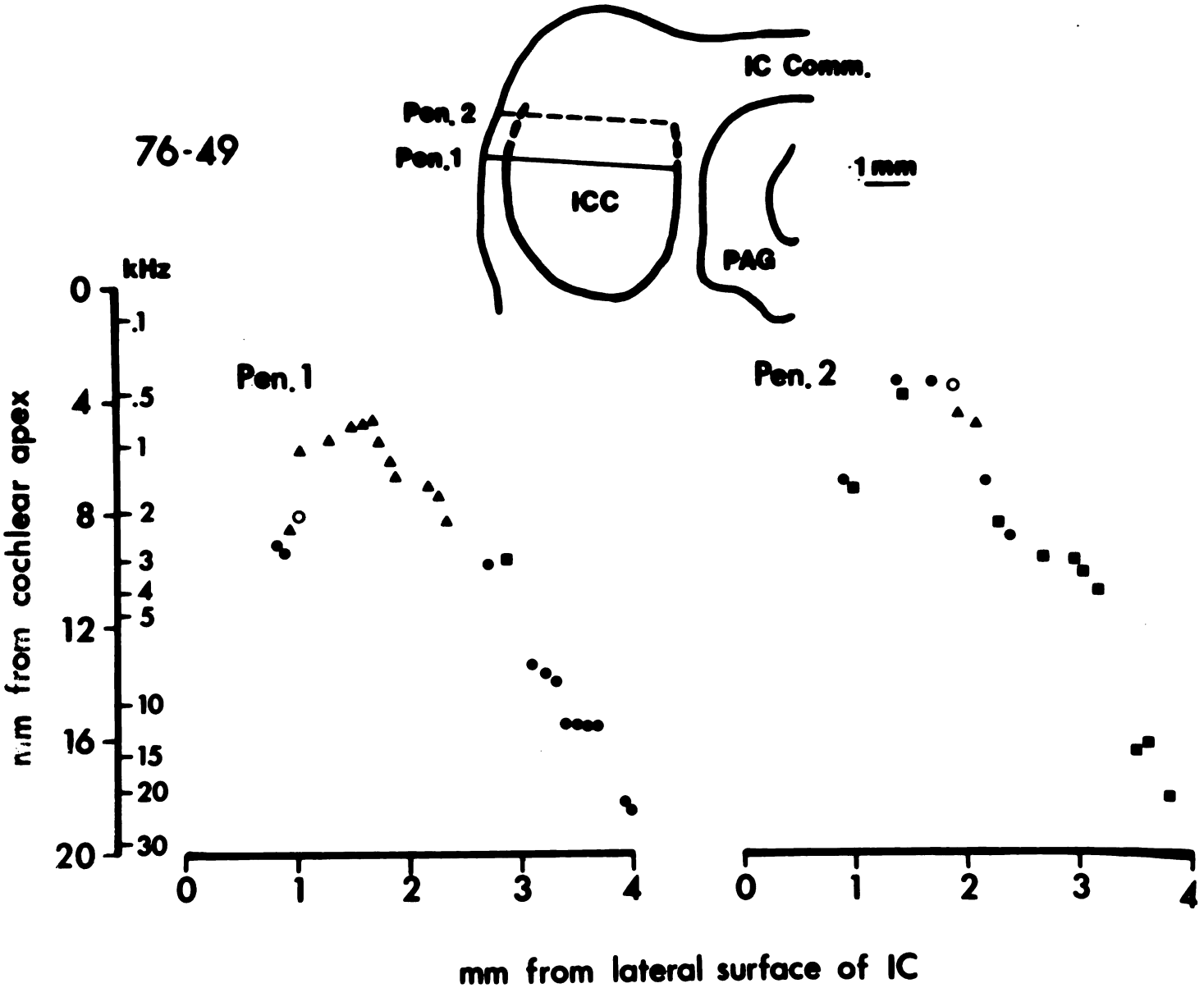
76-49
IC Comm.
Pen. 2
Pen. 1
ICC
PAG
1 mm
kHz
0
.1
4
.5
1
8
2
3
4
12
5
10
16
15
20
20
30
Pen. 1
Pen. 2
mm from cochlear apex
0
1
2
3
4
0
1
2
3
4
mm from lateral surface of IC

Figure 20. Represented cochlear place of ICC neurons isolated in experiment 76-33 in two dorsal-to-ventral microelectrode penetrations in the same frontal plane. CN = Cuneiform Nucleus.

76-33

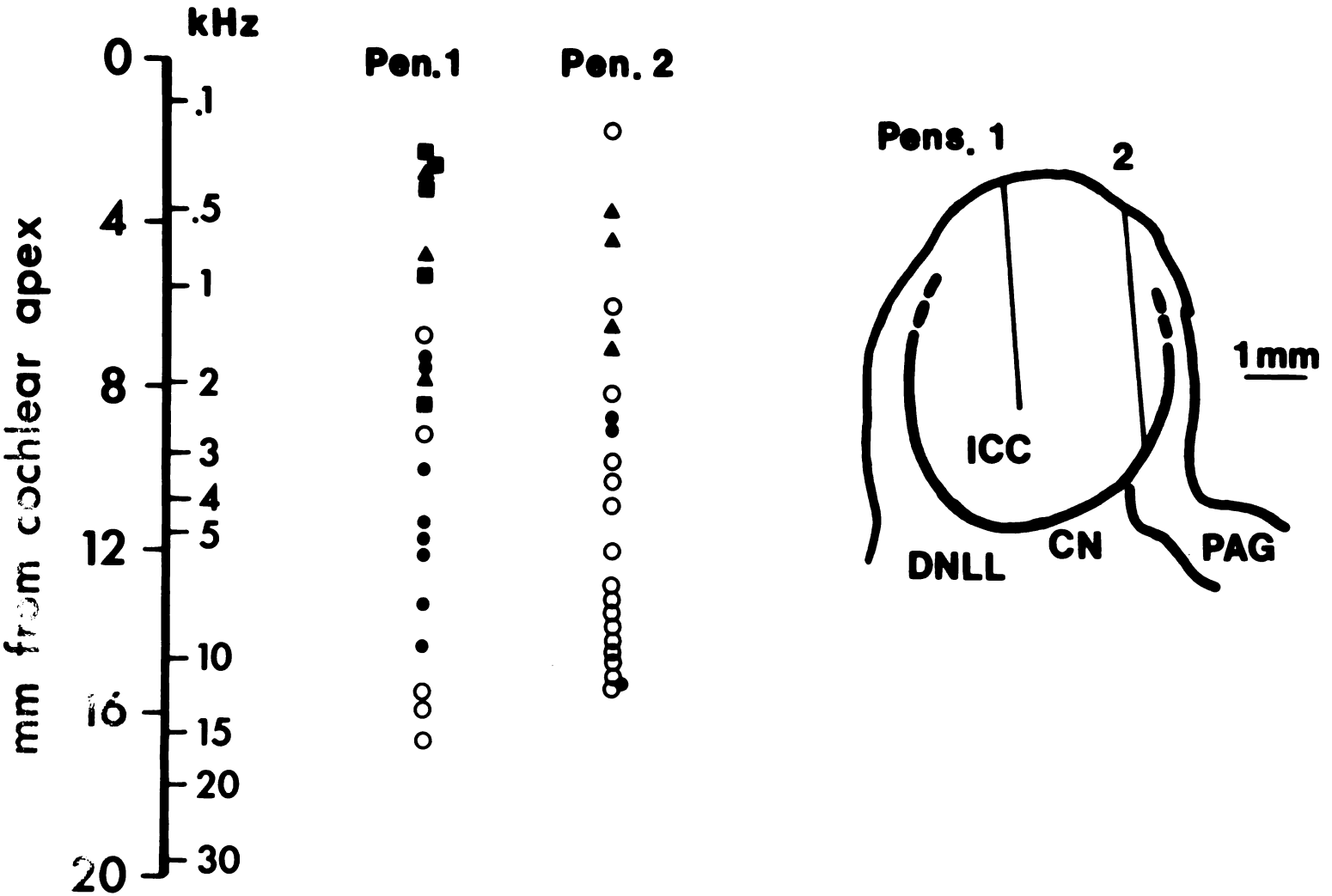
kHz
mm from cochlear apex
0
4
8
12
16
20
.1
.5
1
2
3
4
5
10
15
20
30
Pen. 1
Pen. 2
Pens. 1
2
1mm
ICC
DNLL
CN
PAG

Figure 21. A. Number of neural responses of ICC unit 74-48-9 to ten 250 msec. best frequency tone bursts delivered at each of a series of interaural time differences and at four different intensity levels (different symbols). Each pair of numbers below the abscissa of this and other illustrations indicates the stimulus intensity (in dBA) applied to each ear during each series of trails (see methods). The best frequency for this and other illustrated neurons is given below the unit number, as is the represented cochlear place (in mm from the apex) corresponding to that best frequency.
B. Percentage of the maximum neural response defined for each of these four intensity levels plotted as a function of the interaural time differences. Data shown in this and the following illustrations are representative of all such data derived in this study.

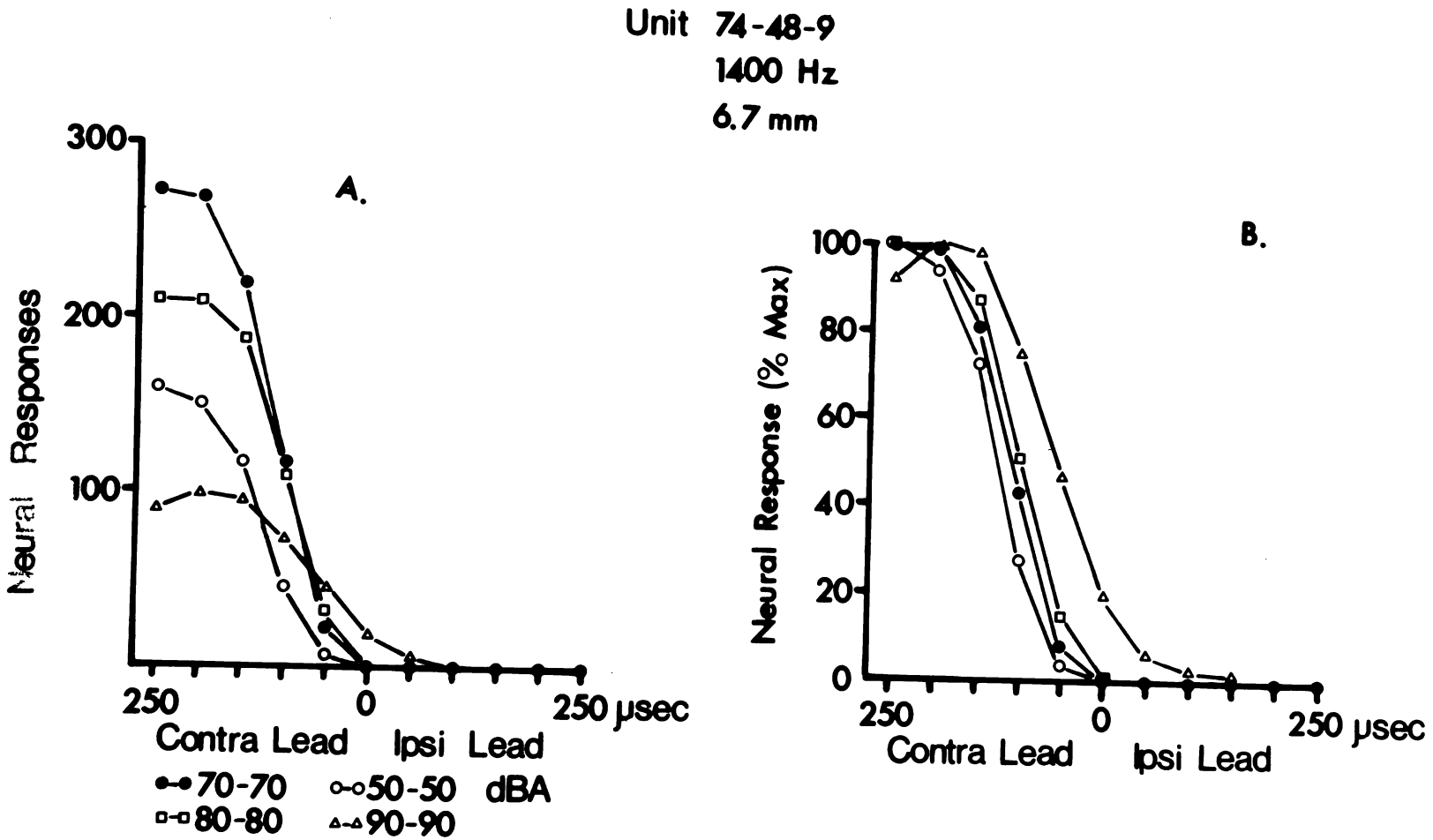
Unit 74-48-9
1400 Hz
6.7 mm
A.
B.
Neural Responses
300
200
100
Neural Response (% Max)
100
80
60
40
20
0
250
0
250 µsec
Contra Lead
Ipsi Lead
70-70
50-50 dBA
80-80
90-90

Figure 22. Responses of two delay-sensitive ICC neurons to tonal stimulation at their best best frequencies (filled circles) and to tonal stimulation below (squares in A) and above (squares in B) their respective best frequencies (as indicated below graphs).

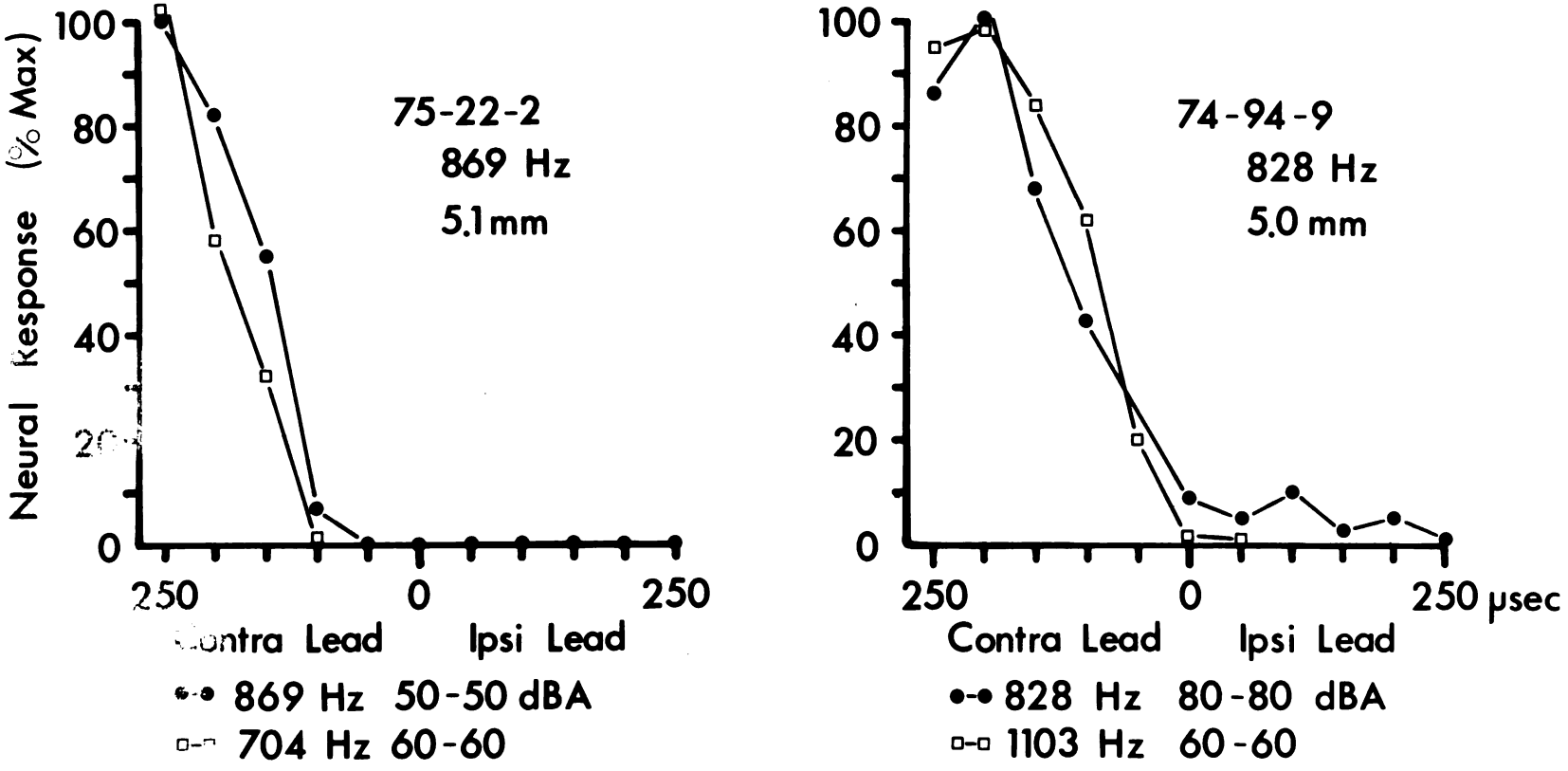
Neural Response (% Max)
100
80
60
40
20
0
250
0
250
Contra Lead
Ipsi Lead
75-22-2
869 Hz
5.1mm
869 Hz 50-50 dBA
704 Hz 60-60
74-94-9
828 Hz
5.0 mm
250 µsec
828 Hz 80-80 dBA
1103 Hz 60-60

Figure 23. Responses of two delay sensitive ICC neurons to tonal stimulation at their best frequency (filled circles), and at a lower frequency (squares in A and B).

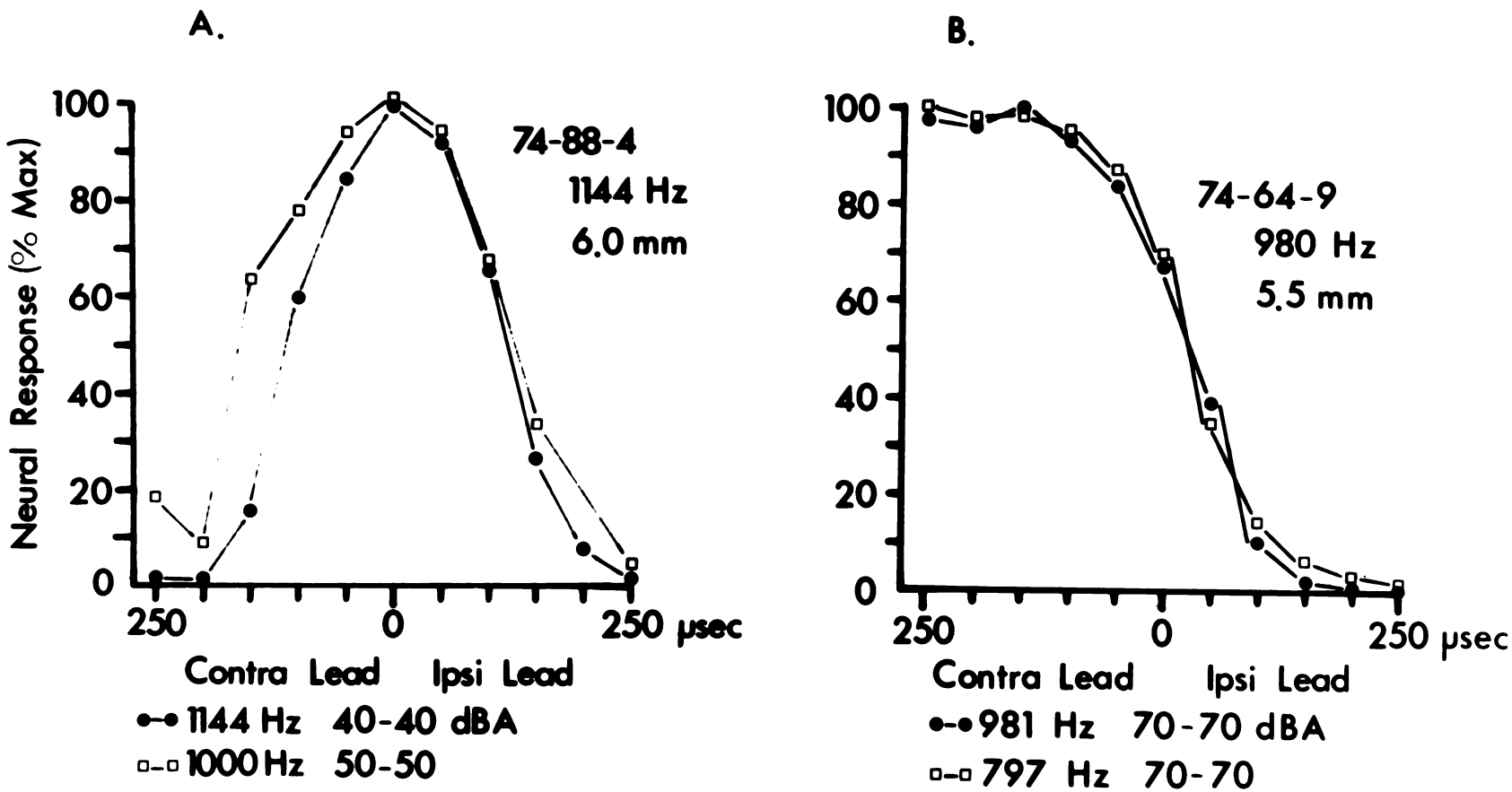
A.
Neural Response (% Max)
100
80
60
40
20
0
74-88-4
1144 Hz
6.0 mm
250
0
250 μsec
Contra Lead
Ipsi Lead
1144 Hz 40-40 dBA
1000 Hz 50-50
B.
100
80
60
40
20
0
74-64-9
980 Hz
5.5 mm
250
0
250 μsec
Contra Lead
Ipsi Lead
981 Hz 70-70 dBA
797 Hz 70-70

Figure 24. Responses of two delay-sensitive ICC neurons to tonal stimulation at their best frequencies (open circles) and to noise stimulation (stars in A and B).

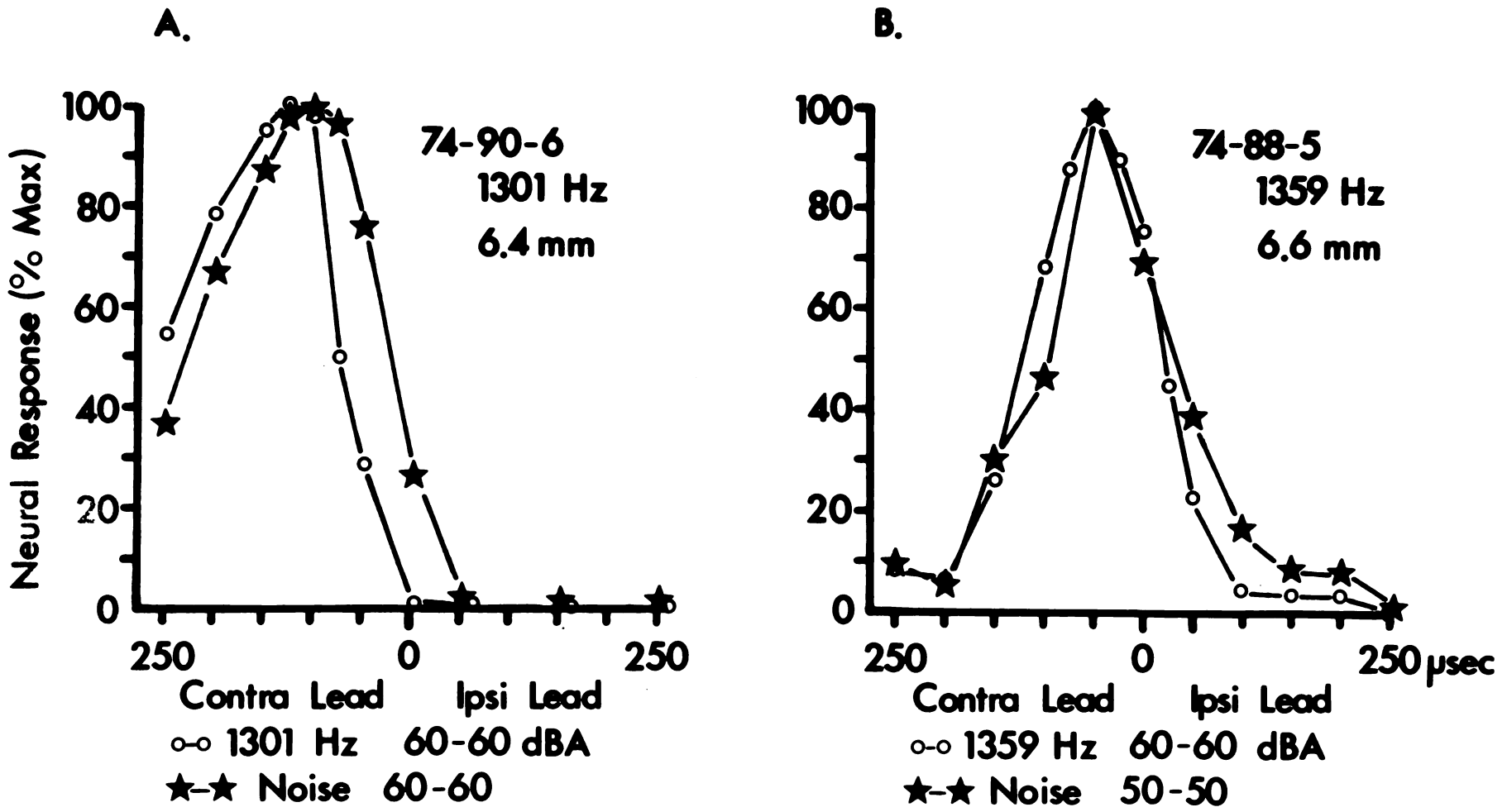
A.
Neural Response (% Max)
100
80
60
40
20
0
74-90-6
1301 Hz
6.4 mm
250
0
250
Contra Lead
Ipsi Lead
o-o 1301 Hz 60-60 dBA
★-★ Noise 60-60
B.
100
80
60
40
20
0
74-88-5
1359 Hz
6.6 mm
250
0
250 µsec
Contra Lead
Ipsi Lead
o-o 1359 Hz 60-60 dBA
★-★ Noise 50-50

Figure 25. Responses of two delay sensitive ICC neurons to best frequency tonal and to noise stimulation.

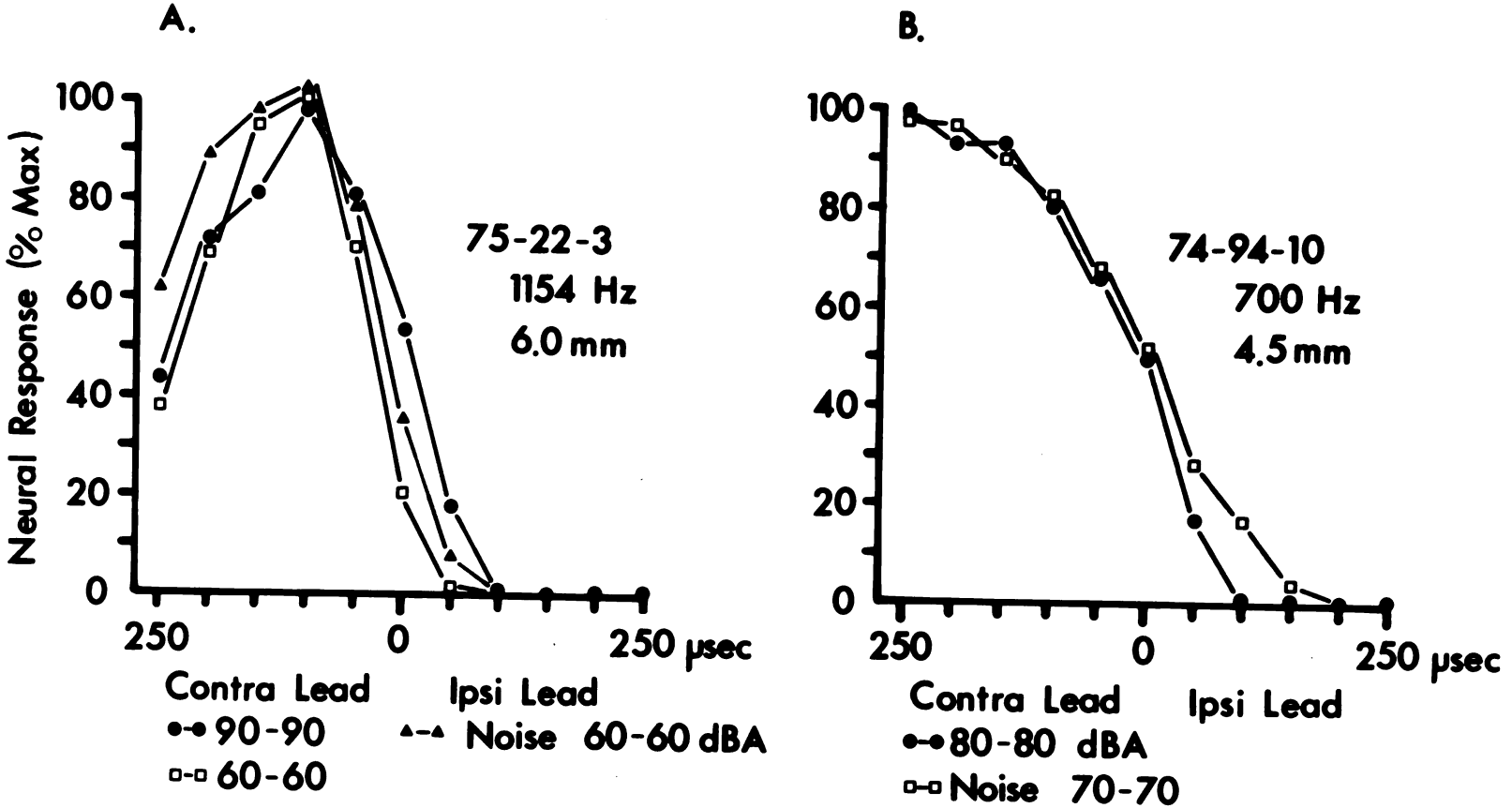
A.
Neural Response (% Max)
100
80
60
40
20
0
250
0
250 µsec
75-22-3
1154 Hz
6.0 mm
Contra Lead
Ipsi Lead
90-90
60-60
Noise 60-60 dBA
B.
100
80
60
40
20
0
250
0
250 µsec
74-94-10
700 Hz
4.5 mm
Contra Lead
Ipsi Lead
80-80 dBA
Noise 70-70

Figure 26. Responses of two delay-sensitive ICC neurons to best frequency tonal stimulation at different intensity levels.

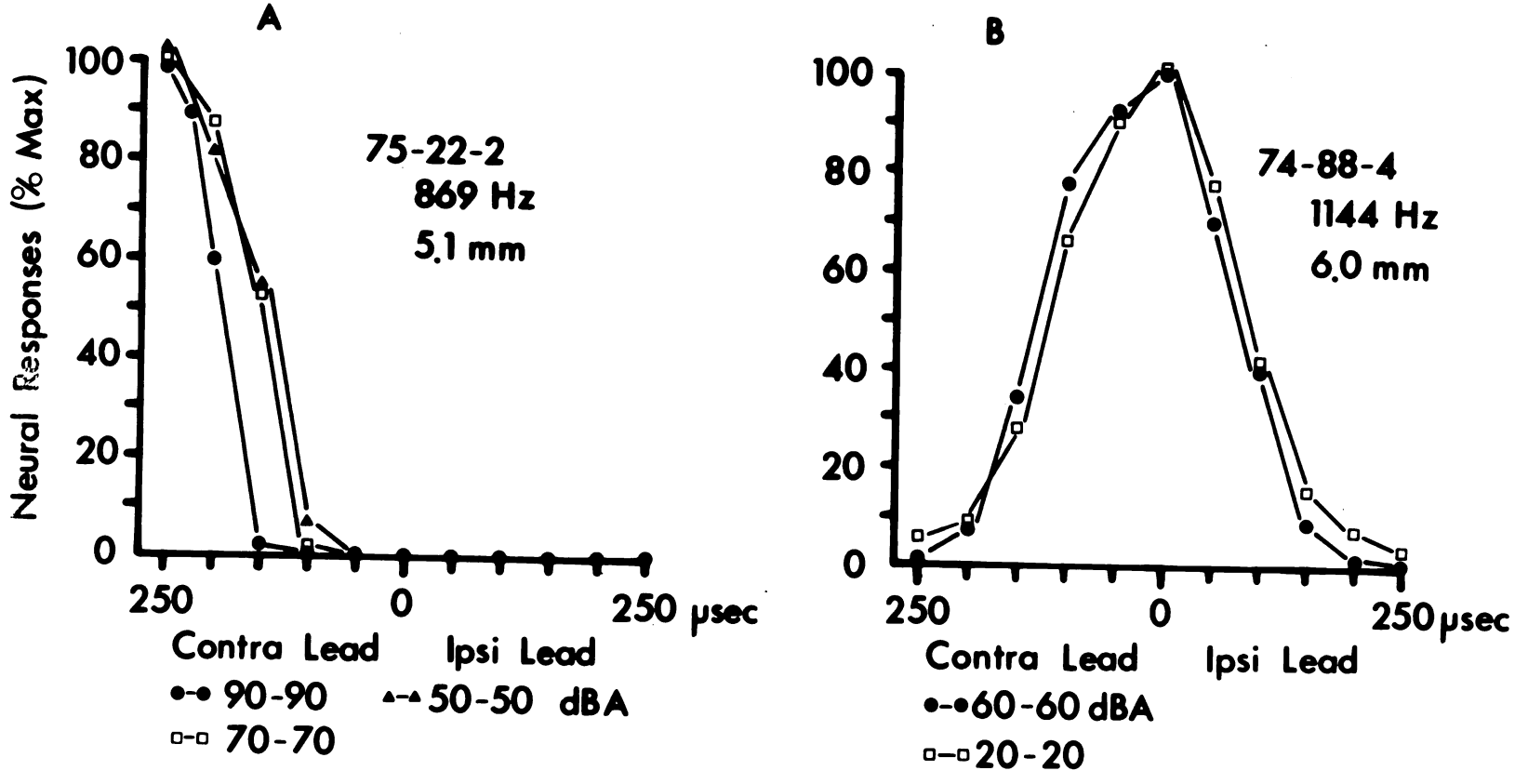
A
Neural Responses (% Max)
100
80
60
40
20
0
75-22-2
869 Hz
5.1 mm
250
0
250 μsec
Contra Lead
Ipsi Lead
●-● 90-90
▲-▲ 50-50 dBA
□-□ 70-70
B
100
80
60
40
20
0
74-88-4
1144 Hz
6.0 mm
250
0
250 μsec
Contra Lead
Ipsi Lead
●-●60-60 dBA
□-□20-20

Figure 27. Responses of two delay-sensitive ICC neurons to best frequency tonal stimulation at different intensity levels.

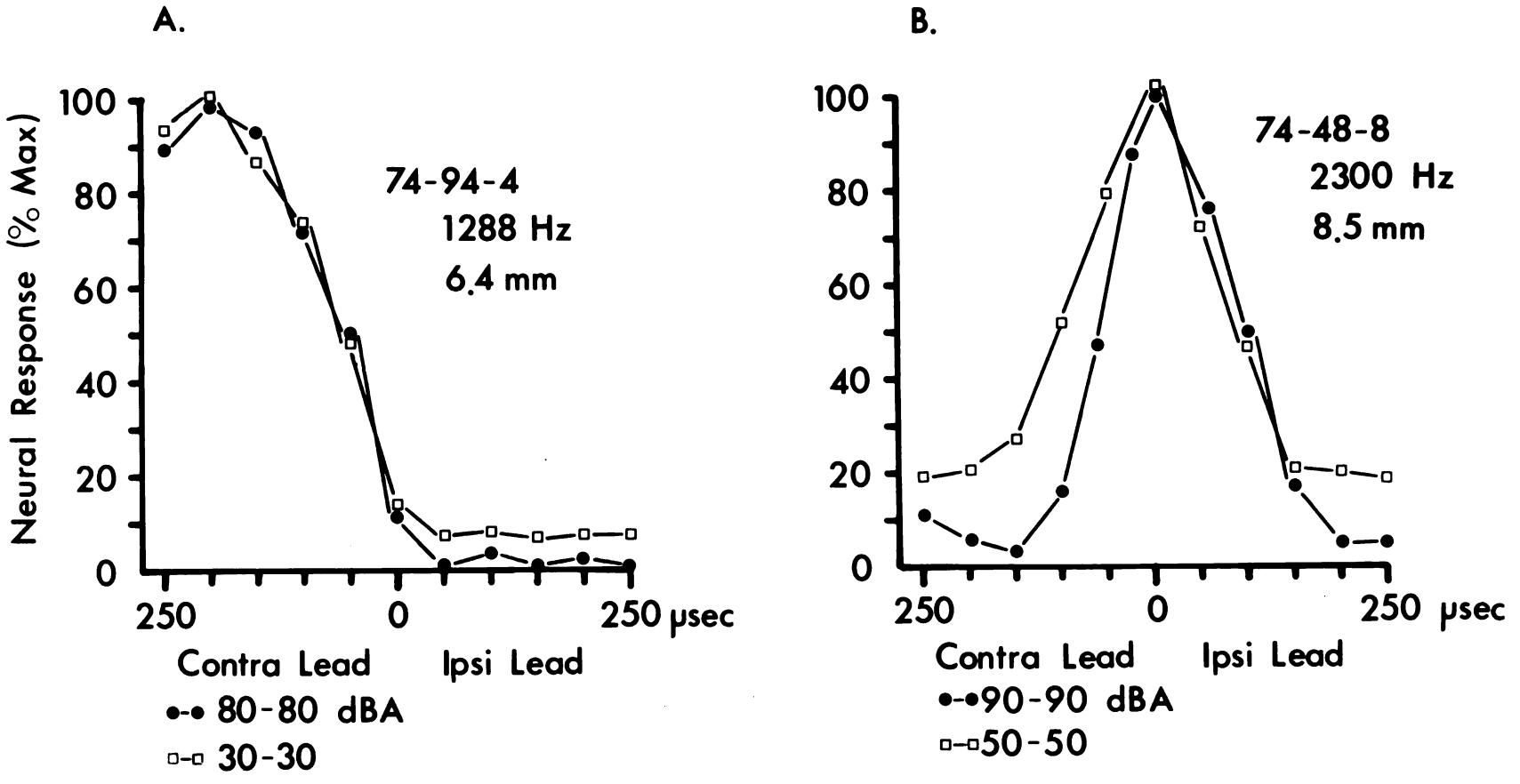
A.
Neural Response (% Max)
100
80
60
40
20
0
74-94-4
1288 Hz
6.4 mm
250
0
250 μsec
Contra Lead
Ipsi Lead
●-● 80-80 dBA
□-□ 30-30
B.
100
80
60
40
20
0
74-48-8
2300 Hz
8.5 mm
250
0
250 μsec
Contra Lead
Ipsi Lead
●-●90-90 dBA
□-□50-50

Figure 28. Responses of six delay-sensitive ICC neurons that discharged maximally to interaural time differences that could be generated by sound sources located in the contralateral side (A,B), ipsilateral side (D,E), and middle (C,F) of the free sound field.

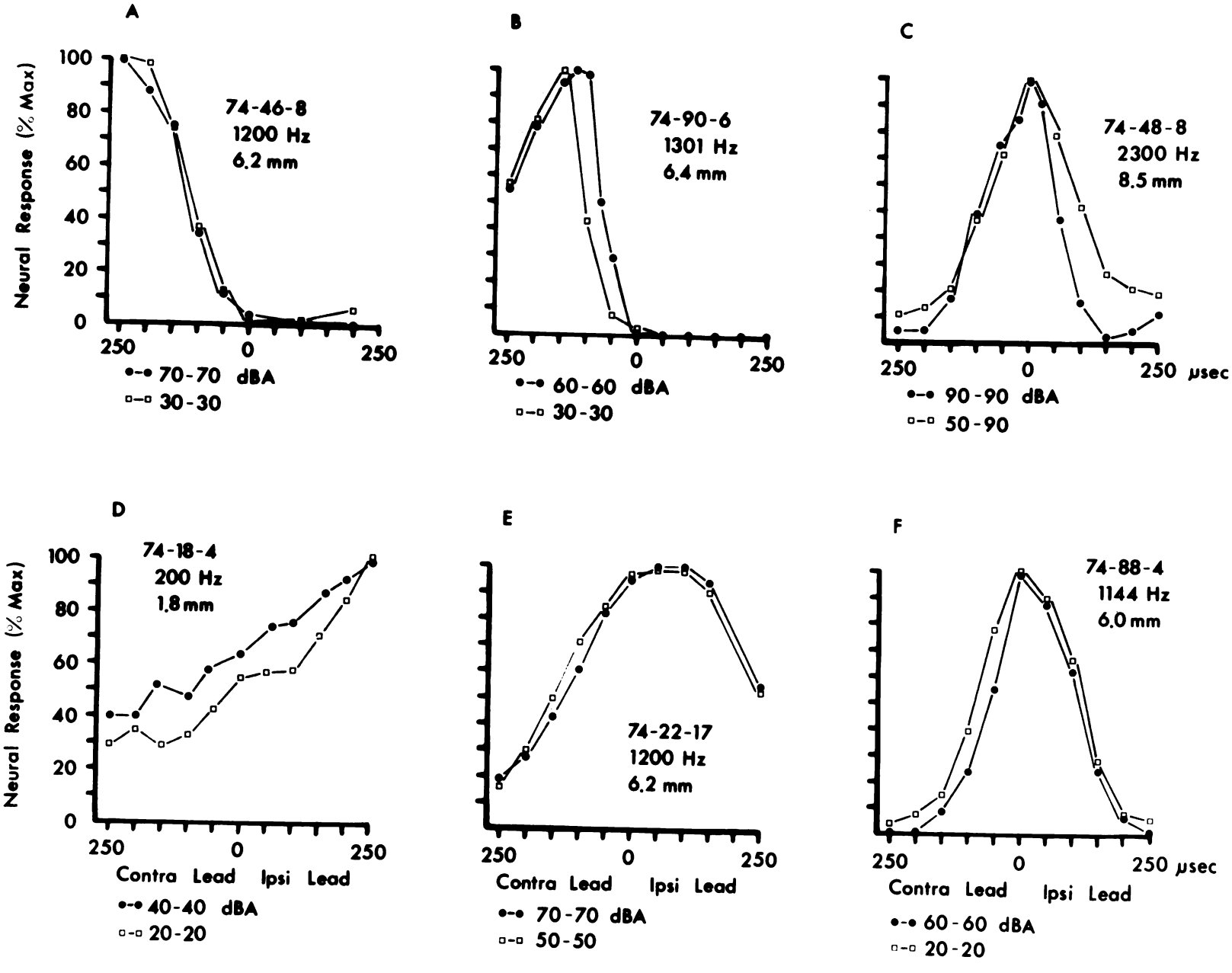
A
Neural Response (% Max)
100
80
60
40
20
0
74-46-8
1200 Hz
6.2 mm
250
0
250
●-● 70-70 dBA
□-□ 30-30
B
74-90-6
1301 Hz
6.4 mm
250
0
250
●-● 60-60 dBA
□-□ 30-30
C
74-48-8
2300 Hz
8.5 mm
250
0
250 μsec
●-● 90-90 dBA
□-□ 50-90
D
Neural Response (% Max)
100
80
60
40
20
0
74-18-4
200 Hz
1.8 mm
250
0
250
Contra Lead
Ipsi Lead
●-● 40-40 dBA
□-□ 20-20
E
74-22-17
1200 Hz
6.2 mm
250
0
250
Contra Lead
Ipsi Lead
●-● 70-70 dBA
□-□ 50-50
F
74-88-4
1144 Hz
6.0 mm
250
0
250 μsec
Contra Lead
Ipsi Lead
●-● 60-60 dBA
□-□ 20-20

Figure 29. A. The distribution of delay-sensitive neurons as a function of the interaural time differences (in 50 μsec bins) at which each neuron charged maximally.

B. The same distribution of delay-sensitive neurons plotted as a function of the interaural time differences representing 22.5^{o} sectors of a hypothetical free sound field (see text).

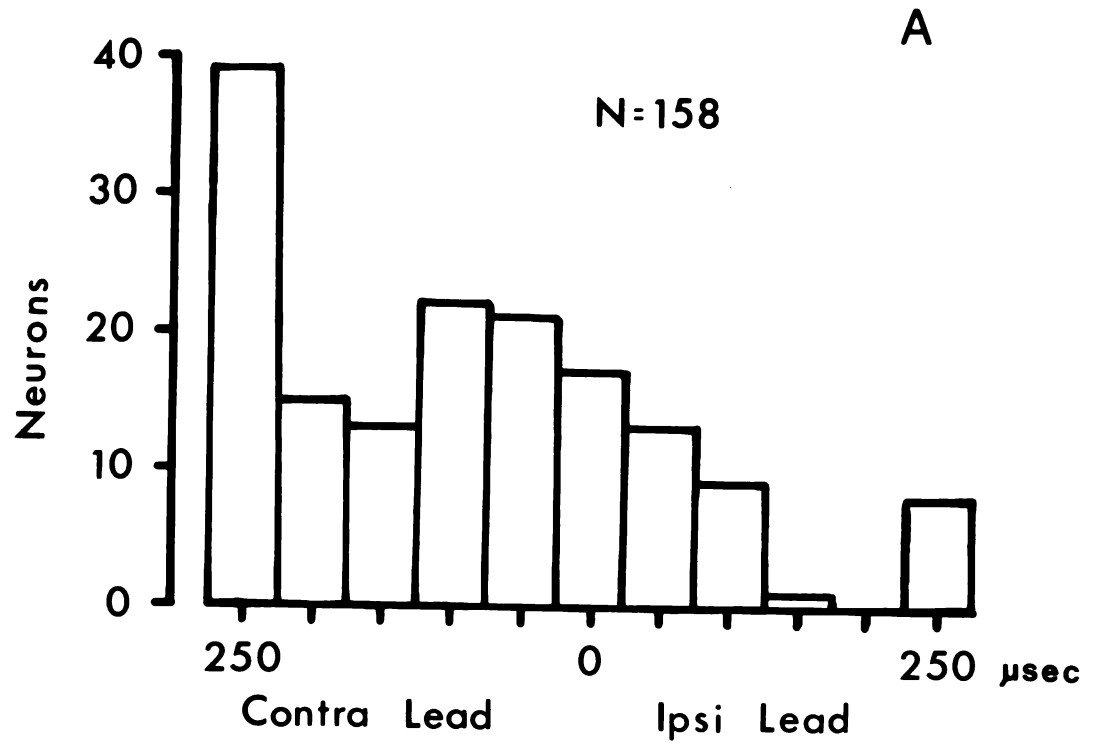
A
N=158
40
30
20
10
0
Neurons
250
0
250 µsec
Contra Lead
Ipsi Lead

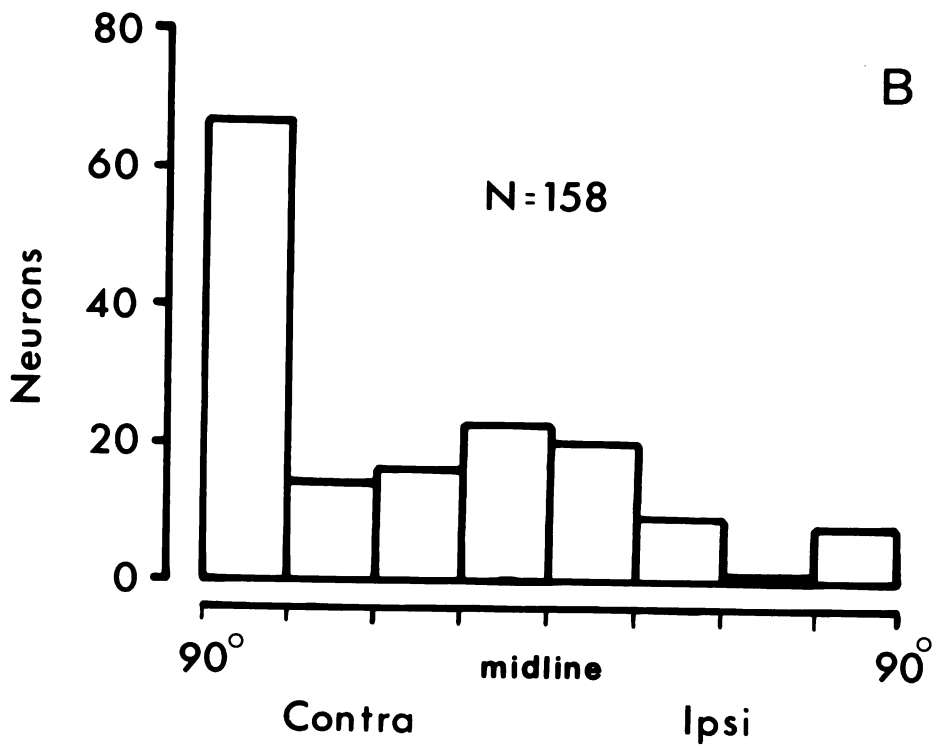
B
N=158
80
60
40
20
0
Neurons
90°
midline
90°
Contra
Ipsi

Figure 30. Represented cochlear place (or best frequency) of 158 delay-sensitive ICC neurons as a function of the preferred interaural time difference at which each discharged maximally.

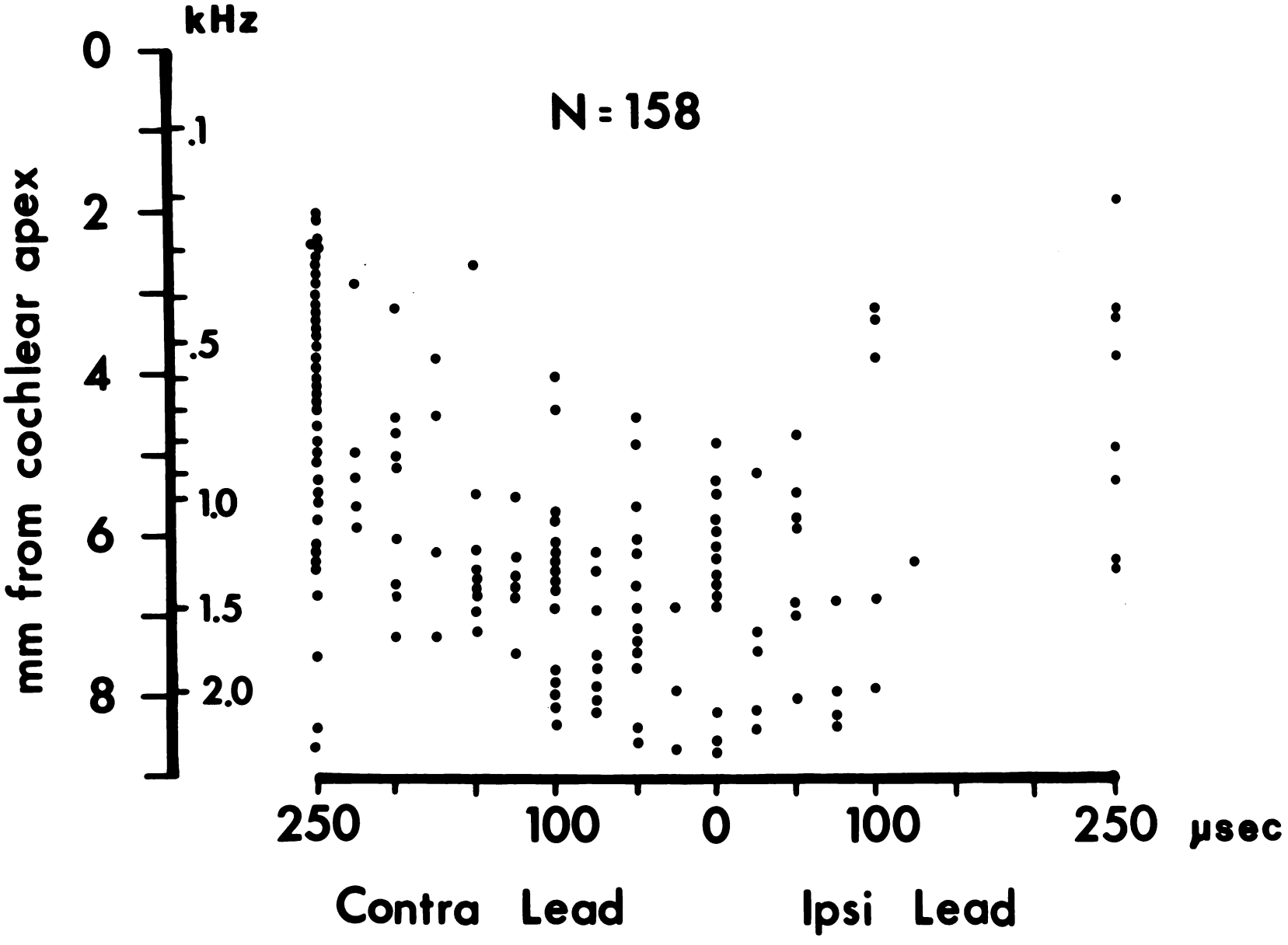
kHz
0
.1
2
.5
4
1.0
6
1.5
8
2.0
mm from cochlear apex
N = 158
250
100
0
100
250
µsec
Contra Lead
Ipsi Lead

Figure 31. Represented cochlear place of delay-sensitive ICC neurons isolated in four dorsal-to-ventral microelectrode penetrations as a function of the preferred interaural time differences at which each discharged maximally.

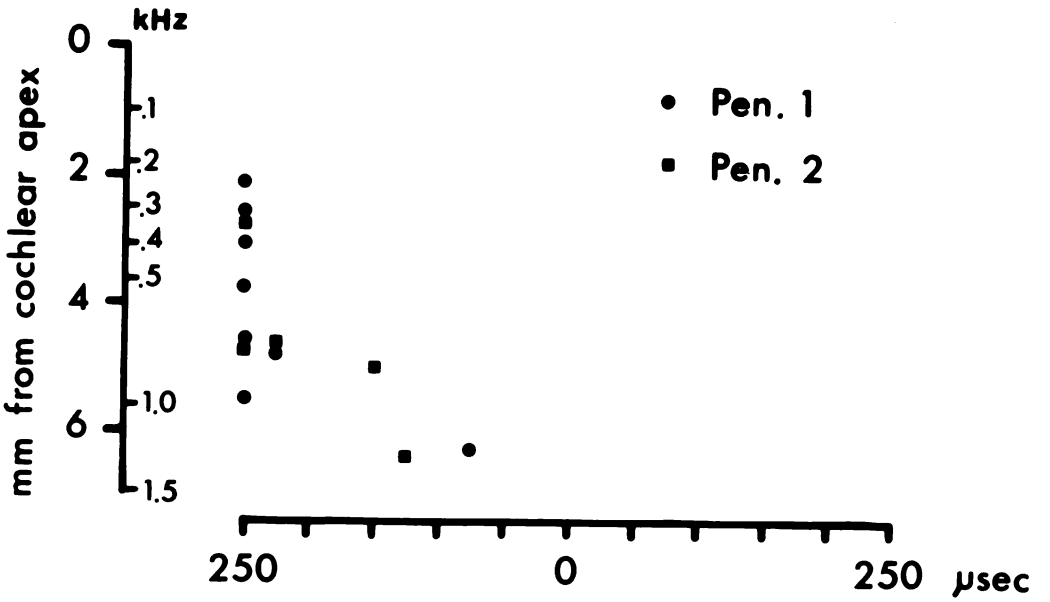
kHz
0
.1
2
.2
.3
.4
4
.5
1.0
6
1.5
mm from cochlear apex
Pen. 1
Pen. 2
250
0
250 μsec

75-18

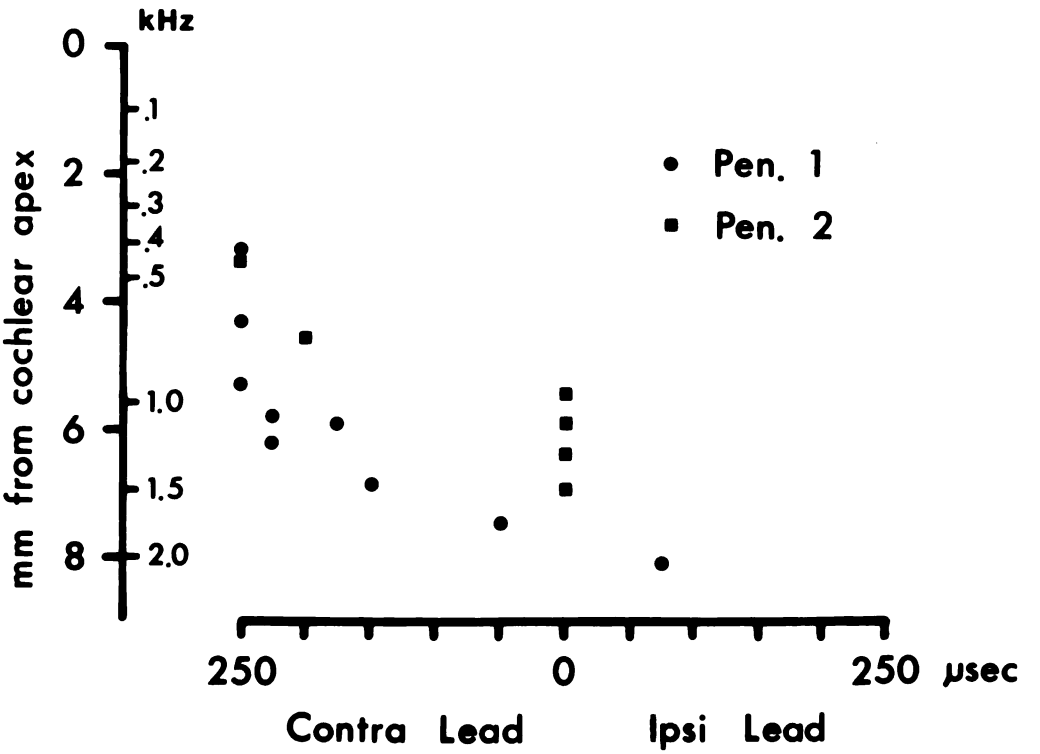
kHz
0
.1
2
.2
.3
.4
4
.5
1.0
6
1.5
8
2.0
mm from cochlear apex
Pen. 1
Pen. 2
250
0
250 μsec
Contra Lead
Ipsi Lead